UNIVERSITÀ DEGLI STUDI DI MILANO

SCUOLA DI DOTTORATO IN SCIENZE FARMACOLOGICHE

DIPARTIMENTO DI
SCIENZE FARMACOLOGICHE E BIOMOLECOLARI

XXVI CICLO

ROLE OF ABNORMAL LIPOPROTEINS IN ATHEROSCLEROSIS AND RENAL DISEASE IN LCAT DEFICIENCY

BIO/14

TESI DI:

Alice Federica Ossoli

Matricola R09312

TUTOR: Chiar.mo Prof. Guido Franceschini

COORDINATORE: Chiar.mo Prof. Alberto Panerai

ANNO ACCADEMICO 2013

INDEX

Introduction

1. ATHEROSCLEROSIS AND LIPOPROTEIN METABOLISM

Cardiovascular disease (CVD) is the main cause of death in worldwide, every day, coronary disease, particularly heart attacks and stroke, kills 4500 people in Europe and more than 17 million people in the world and it is attended by 2030 more than 23 million people will die annually from CVD [1].Atherosclerosis is a pathological condition characterized by the development and progression of plaque within arteries. It is described as inflammatory disease with lesions involving both lipid and cellular accumulation within the vessel wall and reactive intimal thickening of the artery. The onset of disease begins early, often in the childhood, and it is characterized by development of fatty streak followed by lipid deposition and accumulation of both extracellular matrix and intimal smooth muscle cells. Once the characteristic plaque has formed, it may remain asymptomatic for many years. However, as the disease progress, ischemia can appear with progressive occlusion of the vessel, or the plaque can suddenly rupture, resulting in thrombus formation. Rupture of a plaque frequently leads to one of the acute coronary syndromes (ACS), which include sudden death, acute myocardial infarction, or unstable angina.

There are numerous known risk factors involved in development of atherosclerosis, among these, elevated plasma concentration of cholesterol, in particular the low-density lipoprotein (LDL) fraction, hypertension, diabetes mellitus, smoking and genetic predisposition are the most known and studied [2].

Total and LDL cholesterol impact on coronary disease is well established and the cardiovascular risk in linearly correlated to increasing plasma LDL levels.

On the contrary, cholesterol levels associated to high-density lipoprotein (HLD) is inversely correlated to cardiovascular disease.

Among the other lipid parameters, hypertriglyceridemia associated to higher levels of very-low-density lipoprotein (VLDL) and chylomicrons (CM) appears less atherogenic than hypercholesterolemia. Usually, elevated triglyceride levels are associated with lower HDL levels and it is hard to understand which risk factor has high contribution in developing

cardiovascular disease. Lipid are particularly and marked involved in the plaque developing and regression and consequently in the manifestation of cardiovascular disease [3].

1.1 LIPOPROTEIN CHARACHTERISTIC AND METABOLISM

Levels of cholesterol and related lipids circulating in plasma are important predictive factors utilized clinically to estimate risk of a cardiovascular event.

In circulation, cholesterol, requires a transport vesicle because, being a lipid, it need to be shielded from the aqueous nature of plasma. Complex, micelle-like amalgamations of various proteins and lipids accomplish cholesterol transport through the vascular system. These particles, called lipoproteins, are heterogeneous in size, shape, composition and function. Plasma lipoprotein are spherical particles containing a core that consist of nonpolar lipid, mostly triglyceride (TG) and cholesteryl ester (CE), surrounded by a surface coat consisting of proteins (apolipoproteins), and more polar lipids, phospholipids (PL) and unesterified (free) cholesterol (FC). Lipoproteins are classified by their density and electrophoretic mobility into four major groups: chylomicrons, very-low-density (preβ) lipoproteins (VLDL), low-density (β) lipoproteins (LDL) and high-density (α) lipoprotein (HDL). After electrophoresis, chylomicrons remain at origin, and VLDL, LDL, and HDL migrate in the same position as preβ-, β- and α globulins, respectively. The main characteristic of these four classes are resumed in table 1 [4].

	Chylomicrons	VLDL	LDL	HDL
Hydrated density range (g/ml)	< 0.95	0.95-1.006	1.019-1.063	1.063-1.21
Electrophoretic migration	origin	pre-β	β	α
Average composition %				
Cholesterol	3	22	50	20
Triglyceride	90	55	5	5
Phospholipid	6	15	25	25
Protein	1	8	20	50
Major apolipoprtoteins	apoB-48, apoA-I, apoA-IV, apoE	apoB-100 apoC-I, apoC-II, apoC-III, apo-E	apoB-100	apoA-I, apoA-II apoC-I, apoC-II, apoC-III, apo-E
Origin	Intestine	Liver	VLDL	Liver, Intestine

Table 1Classification and property of the major human plasma lipoprotein [4]

Lipoproteins hydrated density is related to their chemical composition and the relative content of lipid and apolipoprotein. Chylomicrons (<0.95% g/ml) are 99% lipid, most of it TG;VLDL (0.95 to 1.006 g/ml) are about 90% lipid, the majority of it TG with smaller amount of cholesterol; LDL (1.019 to 1.063 g/ml) are the major carriers of cholesterol in plasma and CE and FC represent 50% of their weight; HDL (1.063 to 1.21 g/ml) involve about the same equal amounts of apolipoprotein and lipid, principally PL and cholesterol [4].

Beside the main function to transport lipid in plasma, apolipoproteins have other generic functions, among these they are able to release lipoproteins from cells, facilitate the cellular uptake of intact lipoproteins or selective uptake of their lipids and regulate other aspects of lipoprotein metabolism such as intravascular remodeling and lipid transfer. The major lipoproteins have a variety of apolipoproteins associated with them; different

apolipoproteins have one or more specific functions as described in table n.2 [4].

Apolipoprotein	Molecular weight	Chromosomal location	Function
ApoA-I	29.016	11q23	Cofactor LCAT, facilitates both the transfer to cell cholesterol by ABCA1 to nascent HDL and the delivery of CE and FC on HDL to liver through SR-BI
ApoA-II	17.414	1q21-23	Inhibit TG hydrolysis by HL and VLDL
ApoA-IV	44.465	11q23	Activates LCAT, promotes chylomicron formation
ApoA-V	39.000	11q23	Stimulates proteoglycan-bound LPL
ApoB-100	512.723	2p24-p23	Secretion on VLDL from liver; binding ligand to LDLR
ApoB-48	240.800	2p24-p23	Secretion of chylomicron from intestine
ApoC-I	6.630	19q13.2	Inhibits apoE binding to LDLR; stimulates LCAT; inhibits CETP and SR-BI
ApoC-II	8.900	19q13.2	Cofactor LPL
ApoC-III	8.800	11q23.3	Inhibits LPL, binding apoE to LDLR
ApoC-IV	11.000	19q13.2	Regulates TG metabolism
ApoD	19.000	3q26.2	Promotes reverse cholesterol transport
ApoE	34.145	19q13.2	Binding ligand for LRP on chylomicrons remanants and for LDLR on VLDL and HDL
ApoF	29.000	12q13.3	Inhibitor of CETP
ApoH	54.000	17q23	Activates LPL
ApoJ	70.000	8p21-p12	Binding of hydrophobic molecules
ApoL	42.000	22q13.1	Make only in pancreas, affect TG and glucose metabolism
ApoM	25.000	6p21.33	Binding of small hydrophobic molecules

Table n. 2 Description of characteristics and functionality of the major human apolipoprotein. LCAT lecithin:cholesterol acyltransferase, ABCA1 ATP-binding cassette A1, SR-BI scavenger receptor class B type I, LPL lipoprotein lipase, LDLR LDL receptor, CETP cholesteryl ester transfer protein, LRP LDL receptor-related protein [4].

Usually,lipoprotein metabolism is described as consisting of three pathways: the exogenous pathway, the endogenous pathway and the

pathway of the reverse cholesterol transport. The exogenous pathway involves transport of lipid deriving form diet from the intestine to liver; the endogenous pathway involves transport of lipids synthesized in the liver to peripheral tissues. The two pathways meet at the step of hydrolysis by lipoprotein lipase (LPL) in the periphery and by hepatic triglyceride lipase (HTGL) in the liver. Reverse cholesterol transport is the pathway in which cholesterol is removed from peripheral tissues and is carried to the liver [5].

Availability of triglycerides determines the state of lipid transport system. Fatty acids are provided as components of triglyceride in the diet: in the fed state they are primarily sent to the adipose tissue for storage, but in the post-absorptive and fasting state, free fatty acids are provided from storage depots by lipolysis. Muscle and liver capture free fatty acids from lipolysis and depending on cell energy status they are either oxidized to yield energy or re-esterified to form TG [5].

In the exogenous pathway intestine absorbs dietary lipids and in the enterocyte cellslipidsare assembled with apoB -48, apoA-I e apoA-IV into chylomicrons. The microsomal triglyceride transfer protein (MTTP) is the key protein in chylomicrons package, MTTP function is to transfer TG into apoB-48. Chylomicrons, secreted via the lymphatic system, enter the vena cava and circulate until they interact with lipoprotein lipase (LPL) that hydrolyze their triglyceride with glycerol and fatty acids formation. ApoC-II and apoA-V are cofactors for LPL activation, on the opposite,apoC-III has inhibitory proprieties. Aftertriglyceride hydrolysis, chylomicrons has smaller dimension and they are called “remnants”. The remnants are also characterized by altered apoE conformation that is necessary for binding to liver receptor in which remnants are eliminated. There are three different apoE isoforms: apoE-2, apoE-3 e apoE-4, (single aminoacid substitution in regions 112 and 158) with three different homozygous (E2/2, E3/3 e E4/4) and heterozygous (E2/3, E2/4, E3/4) phenotypes. ApoE2 has low affinity to hepatic receptor and it is not able to mediate remnants internalization [6].

In the liver cells (hepatocytes) the MTTP package TG with apoB-100, apoA-V, apoC and apoE to synthetize VLDL particles. In plasma VLDL acquire other molecules of apoC and apoE from HDL. In the same way of

chylomicron metabolism, LPL hydrolyze TG in VLDL with VLDL remnants formation called IDL.

IDL are transformed to LDL by hepatic lipase (HL) that hydrolyze TG and release apoC and apoE. LDL are characterized byenrichment in esterified cholesterol and contain only apoB-100 as protein. In healthy subjects 70% of total plasma cholesterol is consisted to LDL, large part of LDL are removed by liver through interaction with LDL receptor (LDLR), another small part is removed in the peripheral cells through interaction with LDLR or scavenger receptors. apoB-100 is the interact with LDLR that is expressed in all cells; after binding, LDL are internalized through endocytosis pathway and localize into lysosomes in which the esterified cholesterol has been hydrolyzed. The unesterified cholesterol become available for different physiological functions such as cellular membrane building, synthesis of steroid hormones, and if is needed, esterified a second time by ACAT and stored as cholesteryl ester into cell.LDLR expression is regulated by cholesterol content into cell, but on the contrary, scavenger receptor expression is not regulated.The LDL are sensitive to lipolytic hepatic lipase action; thus form small dense LDL characterized by a low ratio lipid/protein. Small and dense LDL are more atherogenic than large and low-dense LDL. The LDL become more atherogenic even when they are modified from oxidative processes in lipid and proteinform that facilitate interaction with receptors scavengers. A slowed down catabolism of LDL prolongs the half-life and promotes the oxidation, with a resulting increase in the deposition of cholesterol in the macrophages of the arterial wall, transformation into foam cells, formation and progress of the plaque [6].The cholesterol removal from arterial wall is mediated by HDL through the reverse cholesterol transport, an atheroprotective process that will be discussed later.Through RCT, cholesterol returns to liver in which it is eliminated through biliary excretion. Transporters ABCG5 and ABCG8 are expressed in liver and intestine and are involved in excretion of cholesterol.

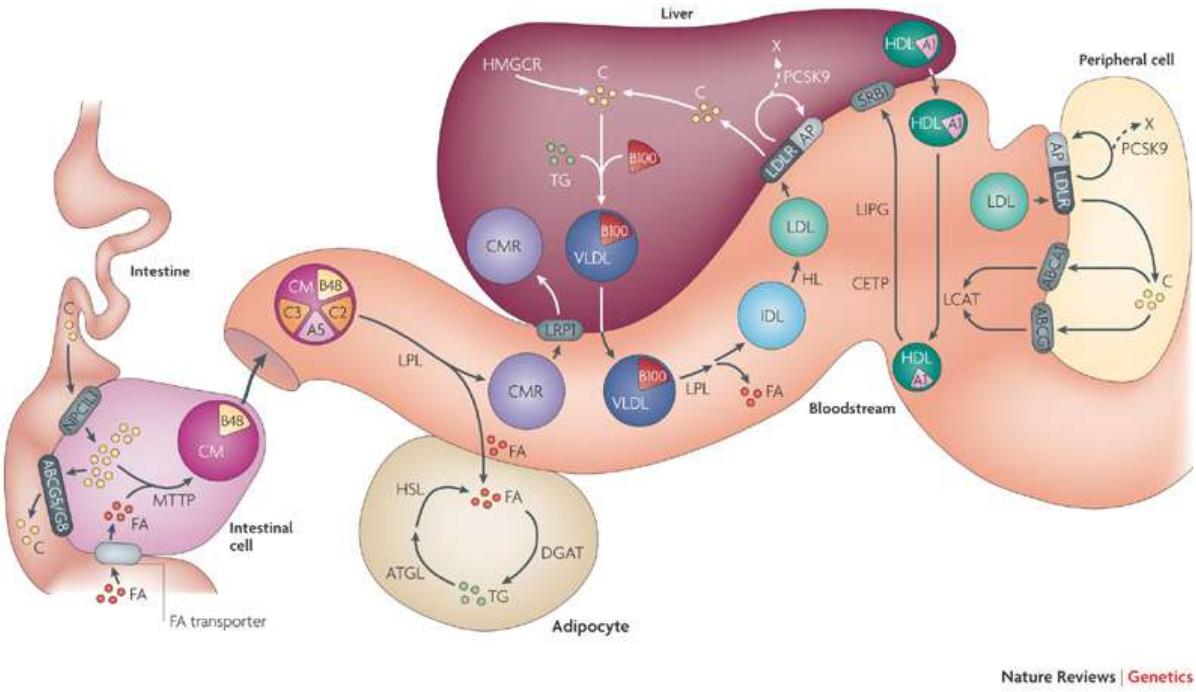

Fig. 1.Schematic drawing of cholesterol metabolism. In intestine fats from diet are hydrolyzed and the reconstituted triglycerides are packed into chylomicrons with apoB48 and cholesteryl ester by MTTP.Cholesterol in the intestinal lumen enter enterocytes via the Niemann-Pick C1-like 1 (NPC1L1) transporter. Some sterols are resecreted by heterodimeric ATP-binding cassette transporter G5/G8 (ABCG5/G8)and other are packed into chylomicrons. Chylomicrons also present other apoliporoteins (APOA5, APOC2 and APOC3) and are secreted via the system. Chylomicrons then enter the vena cava and circulate in the blood until interaction with LPL; after interaction free fatty acids are released and enter in peripheral cells. In adipocytes, triglycerides are resynthesized by acyl CoA:diacylglycerol acyltransferase (DGAT), but they can be hydrolyzed again by adipose TG lipase (ATGL) and hormone sensitive lipase (HSL). Chylomicron remnants (CMRs) are internalized into the liver by hepatic LDL receptor (LDLR), here triglyceride is packaged with cholesterol and the apoB100 to form VLDL particles. In liver, cholesterol packed into VLDL is recycled or synthesized de novo by 3-hydroxy-3-methylglutaryl coenzyme A reductase (HMGCR) that represent rate-limiting step. In plasma LPL hydrolyze triglyceride contained in VLDL with resulting release of fatty acids and VLDL remnants (IDL). Thus IDL are hydrolyzed by hepatic lipase (HL) with the resulting formation of LDL particles.LDL transports cholesterol from the liver to the peripheral tissues in which enter by endocytosis. LDL can return to the liver and enter hepatocytes through LDLR. LDRL expression

is regulated by proprotein convertase subtilisin/kexin type 9 (PCSK9).PCSK9 complexes to LDLR, leading to degradation of the receptor. Inthe peripheral cells, cholesterol is removed from macrophages after interaction of ApoA-I present on HDL particles with ATP-binding cassette A1 (ABCA1) and ABCG1 transporters. Unesterified cholesterol incorporated in HDL particles become substrate of Lecithin-cholesterol acyltransferase (LCAT) enzyme.Esterified cholesterol can be transferred from HDL to apoB-containing particlesby cholesterol ester transfer protein (CETP) or, after remodelling by endothelial lipase (LIPG), enters hepatocytes via scavenger receptor class B type I (SRB1) [7].

1.2 HDLCHARACTERISTIC

HDL are a highly heterogeneous lipoprotein family composedby several subclasseswith different density, shape and size. They have density between 1.063 to 1.21 g/ml, and range in diameter from 70 to130 Å and in mass from 200,000 to 400,000 Dalton. On the average,HDL are formed by 50% lipid and 50% protein. The density ofthe HDL particles is inversely related to their size, reflecting therelative contents of low-density non-polar core lipid, and highdensitysurface protein. Most part of plasma HDL have a globularshape, the central core is composed by non-polar lipids (triglycerides andcholesteryl esters) surrounded by a monolayer of polar lipids(phospholipids and unesterified cholesterol) and apolipoproteins. Current models of HDL describe apolipoprotein molecules disposed like a belt wrapping around the lipid core [8-9]. HDL apolipoproteinshave amphipathic (detergent-like) properties, determined by regionscontaining both polar and non-polar amino acid residues, which areoften located on opposite sides of anα-helix [10]. Hydrophobic forces drivethe association ofpolar lipids and apolipoproteins in HDL, and the fatty acyl chains and the non-polaramino acids side chains are excluded from the aqueous environment.The apolipoproteins and the unesterified cholesterol are soluble in aqueous environment and can exchange easily betweenlipoproteins or with other lipid surfaces (i.e. cell membranes).Phospholipids and non-polar lipids have little potential forexchange, but through the action of specific lipid transfer proteins, theymay be transferred between lipoproteins [8-11]. A minor fraction ofplasma HDL has a non-spherical structure, but they consist in discoidal bilayer of polar lipids, in which non-polar core is lacked; apolipoproteins run from side to sideof the disk, with polar residues facing the aqueous phase and nonpolarresidues facing the acyl chains of the lipid bilayer [12,13].The protein component of HDL is formed mainly byapoA-I (70%) and apoA-II (20%). Two major particle subclasseshave been identified on the basis of major apolipoproteins composition: particles containing apoA-I only(LpA-I), and particles containing apoA-I and apoA-II (LpA-I: A-II); they also carry additional minor proteins and are heterogeneous in size and

composition. Recent shotgun proteomic analysis showed that HDL contain 48 or more proteins, among these apoAIV, apoCs, apoE, lecithin: cholesterol acyltransferase (LCAT),cholesteryl ester transfer protein (CETP), phospholipid transfer protein (PLTP), paraoxonase (PON), and platelet-activating factor acetylhydrolase (PAF-AH) circulate in plasma bound to HDL [8-14]. Most of the proteins carried by HDL are not apolipoproteins, and represent very minor components of HDL.

It is possible to classify HDL on the basis of density, charge, shape and size.Based on density, two HDL subclasses were identified, called HDL2 (1.063 to 1.12 g/ml) and HDL3(1.12 to 1.21 g/ml).

According to charge is possible identify HDL into α- and pre-β-migrating particles on the agarose gel and combining charge and size these two subclasses can be divided into 12 distinct apoA-I-containing HDL particles, referred to as pre-β (pre-β1 and pre- β 2), α (α 1, α 2 and α 3) and pre- α (pre- α 1, pre- α 2 and pre- α 3) on the basis of mobility that is slower or faster than albumin, respectively, and decreasing size. On the basis ofparticle size; five subclasses have been identified and characterized HDL3c, 7.2-7.8 nm; HDL3b, 7.8-8.2 nm; HDL3a, 8.2-8.8nm; HDL2a, 8.8.-9.7 nm; HDL2b, 9.7-12.0 nm [15].

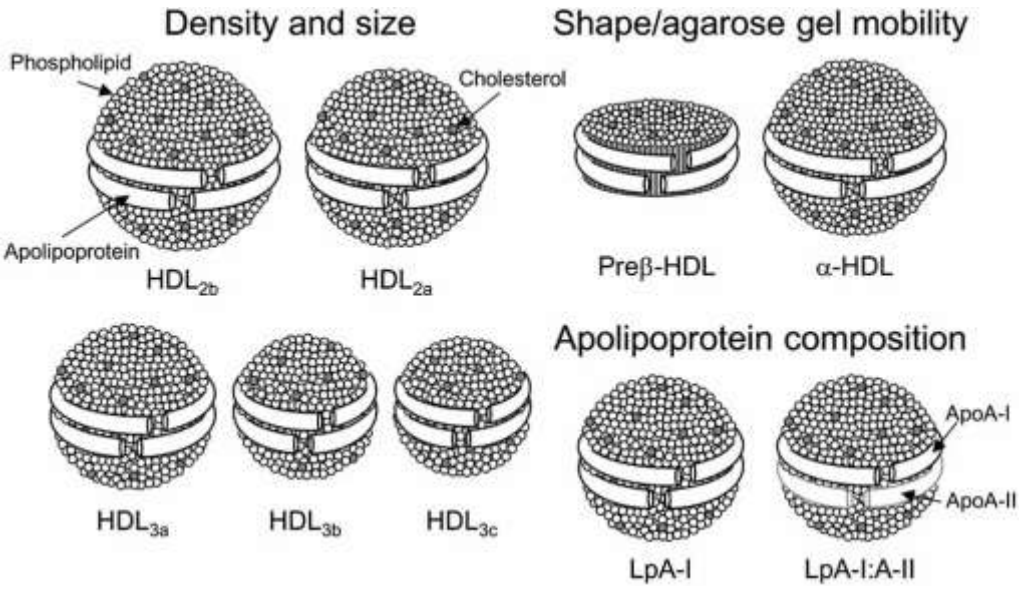

Fig 2.HDL heterogeneity.Schematic representation of HDL subclasses according to density, size, charge and apolipoprotein composition (drawings not in scale) [8].

1.3 HDL METABOLISM

The two major apoliporotein in HDL, ApoA-I and A-II, are synthesized mainly by the liver and, to a lesser extent, by the small intestine [16].

The proteins are secretedas components of triglyceride-rich lipoproteins, chylomicronsarising from the intestine and VLDL from the liver. In circulation, PLTPpromote the transfer of surface components (phospholipids,cholesterol and apolipoproteins) from triglyceride-richlipoproteins during lipolysis to HLD. The regulatory role of PLTP is achieved via its two main functions, phospholipid transfer activity and the capability to modulate HDL size and composition in a process called HDL conversion [17]. Hepatocytes are able to secrete apoA-I in lipid-free or lipid-poor and lipidated forms [18],ApoA-I is secreted as pro-apoA-I and converted to a mature form by a metalloprotease in blood plasma [19]. There are three potential sources of lipid-poor apoA-I in plasma: it may be released as lipid-poor protein after its synthesis in the liver and intestine, it may be released from triglyceride-rich lipoproteins that are undergoing hydrolysis by lipoprotein lipase, and it may be generated within the plasma during the remodeling of mature, spherical HDL particles. Lipid free-apoA-Iacquires phospholipids and cholesterol peri-cellularlythrough the interaction with the ATP binding cassette transporterA1 (ABCA1), to form pre-β-HDL, this pathway is dependent on ABCA1 expression. Only 20% of total apoA-I produced in liver is intracellularly lipidated, and some of the lipidation may not be mediated by ABCA1 [20]. Once in the circulation,pre-β-HDL are acted on by LCAT, which converts lecithin andcholesterol into lysolecithin and cholesteryl esters in a reaction thatuses apoA-I as cofactor [21]. The non-polar cholesteryl esters splitthe bilayer and give rise to the mature spherical α-HDL (HDL3).The HDL3 interact in the plasma with CETP, that exchanges cholesterylesters for triglycerides between HDL and triglyceride-rich lipoproteins,generating large cholesteryl ester-poor and triglyceride-richHDL particles (HDL2) [22]. HDL triglycerides and phospholipidsare hydrolyzed by lipolytic enzymes (lipoprotein, hepatic,and endothelial lipases), converting spherical α-HDL back to discoidal pre-β-HDL particles [23, 24]. During this process, someapoA-I dissociate from

HDL and are cleared from the circulation,mainly through the kidney [25]. Cholesteryl ester-rich HDL3could be also internalized in hepatocytes through two different pathways: the first is mediated by SR-BI, located on the surface of liver and adrenal cells, which mediates the uptake of cholesteryl esters (and unesterified cholesterol) from HDL, without the internalization and degradation of the lipoprotein itself [26]. The generated cholesteryl ester-depleted, small HDL particles are either remodeled into large HDL by incorporation into preexisting HDL, or are cleared through the kidney [27,28]. The second might be independent of SR-BI and involve the uptake and degradation of the holo-HDL particle by unknown receptors. An alternative mRNA splicing variant of SR-BI, named SR-BII, can remove HDL from circulation through internalization and co-localization with transferrin in the endosomal recycling compartment [29], this receptor is identical to the β-chain of ATP synthase [30]; however, this does not seem to be a major pathway for HDL catabolismin.Rather HDL lipids and apoA-Iappear to be catabolized through distinct pathways, which requirethe dissociation of the apolipoprotein from its bound lipids. HDLlipid clearance occurs by the processes of cellular selective uptakethrough SR-BI [26], transfer to other lipoproteins by CETP [22] andPLTP [31], and hydrolysis by lipolytic enzymes [23, 24]. Less isknown about the catabolism of the HDL protein moiety. Numeroustissue uptake studies support the view that the kidney is the principalsite of apoA-I degradation, withpresence of apo-A-I on the brush-border and in apical granules of proximal tubule epithelial cells [32]. Lipid-poor apoA-I has a size, which is lower than thecutoff value of the glomerular barrier, and may be readily removedfrom the circulation by glomerular filtration. The filtered apolipoproteinis entirely reabsorbed in the proximal convoluted tubule,and undetectable in urine [33]. Cubilin,is a multiligand receptorexpressedin the apical membrane of various absorptive epithelia including those of the kidney, intestine, the yolk sac and placenta[34]. Cubulin is the established receptor for endocytosis ofintrinsic factor vitamin B12 , but also binds apoA-I with high affinity,and mediates apoA-I endocytosis [35]. The proximal tubule of the renal cortex is the major site for the uptake of apoA-I and most other proteins filtered in the glomeruli. Cubilin is highly

expressed in this segment of the nephron, and is probably involved in the reabsorption of multiple proteins in the glomerular ultrafiltrate [35].Whether the internalizedapoA-I may escape degradation and recycle back to the plasma isunknown. However, the fact that all known cubilin ligands seeminvolved in lysosome transportation argues against suchtranscytosis of apoA-I [33]. Some studies suggest that the kidney isalso capable of both filtration and re-absorption of HDL particles;both the molecular shape and the charge of the particle influencethe ability of HDL to cross the glomerular barrier, with small,discoidal and positively charged HDL particles being filtered morereadily than mature HDL [36].Metabolic turnover studies in humans have shown that apoA-Ihas a metabolic fate separate from apoA-II, and that apoA-I isgenerally catabolized at a faster rate than apoA-II; moreover, lipidfreeapoA-I is cleared from plasma at a much faster rate than apoAIbound to HDL [37]. It has also been established that the fractionalcatabolic rate of apoA-I is the major determinant of plasma apoA-Iand HDL levels [38]. Apolipoprotein and lipid composition, as wellas particle size, are important determinants of HDL catabolism.LpA-I particles are cleared from the circulation at a faster rate thanLpA-I: A-II particles, with residence times of 4.4 versus 5.2 days,and apoA-I in HDL3 has a substantially faster turnover rate thandoes the apoA-I in HDL2 [39]. Triglyceride enrichment of HDLfurther enhances the clearance of LpA-I particles, without changesin LpA-I: A-II turnover [40].

1.4 HDL FUNCTION

1.4.1 REVERSE CHOLESTEROL TRANSPORT

The most important function of HDL is to promote the removalof cholesterol from peripheral cells, including macrophages withinthe arterial wall, and shuttle it to the liver for excretion through the bileand feces. This process is called reverse cholesterol transport (RCT) and it results in a net mass transport of cholesterol from thearterial wall into the bile. This pathway is described as anti-atherogenic process by preventing arterial cholesterol accumulation,plaque destabilization and development of acute cardiovascularevents. Cell cholesterol efflux is the first process in RCT and also represents the rate-limiting step. In cell culture experiments several distinctpathways have been identified for the exchange of unesterified cholesterol between cells and extracellular acceptors [41]. Thisexchange can occur by several processes: the simply way is characterized by aqueous diffusion according to the direction of cholesterolgradient, or through three main distinct, protein-mediated, pathways [41]. The protein-mediated pathways consistto an unidirectional (cell to acceptor), ATP-dependent pathwaymediated by the ABCA1 transporter; an ATP-dependent pathwaymediated by the ATP binding cassette G1 transporter(ABCG1); an ATP-independent, bidirectional pathway mediated bySR-BI. Lipid-free/lipid-poor apolipoproteins, mainly apoA-I,represent the principal cholesterol ABCA1acceptors [41]. ABCA1 and apoA-I interaction promotes cholesterol and phospholipidefflux from ABCA1 to apoA-I, with generation of small, discoidal pre-β-HDL. These particles can remove further cholesterol from cells through the samepathway [43]. All plasma HDL subclasses, including mature α-HDL particles and discoidal pre-β-HDL, are efficient cholesterol acceptors via the ABCG1 pathway [41, 42]. Both ABCA1 andABCG1 are highly expressed in macrophages, especially after cholesterolloading, suggesting their critical importance for HDL-mediatedcholesterol efflux. SR-BI promotes cell cholesterol efflux to mature α-HDL particles but not to the small pre-β-HDL [41, 42]. Thisreceptor mediates a bidirectional flux of cholesterol resulting that thelarge cholesteryl esters-rich HDL become

cholesterol donorsinstead than acceptors via this pathway. The role of SR-BI in mediating macrophage RCT in vivo is probably not quantitatively important, despite its role to facilitate in vitro cholesterol efflux from macrophages to mature HDL has beenshown. [44].Once accumulated into HDL, cholesterol is esterified in plasmaby the LCAT enzyme with the resulting formation of cholesteryl esters. Thehydrophobic cholesteryl esters move to the core of the HDLparticle, and contribute to the progressive enlargement of HDL.Through this process also unesterified cholesterol is removed from thesurface of HDL, thus helping to maintain a free-cholesterol gradientfrom cells to HDL. LCAT has long been considerednecessary for efficient RCT, but recent data suggest that even if functional LCAT is not present, macrophagecholesterol efflux and RCT can occur [45,46]. Large amount of the cholesteryl esters formed by theLCAT reaction are transferred to apoB containinglipoproteins in exchange for triglycerides through CETP-mediated process (Fig. 3). The apoBcontaininglipoproteins are finally catabolized by the liver. In humans,CETPpathway represents an important mechanism by which HDL-derivedcholesterol is transported back to the liver. Alternatively,HDL-cholesteryl esters are taken-up by the liver through SR-BI. Additional pathway for hepatic cholesteryl ester removal is represented by direct, SR-BI-dependent uptake of HDL unesterifiedcholesterol by the liver [47].

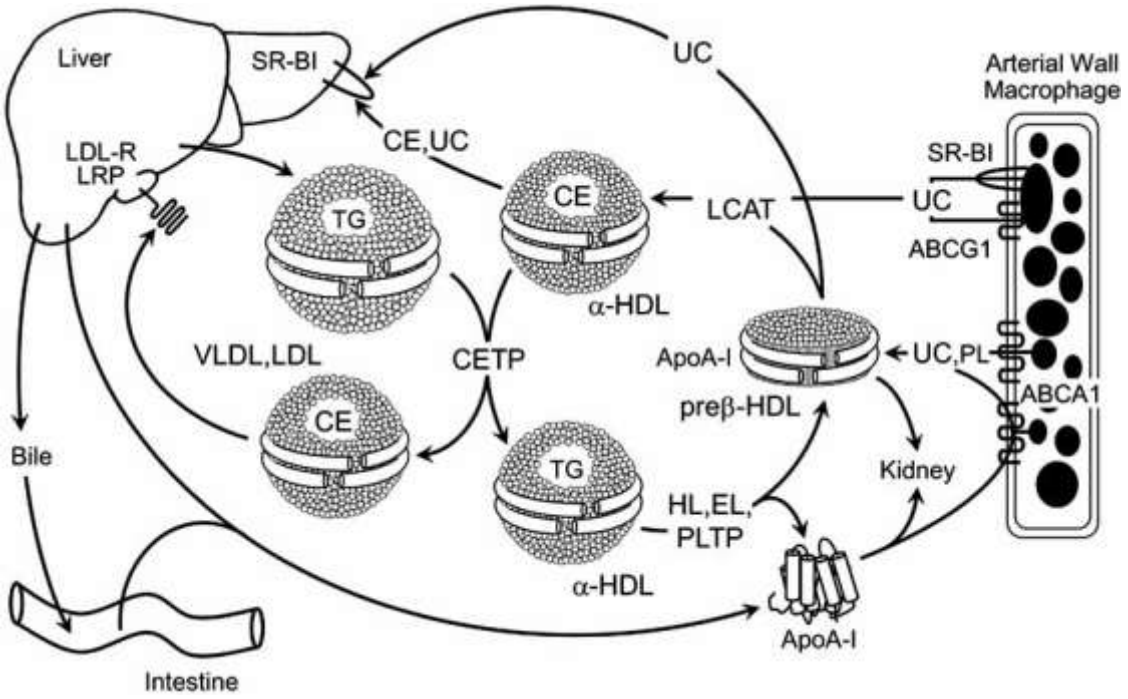

Fig 3Schematic drawing of Reverse Cholesterol Transport [8]

1.4.2 HDL AND ENDOTHELIAL PROTECTION

Atheroprotection mediated by HDL is not only through their major role in RCT, but also through secondary different functions, one of the most important is the ability of HDL to maintain endothelial cell homeostasis and integrity [50].

HDL have potent antioxidant properties, mediated bymolecules carried by HDL (PON-1, PAF-AH, and LCAT) or by apoA-I and apoA-II [48], aswell as anti-inflammatory and antithrombotic activities [49].

Usually, the endothelium has been described such as an inert component of the vessel wall;but during the past two decades it has become evident that the vascular endothelium plays animportant role in maintaining vascular homeostasis through the production of alarge number of substances that modulate vascular tone, inflammation, and hemostasis. Amongthese, nitric oxide (NO) and prostacyclin (PGI2) maintain vascular tone and display antithrombotic proprieties. A decrease in their bioavailability is a typical characteristic ofendothelial dysfunction, and it was demonstrated that HDL are able to increase NO and PGI2 production

bydirect and indirect mechanisms [50]. In *in vitro studies*onendothelial cells, HDL are able to increase endothelialNO synthase (eNOS) protein abundance, by modulating both transcriptional and posttranslationallevels [51-53], prevent eNOS displacement from caveolae, and stimulateeNOS activation. eNOS activation is mediated by the binding of apoA-I to SR-BI; however,apoA-I is necessary but not sufficient for eNOS stimulation, since lipid-free apoA-I are not able to activate the protein[54]. eNOSenzymatic activity is regulated by complex signaltransduction pathways, which include the activation of kinases that modify thephosphorylation state of the enzyme [55]. Akt kinase activates eNOS through directlyphosphorylating at aminoacid position Ser1177; Akt itself is phosphorylated and activated by PI3kinase, which in turn is activated by a tyrosine kinase. In contrast to eNOS-Ser1177, under certain conditions, thephosphorylation of eNOS-Thr495 attenuates enzyme activity. HDL are able to stimulate eNOS activation by phosphorylation at Ser1177 via Akt,and this is mediated by Src family and PI3 kinases. Enzyme activation also requires Srcdependentand PI3 kinase–dependent activation of Erk1/2 MAP kinases [56]. HDL can also mediate eNOS activation through the interaction of sphingosine-1-phosphate (S1P) with itsreceptors [57]. S1P is a bioactive phospholipid associated to HDL, in which is specifically bound to apolipoprotein M (apoM), which thusrepresents a vasculoprotective constituent of HDL [58].

HDL could enhance PGI2 production incultured endothelial cells through several mechanisms. HDL can supply endothelial cellswith arachidonate, that is a substrate for PGI2 synthesis [59], or can activate acalcium-sensitive [60], membrane-bound phospholipase which makes endogenousarachidonate available for PGI2 synthesis [61]. *In vivo* experiments support therelevance of HDL in promoting endothelium-dependent vasodilatation. Inhypercholesterolemic apoE-deficient mice, intravenous injections of synthetic HDL (sHDL)restore endothelium-dependent dilation with a dose-dependent effect [62]. In humans,plasma HDL-C concentration is a strong independent predictor of NO-dependentperipheral vasodilation in healthy individuals, hyperlipidemic, diabetic and coronarypatients [63-66]. As already demonstreted in

animals, the intravenous infusion of sHDL in subjects withhypercholesterolemia or with low HDL-C rapidly restores the altered endotheliumdependentperipheral vasodilation through increased NO bioavailability [67, 68].

Another typical feature of endothelial dysfunction is the increased expression of cell adhesion molecules (CAMs) on the surface ofendothelial cells [50]. Activatedendothelial cells express different adhesion proteins, including vascular cell adhesionmolecule-1 (VCAM-1), intercellular adhesion molecule-1 (ICAM-1), platelet endothelial cell adhesion molecule-1 (PECAM-1) and E-selectin. It was demonstrated that theseadhesion proteins are expressed in arteries in vivo at sites of developingatherosclerosis [69], and soluble forms are present at increased concentrations in theplasma of human subjects with coronary heart disease (CHD) [70]. Adhesion molecules attract circulating monocytes and other leukocytes, which after adhesion through integrins to the endothelial surface can transmigrate into the intima.In particular E-selectins are expressed both in acute and in chronically inflamed endothelium and serve as rolling molecules for monocytes, neutrophils, effector T cells, B cells, and natural killer cells [71]. E-selectin is synthesized only during inflammation and is not constitutively expressed under noninflamed conditions. E-selectin is found on endothelial cells after stimulation by inflammatory cytokines such as tumor necrosis factor (TNF)-α, interleukin (IL)-1α, or platelet factor 4 (PF4). In E-selectin knockout mice was shown a significative reduction in the lesion size in aorta [71].

In response to accumulation of cholesterol within the intima of aortas, VCAM-1 expression is induced by arterial endothelial cells. In human coronary arteries expression of ICAM-1 and VCAM-1 was described. Studies on rabbit demonstrated that also an atherogenic diet rapidly induces VCAM-1 expression in aortic endothelium. More evidence that VCAM-1 expression is regulated by proatherogenic factors are provided by study that demonstrated oxLDL-induced upregulation of VCAM-1. Lipoproteins containing apoCIIIincrease VCAM-1 and ICAM-1 expression in endothelial cells by activating PKCβ and NF-κB pathways. In human coronary atherosclerotic plaques, increased levels of VCAM-1 and ICAM-1

and increased numbers of plaque intimal macrophages and T cells were observed within regions of plaque neovasculazation, but less in the arterial luminal endothelium suggesting that VCAM-1– and ICAM-1–dependent recruitment of immune cells through intimal neovasculature may participate in atherosclerosis [71].

Platelet endothelial cell adhesion molecule-1 (PECAM-1), also known as CD31, is a member of the immunoglobulin gene superfamily. PECAM-1 is mainly expressed at the lateral borders of endothelial cells, but also on the surface of hematopoietic and immune cells, including macrophages, neutrophils, monocytes, mast cells, natural killer cells, lymphocytes, and platelets. PECAM-1 gene polymorphisms and elevated soluble PECAM-1 levels are associated with severe coronary artery disease. PECAM-1 has important signaling properties: acute onset of laminar flow stimulates PECAM-1 phosphorylation of intracellular domain, which may promote activation of PECAM-1 in atherosclerosis-prone regions of the aortic wall. PECAM-1 is a mechanosensitive molecule and is a member of a shear stress responsive complex in association with vascular endothelial cadherin (VE-cadherin) and vascular endothelial growth factor receptor 2 (VEGF-R2) [71].

Integrins are a family of 24 cell-surface receptors composed of 18α and 8β subunits that form αβ heterodimers. Integrins are able to mediate the cell-cell, cell-extracellular matrix, and cell-pathogen contact. Integrins can also regulate leukocyte homing, organize the immunologic synapse; participate in costimulation, migration, and phagocytosis. Integrins rapidly change the conformation of their extracellular domain structure and are able to cluster in response to activation; in parallel, ligation of integrins leads to a signal cascade from the extracellular domain to the cytoplasm. The main integrins that participate in the regulation of leukocyte trafficking are β2 and α4 integrins. All leukocytes constitutively express LFA-1, a member of the β2 subfamily of integrins. LFA-1 binds endothelial molecules that belong to the immunoglobulin superfamily, intercellular cell adhesion molecule-1, and -2 (ICAMs). α4β1 (VLA-4) integrin is a member of α4 subfamily and mostly expressed on monocytes and on lymphocytes with extralymphoid homing potential and it binds to another member of the

immunoglobulin superfamily, VCAM-1, and to the CS-1 peptide of fibronectin [71].

HDL can down-regulate the CAM expressioninduced by pro-inflammatory stimuli in endothelial cells [72, 73], but the mechanisminvolved in HDL-mediated inhibition of CAM expression has not been fully elucidated.Early studies proposed the inhibition of sphingosine kinase activity and of the nucleartranslocation of NF-kB by HDL [74]; but more recent studies described a role for SR-BI and S1P1 receptor inthe HDL-mediated inhibition of CAM expression [75, 76]. HDLcomposition affects HDL anti-inflammatory activity.The protein componenthas little influence on HDL anti-inflammatory activity [77, 78], on the contrary the phospholipid composition of HDL, in particular thelength and the degree of unsaturation of fatty acid residues, affects this activity [79]. In humans, according to*in vitro* data, plasma HDL-C levels are inversely correlated with plasmalevels of soluble CAMs [80]. Subjects with low HDL-C levels also displayan increased sensitivity toward inflammatory stimuli as reflected by enhancedinflammatory response on endotoxin challenge [81]. It is interestingly observed that after the consumption of ameal enriched in saturated fat HDL capacity to inhibit CAM expression inendothelial cells was reduced, while an opposite effect was observed after a meal enriched inpolyunsaturated fat [82].Endothelial cell proliferation and migration are crucial processes to bothneovascularization and replacement of damaged or senescent endothelial cells.Endothelial repair can occur by migration and proliferation of neighboring endothelialcells and through the recruitment of circulating endothelial progenitor cells (EPCs), whichcan differentiate into endothelial cells and facilitate vascular repair and neovascularization[49, 83]. HDL can promote endothelial cell migration and proliferation with mechanisms not been clearly defined [49]. HDL also reduce the loss ofendothelial cells through inhibition of cell apoptosis. Lysosphingolipids associated to HDL areinvolved when the apoptotic process is triggered by growth factor deprivation [84],whereas apoA-I is involved in the HDL-mediated reduction of cell death induced by cytokines [85]. Finally, HDL can modify EPC differentiation and function, thus enhancing progenitor -mediatedendothelial repair [86, 87]; but this direct

effect of HDL on EPC has been recentlydiscussed, and is likely dependent on HDL concentration [88].

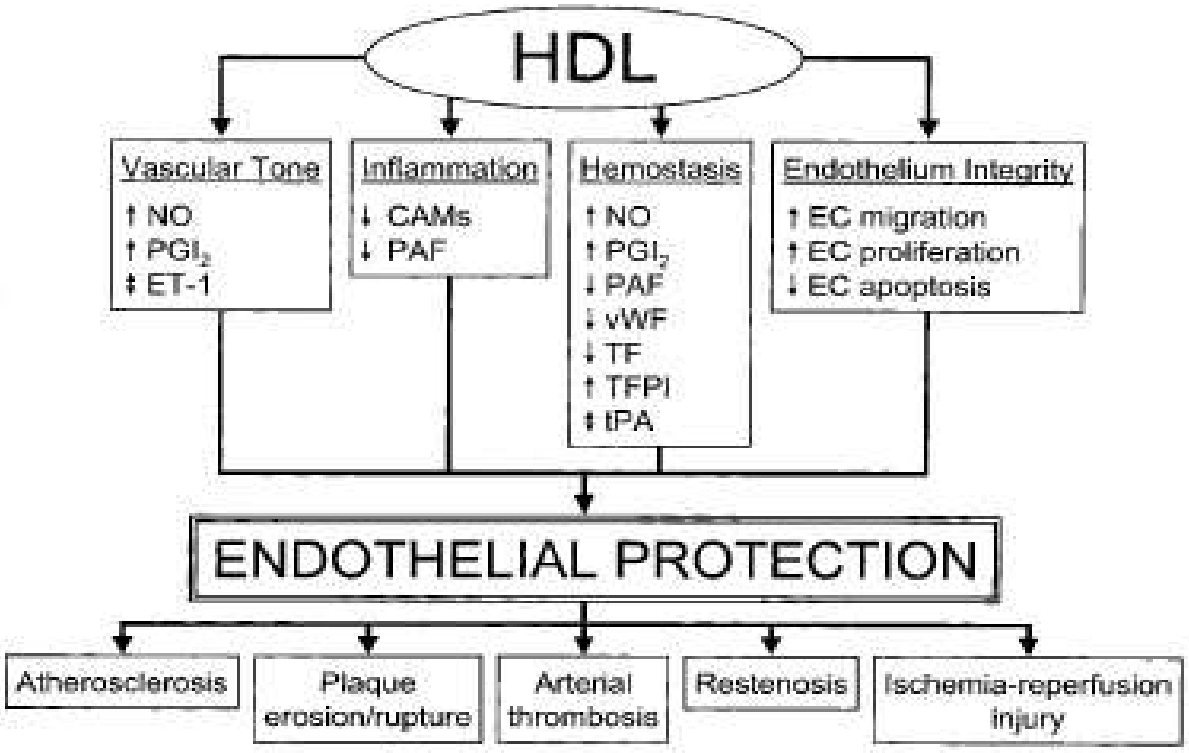

Table 3Schematic depicting potential basis for HDL-mediated endothelial protection in a variety of clinical conditions characterized by endothelial dysfunction [50]

2 LCAT

Inherited HDL disorders represent a heterogeneous group of rare monogenic diseases and include familial hypo- and hyper-alphalipoproteinemias. Familial hypoalphalipoproteinemia is characterized by a plasma HDL cholesterol (HDL-C) level below the 5th percentile for the general population. Known causes of familial hypoalphalipoproteinemia are mutations in the APOA1, ABCA1 and LCAT genes. Familial hyperalphalipoproteinemia is characterized by a plasma HDL-C above the 95th percentile for the general population. The best known monogenic cause of familial hyperalphalipoproteinemia is a mutation in the CETP gene abolishing CETP activity. Other candidate genes include LIPC, LIPG, and SCARBI [89].

HDL inherited disorders also represent a unique tool to evaluatehow specific HDL subpopulations are involved in the atheroprotective activity mediated by HDL. Due to loss of one of RCT key steps, genetic LCAT deficiency permits to evaluate a specific HDL subpopulation and to assess the relevance of LCAT enzyme in atherosclerosis.Carriers of two mutant LCAT alleles have remarkably low plasma HDL-C, apoA-I, and apoA-II levels, associated with multiple alterations in HDL structure and particle distribution, with a selective depletion of large particles and predominance of small preb-HDL [90, 91].

Furthermore the cause of glomerulosclerosis, that is the major cause of morbidity and mortality in FLD patients is not understoodand it is necessary to be investigated.

2.1 THE LCAT BIOCHEMISTY AND REACTION

A single copy of the human LCAT gene (~4.5 kb) is localized on chromosome 16 (region 16q22); it contains six exons with ~1.5 kb of coding sequence [92]. The mRNA for LCAT is found almost exclusively in the liver, with smaller amounts in the brain and testes. The synthesized protein is secreted into the plasma compartment. The mature LCAT is a glycoprotein of 416 residues, with a molecular mass of approximately 67

kDa, which is more than 20% greater than the predicted protein mass. The extra mass is due to both N-linked and O-linked glycosylation [92]. The 3D structure of LCAT is not known, but a partial structural model for LCAT has been built, based on its homology with lipases [92]. The model proposes that LCAT belongs to the α/β-hydrolase fold family. The central domain consists of a mixed seven-stranded β-sheets with four α-helices, and loops linking the β-strands. The catalytic triad, identified by site-directed mutagenesis, includes residues Ser181, Asp345, and His377 [92].

The plasma concentration of LCAT (about 5 mg/L) correlates with plasma enzyme activity, as assessed with endogenous lipoproteins (cholesterol esterification rate) or a standardized exogenous substrate (LCAT activity) [92]. The plasma LCAT level varies little in adult humans with gender, age, alimentary habits, and smoking. In blood, LCAT preferentially binds to HDL; a minority of plasma LCAT circulates bound to apoB-containing lipoproteins [92].

Three catalytic activities have been demonstrated for the LCAT enzyme: acyltransferase activity, phospholipase A2 and lysolecithin acil transferase(LAT) activity.The most important are acyltransferase and phospholipase activity. First, it cleaves the fatty acid in sn-2 position of lecithin and transfersit onto Ser181; then, the fatty acid is transesterified to the free3-β hydroxyl group of cholesterol, generating cholesteryl ester (CE)[21].

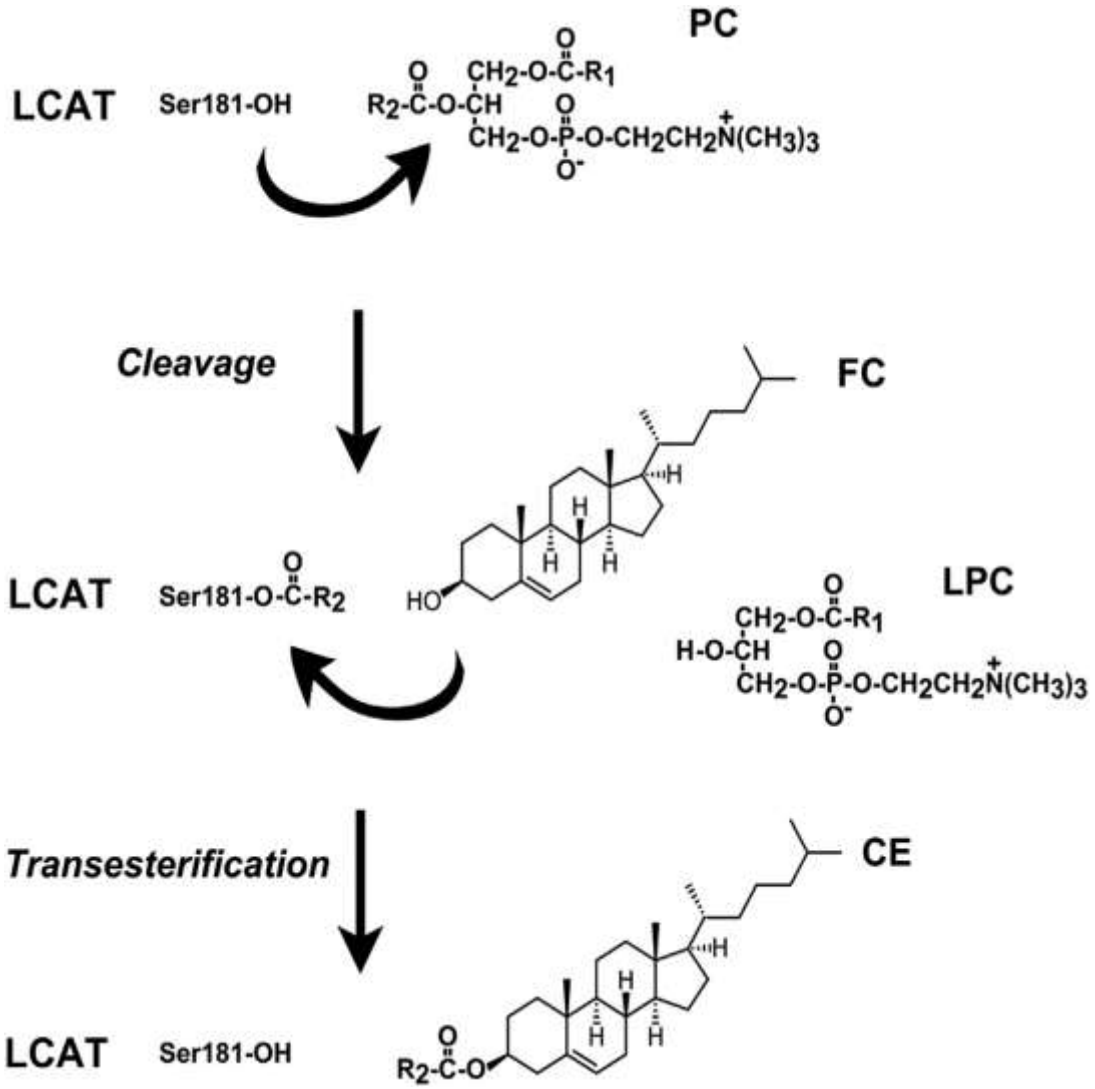

Fig. 4.Diagram of LCAT Reaction. Step 1: Cleavage—Phospholipase cleavage of fatty acid from sn2 position of phosphatidylcholine (PC) with formation of lysophosphatidilcholine (LPC). Step 2: Transesterification— Transfer of fatty acid bound to Ser181 of LCAT to the hydroxyl group of cholesterol or other sterol acceptor[93].

By this way, the LCAT reaction accounts for the synthesis ofmost of the plasma CE. The lipid substrates for LCAT reside preferentiallyin small, discoidal and pre-β-migrating HDL [92]; within these particles LCAT is activated by apoA-I and esterifies cholesterol via α-LCAT activity. LCAT has also been found on LDL particles but is not as active as on HDLand esterifies cholesterol within apoB-containing lipoproteins, via β-LCAT activity with apoE as cofactor [92]. The affinity of human LCAT (purified

from human plasma) for LDL is 2.3 to 4-fold lower than for HDL, with apparent Km's (in nmol CE/hrM) of 0.98 (LDL), 0.19 (HDL2), 2.4 (HDL3) and 14 (rHDL) (all x 10 -4) and relative reactivities (app Vmax/app Km) compared to rHDL of 6.5% for LDL, 1.3% for HDL2, 16% for HDL3, and 100% is rHDL [94]. Nonetheless, human LCAT does esterify cholesterol on LDL, and mutations that abolish α-LCAT activity (activity on HDL) but retain some LCAT activity on apoB-Lipoproteins (β-LCAT activity) produce a less severe phenotype than LCAT mutations that have lost activity on both HDL and LDL. In fact, a school of thought holds that the difference between FLD and FED is that FED patients have LCAT mutations that lack α-LCAT activity but still retain some β-LCAT activity. Despite the ability of LCAT to esterify cholesterol on apoB-Lipoproteins, a substantial portion of CE in human LDL arises from HDL CE's (made by LCAT) that are transferred to LDL via CETP. Either way, LCAT is the primary source of cholesteryl esters on apoB-containing lipoproteins [92]. The remainder of cholesteryl esters present on lipoproteins are derived from the liver and intestine when VLDL and chylomicrons are secreted and are produced by one of the two the intracellular enzymes for Acyl-CoA:Cholesterol Acyltransferase (ACAT) [95].

The third activity of LCAT, the LAT activity, consists in conversion of lysophosphatidylcoline to phosphatidylcholine and requires LDL particles. Part of the lysolecitihin produced by LCAT reaction may be reacylated in the plasma itself presumably on the LDL surface; this reaction is indeed stimulated by LDL and does not require apoA-I as cofactor [96].

Among exchangeable apolipoproteins, apoA-I is the most efficient activator of LCAT and many apolipoprotein coding sequence mutations are associated with poor enzyme activation. Three arginine residues in apoA-I (R149, R153, and R160) have been suggested to be involved in LCAT binding, with multiple hydrogen bonds between the arginine guanidinium group and lipid polar groups and phosphatidylcholine ester bond may be suggested to become exposed to active center [97]. ApoA-I may alternatively influence LCAT activity by activating phosphatidylcholine; ApoA-I influences both dynamics and conformation of substrate molecule in the boundary layer of phosphatidylcholine molecules

adjacent to apolipoprotein molecule at the disc periphery. Data at high cholesterol content do not indicate a saturation phenomenon, thus giving no evidence for a binding of cholesterol to the enzyme [98].In addition to LCAT activation by apoA-I, LCAT is less effectively activated also by apoE. apoA-IV and apoC-I. apoE has been reported as the LCAT activor on apoB-Lps, which do not have apoA-I but it is possible apoC-I and possibly apoA-IV may play a similar role [96]. The requirements for LCAT activation by apolipoproteins and peptides are lipid binding and amphipathic a-helical structures with a nonpolar face of approximately 100 degrees, a central region of acidic residues opposite to the nonpolar face, and, possibly, a distribution of basic residues at the polar-nonpolar interface. ApoA-I residues between 143 and 187 are required for LCAT activation. If these residues are altered by site-directed mutagenesis apoA-I can no longer activate LCAT [21]. Importantly, LCAT is also produced in the brain by primary astrocytes, and esterifies free cholesterol on nascent APOE-containing lipoproteins secreted from glia and influences cerebral spinal fluid (CSF) APOE- and APOA1 levels. Together with APOE and the cholesterol transporter ABCA1, plays a key role in the maturation of glial-derived, nascent lipoproteins [99]. So although apoE may be not as effective an activator as apoA-I, apoE activation is very important in brain lipoprotein metabolism.

Inhibitors of LCAT include sphingomyelin, hydroperoxides of PC, PC with trans-fatty acids and chains of 18 carbons, and apoA-II.Sphingomyelin is a strong inhibitor of LCAT activity. Its action is mediated by several mechanisms, including a decreased interfacial binding, structural effects on apoA-I that may alter apoA-I conformation and charge, and principally by a competition with phosphatidylcholine, the acyl donor in the reaction, that lead to non-productive binding of sphingomyelin to the active site of LCAT [100,101].Hydroperoxides of phosphatidylcholine generated during mild oxidation of lipoprotein lipids inhibit LCAT with apparent competitive kinetics. Oxidation caused a reduction in plasma phosphatidylcholine (PC), an increase in a short-chain polar PC (SCP-PC), and an inhibition of the transfer of long-chain acyl groups to cholesterol (LCAT activity) or to lyso PC (LAT activity). While oxidation of plasma causes a loss of LCAT's

ability to transfer long-chain acyl groups, its ability to transfer short-chain acyl groups, from SCP-PC is retained, and even stimulated, suggesting that LCAT may have a physiological role in the metabolism of oxidized PC in plasma[102]. Trans-fatty acids and chains of 18 carbons also inhibit LCAT. The trans unsaturated fatty acids (TUFA) decrease high density lipoprotein through their inhibition of LCAT activity, and also alter LCAT's positional specificity, inducing the formation of more saturated cholesteryl esters, which are more atherogenic. LCAT exhibited significantly lower activity with PCs containing 18:1t or 18:2t; the inhibition depended on the position occupied by TUFA in the PC, as well as on the paired fatty acid. Thus, for human LCAT, 18:1t was more inhibitory when present at sn-2 position of PC, than at sn-1, when paired with 16:0. In contrast, when paired with 20:4, 18:1t was more inhibitory at sn-1 position of PC. Human LCAT, which is normally specific for the sn-2 acyl group of PC, exhibited an alteration in its positional specificity when 16:0–18:1t PC or 16:1t–20:4 PC was used as substrate, deriving 26–86% of the total acyl groups for cholesterol esterification from the sn-1 position [103].

ApoA-II does not activate LCAT and may in fact prevent activation of LCAT by apoA-I. The mechanisms involved are probably due to masking of sites on apoA-I by apoA-II. Alternatively, apoA-I and apoA-II may compete for binding sites on the phosphatidylcholine -cholesterol vesicles [104]. Moreover, the transfer of cholesterol from preβHDL to αHDL was shown by Castro et al. to be slower in human apoA-I/apoA-II than in apoA-I transgenic mice; correlating with a more efficient cholesterol efflux in the latter [105].Although apoA-II does not activate LCAT, the presence of LCAT does enhance fusion of lipidated apoA-I-only (LpA-I) and apoA-II-only (LpA-II) particles [106]. Kinetic studies show that apoA-II is secreted independently of apoA-I particles and the data indicate that LCAT esterification of LpA-I and LpA-II particles may enhance formation of LpA-I:A-II particles [106].

2.2 LCAT, HDL METABOLISM AND REVERSE CHOLESTEROL TRANSPORT

Discoidal pre-β-HDL are the preferred lipoprotein substrate for LCAT. These particles are generated through the interaction of lipid-free or lipid-poor apoA-I with the ABCA1 transporter located on the cell membrane, and resulting efflux of cholesterol and phospholipids [107]. The cholesterol esters generated by LCAT activity are more hydrophobic than cholesterol and they migrate into the hydrophobic core of the lipoprotein, with the resulting conversion of small, discoidal preβ-HDL into mature, spherical and α-migrating HDL (α-HDL), that represent most of the plasma HDL. α-HDL can be converted back to preβ-HDL through the CETP and of a variety of lipases activities. plasma half-life of preβ-HDL is short, they are rapidly cleared through the kidney, while mature α-HDL have a slower turnover [108]. LCAT thus plays a central role in intravascular HDL metabolism and in the determination of plasma HDL level.

Beside to its function in HDL metabolism, LCAT has also long been believed to play a crucial and critical role in macrophage RCT. It was initially proposed by Glomset that the LCAT reaction contributes to cell cholesterol efflux, the first and rate-limiting step in RCT, by maintaining the cholesterol gradient between the cell membrane and extracellular acceptors, thus facilitating cholesterol efflux by passive diffusion [109], or through the ATP-binding cassette transporter G1 (ABCG1) transporter [110]. Esterification of cholesterol in plasma by LCAT is also necessary for cholesterol uptake from the liver, either directly through the scavenger receptor SR-BI or indirectly through CETP, and theresulting elimination process.However, there are some evidences to doubt about thecritical role of LCAT in reverse cholesterol transport. Among these, the evidence that LCAT converts pre-β- HDL into α-HDL with the resulting deprivation of the best acceptors for cell cholesterol efflux via ABCA1 [111], that represents the major player in cholesterol removal from macrophages [112].

2.3 FAMILIAL LCAT DEFICIENCY AND FISH-EYE DISEASE: CLINICAL SIGNS AND SYMPTOMS

Genetic LCAT deficiency is a rare autosomal recessive disorder with anincidence of less than 1 in 200,000, although the frequency is likely to be higher because of misdiagnosis or underdiagnosis.LCAT deficiency was first described by Norum and Gjone in 1967 in a 33-year-old woman living in Norway, who presented with corneal opacities, anemia, proteinuria, mild hypoalbuminemia, and hyperlipidemia [113]. The renal function was normal, but a kidney biopsy revealed foam cells in the glomerular tufts. Plasma cholesterol, triglycerides and phospholipids were moderately increased, with most of cholesterol being unesterified; HDL could not be detected on agarose gel electrophoresis. Similar clinical and biochemical findings were later reported in the proband's two sisters [114]. All three siblings were shown to lack LCAT activity in plasma. About 60 isolated cases and 70 small nuclear families with partial or complete LCAT deficiency were subsequently described. At the best of knowledge, 86 different molecular defects, spread all along the LCAT gene, have been identified in subjects presenting with this rare genetic disorder [115]. Large number of LCAT gene mutations has been identified through the investigation of single cases, or small families in which a defect in the LCAT gene was predicted from the biochemical or clinical presentation. Homozygous carriers have a highly variable clinical phenotype; most subjects develop corneal opacities and hemolytic anemia; progressive and chronic renal insufficiency, often leading to end-stage renal disease, is also observed. Heterozygotes reportedly do not have a severe clinical phenotype, and LCAT deficiency seems to be transmitted as an autosomal recessive disorder. Subjects with loss-of-function mutations in both alleles can develop two different LCAT deficiency syndromes, familial LCAT deficiency (FLD) and fish-eye disease (FED). All of them are characterized by low plasma HDL cholesterol levels; but plasma LDL cholesterol and triglyceride levels are widely variable [116]. FLD cases have very little amount of esterified cholesterol in plasma and cholesterol accumulates in all plasma lipoprotein fractions is basically unesterified. FLD subjects

present clinical phenotype with corneal opacity and hemolytic anemia,and many of them unpredictably develop renal disease, since the second decade of life [117]. FED patients have subnormalplasma esterified to unesterified cholesterol ratio and a milder clinicalphenotype [116].

Mutations causing FLD can abolish LCAT production, or resultin the synthesis of an inactive LCAT enzyme which lacks both α-LCAT andβ-LCAT activity; mutations causing FED abolish αLCAT activity butβ-LCAT activity is retained [116]. The differential diagnosis of FLD andFED in carriers of two mutant LCAT alleles requires measurementof the ability of plasma to esterify cholesterol incorporated intoendogenous lipoproteins (α-LCAT plus β-LCAT activity) and intoa synthetic HDL substrate (α-LCAT activity) [118]. It is not possible classify carriers ofone mutant LCAT allele as FLD or FED basedon biochemical or clinical criteria [116].Differential diagnosissuch as transient expression of LCAT mutants in cultured cells, andmeasurement of LCAT concentration and activities (α-LCAT and β-LCAT activity) in cell media [119] are utilized to classify heterozygous subjects.

2.3.1 LIPOPROTEIN, OCULAR AND HEMATOLOGICAL FINDINGS

LCAT deficiency leads to dramatic changes in laboratory analysis in FLD patients: plasma analysis are characterize by an increased percentage of unesterified cholesterol (> 75%) and the absence of significantlevels of HDL-C (< 10 mg/dL, < 0.26 mmol/L).ApoA-I levels are also typically reduced (< 30 mg/dL) Triglyceride levels are also variable and can range fromnormal to markedly elevated, depending on the degree of proteinuria andrenal dysfunction. Unfortunately, there is no routine clinical laboratorymethod for detecting LpX, but depending on the gel system, it can sometimesbe observed by lipoprotein electrophoresis and is thought to formprimarily in FLD and not FED patients.

The analysis of HDL by bidimensional electrophoresis,that separate HDL for surface charge and size, in LCAT deficient subjects showed a drastic redistribution of apoA-I-containing-HDL. Heterozygotes had one extra particle in the preβ-1 region (preβ-1×); however, all of their other apoA-I-containing HDL subpopulations were comparable to controls in

electrophoretic mobility and size. ApoA-I distribution in heterozygotes was shifted toward the smaller HDL particles: there was a 2-fold increase in preβ-1 level, a 23% increase in α-4, and a 45% increase in preα-4 levels compared with controls. There were significant decreases in the concentrations of all the other HDL particles, whereas the mean concentration of α-3, an intermediate-sized particle, was similar to that of controls. In homozygotes, the majority of apoA-I was detected in small, lipid-poor, disc-shaped HDL particles (preβ-1 and α-4). Despite the low plasma concentrations of apoA-I in homozygous subjects, the apoA-I concentrations of these particles were comparable to those of controls [120].

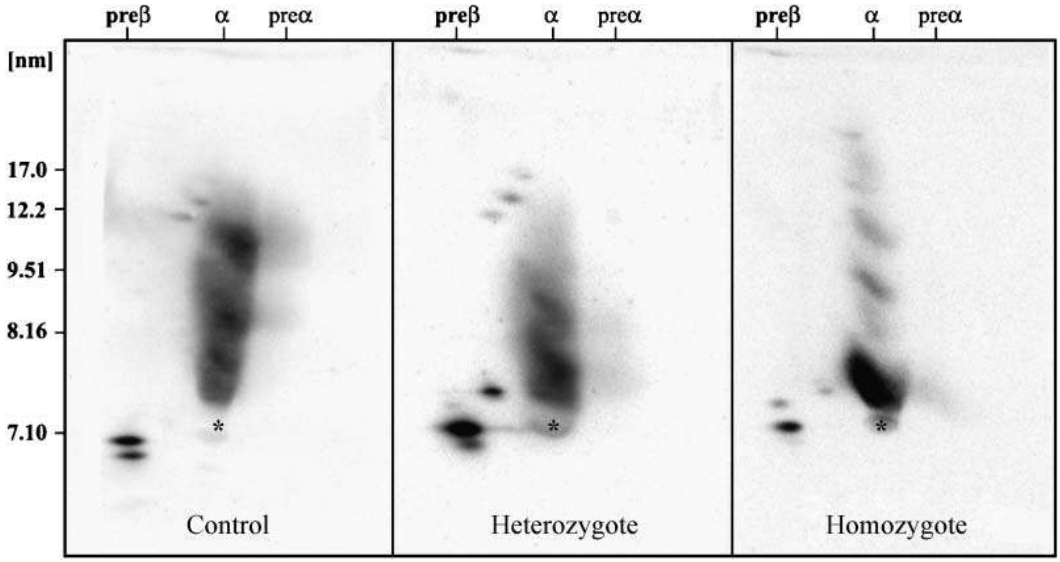

Fig.5Apolipoprotein A-I (apoA-I)-containing HDL subpopulations of representative control, heterozygous, and homozygous LCAT-deficient subjects separated by two-dimensional, nondenaturing agarose- PAGE. The asterisk represents the endogenous human serum albumin marking the a-mobility front [120].

Corneal opacity is the most constant and impressive characteristic in FLD and FED patients. Corneal opacity appears since childhood and progress over years.Despite the cloudy appearance of the cornea, most FLD and FED patients retain relatively normal vision under good lighting conditions. Ophthalmological examination of these patients typically shows diffuse haziness of the corneal stroma, with more pronounced opacity near the

limbus, often arranged in diffuse, grayish, circular bands [116,121]. At first analysis it could be identified as general corneal dystrophy and similar medical case has been reported in other ipoalfalipoproteinemia such as Tangier disease.The diffuse haziness of the corneal stroma is constitute by 5-200 nm vacuoles, enhanced by histochemistry and electron microscopy, the membranous deposits in the vacuoles of FLD and FED patients probably mostly contain unesterified cholesterol and phospholipids, which suggests that LCAT either directly or because of its effect on increasing HDL levels normally leads to the removal of unesterified cholesterol and phospholipids from the cornea, but this process is inadequate in FLD and FED patients [116, 121].

Fig. 6Typical corneal opacity in LCAT deficiency patients [146].

Most FLD patients have a mild chronic normochromic anemia associated with increased reticulocyte.Hematological results showed the changes were mainly in erythrocytes with mean corpuscular volume increased by 7%. Moreover, the erythrocytes were heterogeneous in shape and about 20% of the cells were represented by Target cells or Knizocytes [122].
Erythrocytes presents in subjects with LCAT deficiency have an abnormal intramembranedistribution of lipids: total lipid amount of free cholesterol and phosphpolipids increased by 27% associated with the completely different phospholipid compositions (incrased phosphatidylcholine, and

decreased phosphatidylethanolamine); these changes areassociated with abnormal properties such as deformability, membrane fluidity [122].

Anemia, abnormal shape and the increased mean corpuscular volume of this patient'serythrocytes may be related tomembrane instability owing to the abnormal distribution of membrane lipids such as cholesterol, phosphatidylcholine andphosphatidylethanolamine [122].

Renal disease, that represents the main medical complication in FLD patients, will be discussed in a separate paragraph.

2.4 LCAT AND RENAL DISEASE

Glomerulosclerosis is the major cause of morbidity and mortality in FLD patients and may ultimately lead to renal failure. The cardinal feature is progressive glomerular scarring. Early in the disease course, glomerulosclerosis is both focal, involving a minority of glomeruli, and segmental, affecting a portion of the glomerular globe. With progression, more widespread and global glomerulosclerosis develops [123].

Proteinuria is the early sign of the disease and usually FLD patients during the third and fourth decade of life develop renal failure with symptomatic edema and hypertension. The rate of progression of renal disease is unpredictable, with some patients rapidly going from mild proteinuria to a rapid deterioration in their renal function even in their early 20s. In most patients the urine contains protein, erythrocytes and hyaline casts. Most urinary protein migrates in the position of albumin on electrophoresis. Indices of renal function such as serum creatinine and creatinine clearance usually remain normal in the first three decades of life. Deterioration of renal function may occur suddenly with progression of renal insufficiency and increase of proteinuria. The phenotypic expression of FLD is different and depends on diet, abnormal lipoproteins, and previous kidney disease [123, 124]

2.4.1 RENAL MANIFESTATION

Renal biopsy permit a quite accurate diagnosis: light microscopy enhances characteristic of focal segmental glomerular sclerosis with mesangial expansion, a mild increase in mesangial cellularity, and irregular thickening of the glomerular capillary walls [124]. By Oil Red O staining, gold standard to stain neutral lipid, is possible detect lipid deposits with resulting vacuolization of the glomerular basement membrane and a typical “foamy” appearance. Lipid analysis of isolated glomeruli shows that the amounts of unesterified cholesterol and phospholipids are markedly higher than normal [124].

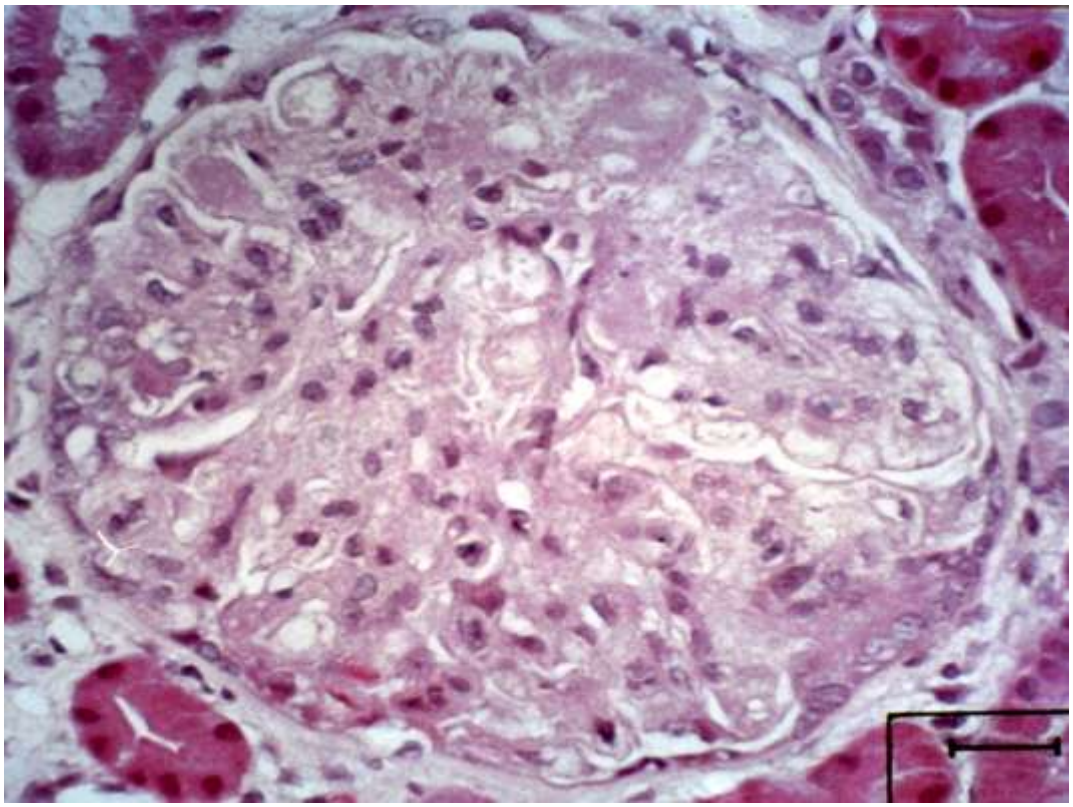

Fig.7 Renal biopsy from FLD patients analyzed by light microscopy: mesangial expansion; basement membrane with “foamy” appearance; foam cells in mesangium and in capillary walls[124].

Immunofluorescence microscopy reveals IgM deposit and bright granular staining for C3 is detected in the capillary loops, mesangium, and arteriolar walls [125,126]. This lipid deposit could activate complement protein and accelerate the injury.

Electron microscopy also highlights the presence of typical lipid electronlucent vacuoles and electron-dense lamellar structures in the mesangial matrix, glomerular and tubular basement membrane, and Bowman’s capsule [127]. Electrolucent expansion in subendothelium and in subephitelial area, intracitoplasmatic lipid droplet in mesangial and endothelial cells are also shown. The basement membrane has irregular thickening and fused endothelial foot processes. Capillary walls are abnormal, showing loss of endothelial cells, irregular thickening of the basement membrane, and fused endothelial foot processes. It often has the appearance of “moth-eaten holes” in the mesangial and basement membrane and can contain lamellar osmiophilic deposits.

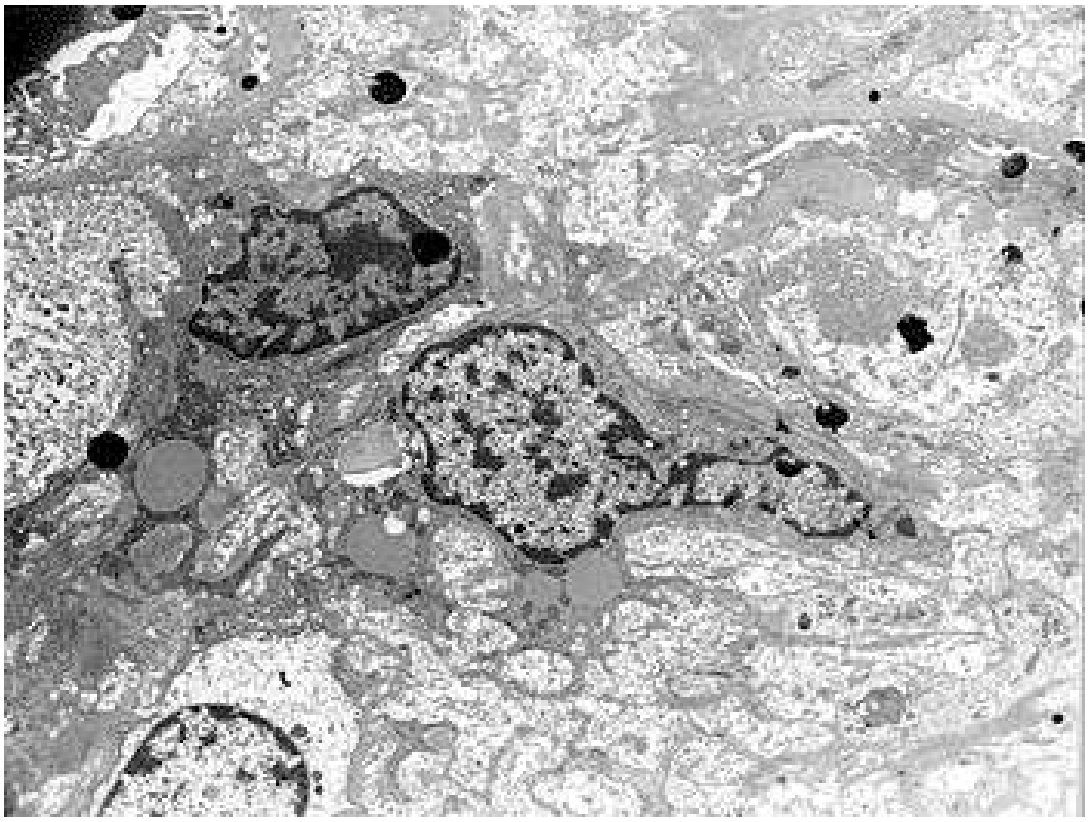

Fig. 8 Mesangial matrix expansion; mesangial cells nuclei are hypertrophic and irregular; lipid droplets in cytoplasmic region (electron microscopy, x 3000 magnification)[124].

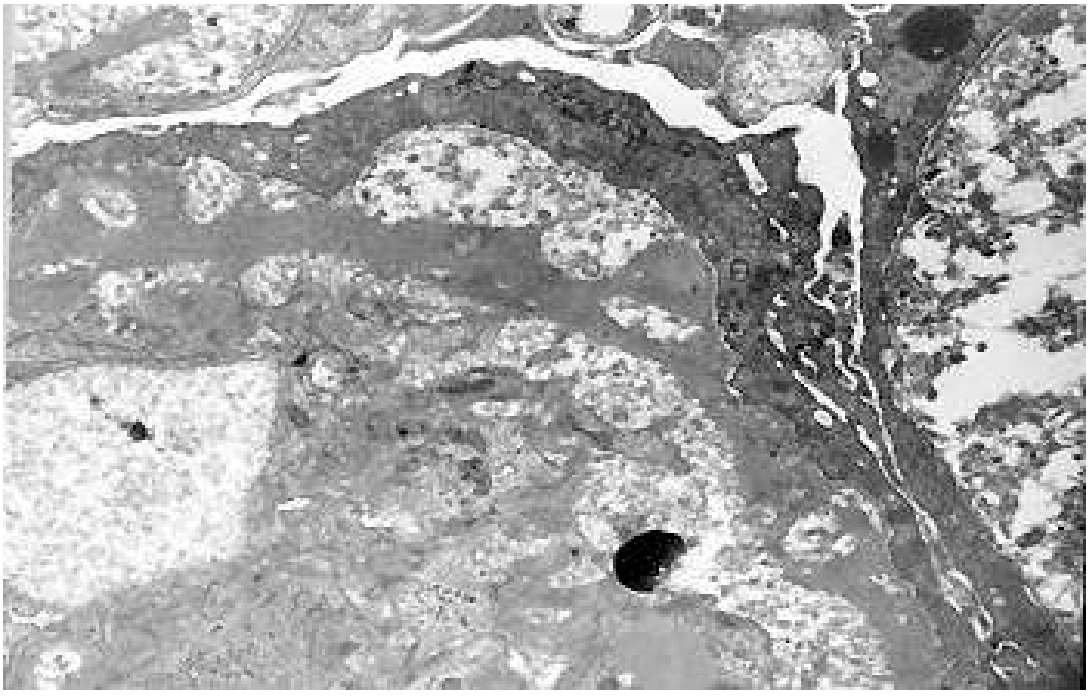

Fig. 9 Basal membranes expansion with irregular bubble aspect (electron microscopy, x 7000 magnification)[124].

Sessa et al. [128] observed that patients with FLD showed glomerular histological lesions and an immunofluorescent glomerular pattern typical of a dense-deposit disease called hypocomplementemic type II membranoproliferative glomerulonephritis.

Besides glomerulopathy, tubular pathology is also been descripted like diffuse tubular atrophy with thickening of the tubular basement membranes, along with focal interstitial fibrosis and mononuclear cells infiltrates [129].

The pathogenesis of the renal disease in FLD is not completely understood. The dramatic changes in lipoprotein profile could be related to renal disease, in particular it has been proposed that presence of LpX particles and/or possibly large molecular weight LDL (LM-LDL), which accumulates in plasma of FLD patients are involved in glomerulosclerosis development [126]. The absence of renal disease in FED is presumably prevented by the residual LCAT activity, and the lack of formation of a significant amount of LpX. LpX and LM-LDL appear to become trapped in capillary loops of the glomerulus and induce endothelial damage and vascular injury [126]. However, these abnormal lipoprotein particles are not always detected in FLD patients with renal disease [125].

2.4.2 BIOCHEMISTRY OF LIPOPROTEIN X (LPX)

Lipoprotein X is an abnormal particle present in the plasma of patients LCAT deficiency syndromes or cholestatic liver disease. LpX is principally composed by phospholipid and cholesterol, contains a high content of phosphatidylcholine (60%) and unesterified cholesterol (30%). LpX is associated with the LDL fraction isolated in a density gradient of 1.019-1.063 g/ml [130]. Under electron microscopy analysis LpX appears as a multilamellar vescicle with bi- or multi-layer of phospholipids. The size in variable with a diameter from 30 to 70 nm (10-13) Phosphatidylcholine is the major phospholipid in LpX and sphingomyelin constitutes the minor fraction. It also contains cholesteryl ester (2%), triglyceride (2%), and a small amount of protein (6%). The major proteins in LpX are albumin and C apolipoprotein (apoC-I, C-II and C-III) [130]. Albumin is trapped in the

center of the particle and the apoCs are present on the surface. Some apoA-I and apoE may also be associated with LpX particles [130].

The mechanism of formation of LpX is still poorly understood. It was initially believed to be an intestinal lipoprotein, normally catabolised by the liver, and accumulating as a result of liver dysfunction.

In familial LCAT deficiency LpX is likely derived from the surface of chylomicron remnants that are not further catabolized due to the lack of LCAT activity. An inverse relationship between plasma concentration of LpX and LCAT activity has been observed in patients with familial LCAT deficiency after blood transfusion, indicating that lack of LCAT activity is a prerequisite for LpX formation [131]. LpX-positive sera were identified by 1% agarose gel electrophoresis followed by staining with Sudan Black, but sometimes are hard to detect, especially in frozen samples. LpX did not migrate to the anode as opposed to the anodic migration of other plasma lipoproteins.

LpX may also appear in patients with cholestasis from various causes, most likely because of the regurgitation of bile salt micelles rich in phospholipid into the plasma compartment [130].

In patients with cholestasis appears dyslipidaemic features include hypertriglyceridaemia with persisting apoB48, increased plasma phospholipids, decreased LCAT activity, and hypercholesterolaemia. The hypercholesterolaemia is mainly due to unesterified cholesterol, which is principally transported in the form of LpX. Deficiencies of hepatic lipase, lipoprotein lipase and LCAT may also occur in cholestasis [132].

2.5 LCAT AND ITS ROLE IN ATHEROSCLEROSIS: HUMAN AND *IN VITRO* STUDIES

The role of LCAT in the pathogenesisof atherosclerosis is controversial.

In early cross-sectional studies in patients with angiographically proven CHD is reported either decreased[133,134] or increased [133] LCAT activity. Moreover, an enhanced cholesterol esterificationrate was strongly associated to the presence [135,136] and progression[137] of angiographically proven atherosclerotic lesions. Carotid intima-media thickness (cIMT) was measured as a surrogatemarker for human atherosclerosis [138] and increased LCAT activityand cIMT were reported in a relatively small number of patientswith the metabolic syndrome.In these patients a highly significant positivecorrelation between LCAT activity and cIMT was found [139]. Ina significant large number of subjects at high cardiovascular risk, no associationbetween LCAT concentration and cIMT was found in men,but raised LCAT concentration was associated with increasedcIMT in women [140]. Others two prospective studies examinedthe relationship between LCAT and prediction of cardiovascular events.In PREVEND [141] and EPIC-Norfolk studies [52] were shown that LCAT activity or concentration did not predict cardiovascular riskin men. In the latter, a high LCAT concentration was associated with a higher risk in women [142]. In these studies different measures of LCAT function and clinical end-points were employed, but is not possible to draw definiteconclusion.These studies suggest that enhanced LCAT activity or concentration may not be beneficial for human arteries, or even detrimental in women. However,in a small case-control study was shown that decreased LCAT activity in related with ischemic heart disease. Theoretically, carriers of LCAT gene mutations should have an increased CHD risk, due to low HDL cholesterol level in plasma. Analysis of all the cases reported till 1997 indicated that premature CHD is not a consistent finding among individuals with LCAT deficiency [143]. In particular, CHD was only sporadically reported in FLD cases, on the contrary one third of FED cases suffered from premature CHD [143]. Vascular structure in individuals with genetic LCAT deficiency was

investigated by cIMT measurement.In a first study, 9 carriers of LCAT gene mutations, 2 homozygotes and 7 heterozygotes, from large Canadian kindred with FLD have been followed for over 25 years, and none of these subjects showed any vascular events [144]. In this study, unaffected subjects were not included for comparison. The 2 homozygous subjects had a cIMT slightly greater than expected from age and gender, which did not progress over 4 years. In the heterozygotes were revealed cIMT greater than homozygotes and an average cIMT 0.24 mm greater than the expected reference value [144]. In the second study 47 heterozygotes from five Dutch FED families, two with premature CHD were involved [145]. Subjects with LCAT deficiencyshowed a modest increase in average cIMT compared to unaffected subjects (0.03 mm), which became statistically significant after adjustment for a variety of confounding factors [145]. Finally, cIMT has been recently investigated in 40 Italian LCAT deficient subjects (12 homozygotes or compound heterozygotes, and 28 heterozygotes) and compared with 80 matched control subjects [119]. Average cIMT was 0.07 mm smaller in the carriers of LCAT mutations than controls, and the inheritance of a mutated LCAT genotype had a remarkable gene-dose dependent effect in reducing cIMT. Results from the three cIMT studies in carriers of LCAT gene mutations suggest that LCAT deficiency does not remarkably increases preclinical atherosclerosis, and could even be protective for human arteries[92].The absence of cardiovascular events observed in FLD patients could be partially explained by in vitro study in which it was demonstrate that functional LCAT is not required for macrophage cholesterol efflux to human serum.In this study fasting blood was collected from forty-one carriers of LCAT gene mutations, including 14 carriers of two mutant LCAT alleles (8 FLD and 6 FED) and 27 heterozygotes. The authors demonstrates for the first time that serum from carriers of LCAT gene mutations has a greater capacity for cell cholesterol efflux through ABCA1 than serum from control subjects, due to the very high content of preβ-HDL. In contrast, serum from carriers of mutant LCAT alleles is less efficient than serum from control subjects in promoting ABCG1- and SR-BI-mediated cell cholesterol efflux. This is

probably due to the reduced concentrations of mature HDL. HDL particle distribution is drastically altered in LCAT deficient carriers and it is characterized by a reduced content of large HDL2 particles and by an accumulation of preβ-HDL, which in homozygous carriers represent the majority of plasma HDL [146]. The serum content of small preβ-HDL is correlated with ABCA1-mediated efflux in control serum, and the enrichment of HDL fraction or whole serum with preβ-HDL result in parallel increases in ABCA1-dependent cell cholesterol release. Therefore, the enhanced ABCA1-mediated cholesterol efflux observed in LCAT deficient serum is likely due to the increased serum content of preβ-HDL particles; on the contrary sera from carriers of LCAT gene mutations have an impaired capacity to efflux cholesterol via ABCG1 and SR-BI. This is possibly due both to the reduced content of large, phospholipid-rich HDL2 particles, and both to the reduced or absent LCAT activity, which contributes to maintain the cholesterol gradient that promotes efflux [147, 148]. The authors concluded that functional LCAT is not required for appropriate macrophage cholesterol depletion and RCT, since cell cholesterol can be taken up by discoidal preβ-HDL, which accumulate in plasma when LCAT function is compromised and then delivered to hepatocytes, possibly through an SR-BI-dependent pathway, for subsequent excretion in the bile [146].

2.6 LCAT IN ANIMAL MODELS: STUDIES ON ATHEROSCLEROSIS AND RENAL DISEASE

To better understand the LCAT role in HDL metabolism, in atherosclerosis and in renal disease several genetically modified animal models have been developed.

2.6.1 LCAT AND ATHEROSCLEROSIS IN HUMAN LCAT TRANSGENIC MOUSE MODELS

The effects of overexpression of human LCAT in mice were investigated since 1995 fromdifferent independent groups. Vaisman and colleagues generated transgenic mice containing the entire human LCAT gene, including 0.851 kb of the 5′ flanking region and 1.134 kb of the 3′ flanking region on a C57Bl/6 background [149]. This mice contained 15–120 copies of the transgene, LCAT mass of 11–109 μg/ml and α-LCAT activity of 607–3513 nmol/ml/h were reported. α-LCAT activity in control mice was only 32 nmol/ml/h. A second group generated transgenic mice expressing the human LCAT gene (FVB background), under control of either the natural or the mouse albumin enhancer and promoter. [150]. This mice also express human CETP. α-LCAT activity was 27.6 nmol/ml/h in the transgenic mice under control of the natural promoter and 33.7 nmol/ml/h under control of the mouse albumin enhancer and promoter, compared with 23.0 nmol/ml/h in wild-type mice. Coexpression of human apoAI or human apoAI and apoAII leads further increase in LCAT activity. Other investigators generated C57Bl/6 mice containing the full-length human LCAT gene, including 0.1932 kb of the 5′ flanking region and 0.908 kb of the 3′ flanking region [151]. About 30 copies of the transgene were integrated into one site. α-LCAT activity was increased from 106 nmol/ml/h in controls to 4,431 nmol/ml/h in the transgenic mice. In all three studies, human LCAToverexpression increased total cholesterol, basically related to an increase in the amount of cholesterol esters transported by HDL. The enhanced esterification of free cholesterol in HDL leads accumulation of abnormally large HDL particles that were rich in apoE in the circulation of these animals [152].

Vaisman LCAT transgenic mice fed for 16 weeks with atherogenic dietdeveloped from 1.8-fold to 3.5-fold larger atherosclerotic lesions correlated with the number of copies of the human transgene integrated [153]. In the Francone mice on the FVB background, a 2.5-fold non-significant increase in lesion size was observed [154]. However, in the presence of human apoAI a 3.4-fold increase in lesion size was observed. The Mehlum reported a 3.2-fold increase in lesion size in human LCAT transgenic miceafter 17 weeks of atherogenic diet feeding [153].

The results obtained from these studies suggest that LCAT overexpression did not protect against atherosclerosis.This is probably due to the accumulation of dysfunctional large apoeE-rich HDL in the plasma of transgenic mice, which were shown to be defective in the delivery of cholesterol to the liver through SR-BI pathway[153].

In humans, CETP represents an alternative pathway for delivery of HDL cholesterol esters to the liver through the transfer of cholesteryl ester to apoB-containing lipoproteins. However, in CETP/LCAT double transgenic animals, lesions were still 1.9-fold bigger compared with lesions in control and single CETP transgenic animals, suggesting that also in the presence of CETP, high expression levels of human LCAT is confirmedto be proatherogenic in mice[155].

2.6.2 LCAT AND ATHEROSCLEROSIS IN LCAT KNOCKOUT MOUSE MODELS

On other side, the effects of LCAT lacking in mice were investigated. Mouse model for human LCAT deficiency was generated by targeted disruption of the LCAT gene in mouse embryonic stem cells [153]. Sakai and colleagues generated an LCAT knockout (LCAT KO) mouse in which exons 2–5 of LCAT allele were disrupted [156], and another group generated a mouse lacking exon 1 [157]. In both cases, α-HDL activity was no detectable in the homozygous LCAT knockout mice, whereas activity in heterozygous mice was reduced to 30–55% respect control mice. In contrast with evidences in human FLD patients, there was no sign of corneal opacities or renal insufficiency in homozygous LCAT knockout mice at the age of 2–3 months. On chow diet, the plasma concentrations

of total cholesterol and HDL cholesterol of the LCAT knockout mice were reduced to approximately 24% and 30%, and 7% and 8.4% in the mice generated by Sakai and Ng, respectively. Also plasma apoA-I levels were reduced to 13% and 19%, respectively. α-HDLlevels and size were significantly reduced in the LCAT knockout mice, whereas preβ-HDL was increased. In LCAT knockout mice of Sakai et al. fed with atherogenic diet, HDL levels in plasma were not detectable. Beside HDL absence,an also remarkably lower plasma level of proatherogenic apoB-containing lipoproteins was observed. [153, 156]. In addition, some mice accumulated LpX and in these mice fed with atherogenic diet, proteinuria and glomerulosclerosis characterized by mesangial cell proliferation, sclerosis, lipid accumulation, and deposition of electron dense material throughout the glomeruli were observed [158]. However, no ocular abnormalities were found, even though corneal opacities are associated with FLD and FED in humans.

When LCAT KO mice were crossed with LDL receptor knockout mice, CETP transgenic mice, kept on high fat high cholesterol diet (HF/HC) diet, or with apoE knockout (apoE KO) mice on normal chow diet, LCAT deficiency appeared to be atheroprotective [158]. Similar results were also confirmed by Ng and colleagues in experiments on apoE knockout mice [157]. In all the cases described, LCAT deficiency was associated with significant reduction in the cholesterol content of pro-atherogenic apoB-containing lipoproteins. It wasalso reported that when LCAT-KO/apoE-KO mice were fedwitha high-fat diet without cholate, mice had an elevated level of apoB lipoproteins and increased incidence of atherosclerosis [159]. It was suggested that the anti-atherogenic effect of LCAT deficiency closely correlates with its ability to lower plasma levels of apoB lipoproteins, probably also through upregulation of the LDL receptor [158]

2.6.3 LCAT AND ATHEROSCLEROSIS IN RABBIT MODELS

Rabbitsexpress CETP and can develop spontaneous atherosclerosis. In 1996, transgenic New Zealand White rabbits were create by Hoeg and colleagues with a 6.2 kb genomic fragment consisting of the entire human LCAT gene, including 0.851 kb of the 5′ flanking region and 1.134 kb of

the 3′ flanking region [160]. The LCAT transgenic rabbits contained 38–1,436 copies of the human transgene with an LCAT mass of 1.9–54 μg/ml and α-LCAT activity of 219–3,217 nmol/ml/hα-LCAT activity detected on the control rabbits was 202 nmol/ml/h. Overexpression of human LCAT in the rabbit led to markedly increased of plasma concentrationof large HDL particles containing apoE and reduced the concentrations of the apoB-containing VLDL and LDL particles [160]. Overexpression of LCAT reduced also apoAI catabolism, indeed the fractional catabolic rate was decreased, whereas apoA-I pool size was increased. In theseanimalsthe total surface of aortic lesions in LCAT transgenic rabbits was 7-fold smaller than in control rabbits, after 17 weeks of an atherogenic diet. In rabbits, overexpression of human LCAT protects against atherosclerosis, probably due to the combined effect of the increase in HDL cholesterol and the lowering of proatherogenic apoB-containing lipoproteins [161].

2.6.4 LCAT AND RENAL DISEASE IN MOUSE MODELS

In 2001, Lambert et al., described renal disease associated with plasma Lpx appearance in a subset of LCAT knockout mice on high fat high cholesterol diet (HF/HC) [158]. The authors histologically described that lesions were characterized by significant reductions in the vascular space, expanded mesangial region with increased number of mesangial cells and mesangial sclerosis, and increased extracellular matrix with accumulation of lipid droplets and macrophages. Filipin and oil red-O staining demonstrated the accumulation of free cholesterol and polar lipids in the glomeruli. Ultrastructurally, the endothelial cytoplasm and the vascular spaces were smaller in LCAT knockout than in controls, and the mesangial regions contained an increased amount of extracellular matrix. The development of glomerulosclerosis in LCAT knockout mice only while on the HF/HC diet, when the plasma levels of apoB-containing lipoproteins were increased. Both large LDL and LpX were present in the plasma of LCAT knockout mice only on the HF/HC diet. Furthermore, renal lesions were only detected in the group of mice that accumulated LpX. These findings support the importance of large LDL and LpX in the development of renal disease in FLD [158]

In 2004, Zhu and colleagues generated a LCAT knockout mice crossed with sterol regulatory element binding protein (SREBP) 1a transgenic mice (S+) that selectively accumulate LpX in the circulation and this mouse model (S+lcat−/−) develops spontaneous chronic glomerulopathy. The light microscopic and ultrastructural features of the S+lcat−/− mouse kidneys are remarkably similar to those seen in familial human LCAT deficiency [162]. This mouse model and the nephropathy seen in human LCAT-deficiency both show light microscopic mesangial matrix expansion, glomerular hilar foam cell infiltrates, and lipid deposits in the glomeruli and tubulointerstitium. Ultrastructural features are also similar in both, showing lamellar osmiophilic deposits in the mesangium, in proximity to the glomerular basement membrane, and in the interstitium. The S+lcat−/− mice show evidence of mesangial injury, mesangial matrix expansion, and glomerulosclerosis progressing from 6 to 10 months of age. This is also similar to that seen in human LCAT-deficiency nephropathy, where the lesions chronically are associated with progressive mesangial and glomerular sclerosis [162]. This mouse model provided in*in vivo* evidence that LpX plays an important role in the spontaneous development of a glomerulopathy, very similar to that seen in human LCAT deficiency [162].

2.7 THERAPIES

Specific treatment for genetic LCAT deficiency is not currently available and patients are usually treatedsymptomatically. Patients are candidates for corneal and renal transplantation, but thedisease can reoccur in transplanted tissue. Probably due the rareness of the disease, therapeutic options for FLD are poorlydefined.

The therapy of LCAT deficiency nephropathy consists mainly to delay the evolution of chronic nephropathy on the basis of current available therapies such as changes in life style and diet, control hypertension, containment of the proteinuria, control of complications. When there is a nephrotic syndrome, its conservative management will further problems [124].

Recently, combined treatment withnicotinic acid and fenofibrate showed an amelioration of the lipid profile, a reduction of LpX and areduction of proteinuria in one FLD patient. The authors suggest that the LpX levels reductionis due to low levels of VLDL and chylomicrons after treatment, that represent the phospholipid pool for LpXformation [163]. Therapy with angiotensin II receptor blockers and lipid-lowering drugs showed in a case report study benefit in blood pressure, lipid abnormalities, proteinuria and also kidney function, probably delaying progression to renal failure [164].In some severe case kidney transplantation is necessary, but often, after renal transplantation the pathology quickly reappearswith lipid may be deposited soon after transplantation [165].

Early successfulstudies focused to correct the biochemical LCAT deficient phenotype through the infusion ofnormal plasma [166] give the basis for the development of enzyme replacement therapyas a therapeutic strategy for LCAT deficiency. Specific characteristic of LCAT enzyme such as its relatively longhalf-life and the fact that LCAT acts in the plasma compartment and does not need to bedelivered to a specific tissue or cellular compartment support the development of this enzyme replacement therapy. Indeed, a recombinant LCAT provedto rapidly restore the normal lipoprotein phenotype in LCAT deficient mice, and it ispresently under clinical development [167].

AIM

The lecithin:cholesterol acyltransferase (LCAT) is the unique enzyme in human plasma responsible for the synthesis of cholesterylesters and plays a critical role in high density lipoprotein (HDL) metabolism. GeneticLCAT deficiency is a rare metabolic disorder characterized by abnormal plasma lipoprotein profile characterized by low HDL level, mainly small discoidal pre-β particles, and by presence of LpX, an abnormal lipoprotein usually absent in normal plasma and detectable only in some pathological cases.

The impact of LCAT on human atherogenesis is controversial and studies with genetically modified animal models in which LCAT was lacked or overexpressed leaded to contrasting results; further investigations are still required to assess the LCAT role in atherosclerosis [92].

Furthermore, renal disease is the major cause of morbidity and mortality in LCAT deficiency patients but the cause of kidney failure is poorly understood. The rate of progression of renal disease in FLD patients is unpredictable, with some patients rapidly going from mild proteinuria to a rapid deterioration in their renal function even in their early 20s [124].

Aim of my project was to analyze the peculiar characteristic of abnormal lipoprotein accumulated in LCAT deficiency subjects and to evaluate LCAT role in atherosclerosis and renal disease.

In Prof. Franceschini's laboratory at the University of Milan I had access to large number of plasma samples from LCAT deficient patients. First aim of my project was to assess the role of LCAT in atherosclerosis by evaluation of ability to maintain endothelial cell homeostasis mediated by peculiar HDL subclass accumulate in LCAT deficient patients. In order to evaluate the capacity of HDL to prevent endothelial dysfunction, HDL were isolated from plasma of homozygous and heterozygous LCAT deficient subjects and from control subjects, and tested on endothelial cells (HUVEC) to prove their ability to promote nitric oxide production and to inhibit adhesion molecules expression.

The project was ended with addition of analysis of expression of genes involved in endothelial cell biology homeostasis in animal models that overexpress LCAT gene in Dr. Remaley's laboratory at National Institutes of Health (United States).

Second aim of my project was to analyze the role of abnormal lipoprotein accumulated in LCAT deficiency patients on renal disease.

Project was started in Prof. Franceschini's laboratory in which sera from LCAT deficient subjects were tested on renal tubular cells, and inflammation, apoptosis and oxidative stress were evaluated. In Dr. Remaley's laboratory in vivo and in vitro studies were performed in order to evaluate the role of LpX in renal cells and in glomerulosclerosis development in LCAT knockout mice. Proteinuria was evaluated in urine from mice after acute and chronic LpX exposure and kidneys from LCAT KO mice injected with LpX were evaluated by confocal microscopy and histological analysis. Expression analysis of genes involved in nephrotoxic pathway was also performed in order to evaluate which pathway is involved in kidney injury mediated by LpX.

In vitro studies were also performed on mesangial and podocyte cell cultures incubated with LpX to clarify which specific cell population is involved.

Materials and Methods

1. LCAT AND ATHEROSCLEROSIS

1.1 STUDIES ON SUBJECTS WITH GENETIC LCAT DEFICIENCY

Subjects

Seventy-seven carriers of LCAT gene mutations, including 15 carriers of two mutant LCAT alleles and 62 heterozygotes, and 32 family controls, all belonging to Italian LCAT deficient families, volunteered for the study. All subjects were fully informed of the modalities and end points of the study and signed an informed consent. Fasting blood was collected and plasma prepared by low speed centrifugation at 4 °C. Aliquots were immediately frozen and stored at −80 °C until assayed.

Measurement of cell adhesion molecules

Plasma levels of the soluble forms of intracellular adhesion molecule-1 (ICAM-1), vascular cell adhesion molecule-1 (VCAM-1) and E-Selectin were measured by commercial ELISA kits (R&D Systems).

These assays employ the quantitative sandwich enzyme immunoassay technique. A monoclonal antibody specific for sVCAM1 or sICAM-1 or sE-Selectin has been pre-coated onto a microplate. Standards, samples, controls are added and any sVCAM1 or sICAM-1 or sE-Selectin presents were bound by the immobilized antibody and the enzyme-linked monoclonal antibody specific for sVCAM1 or sICAM-1 or sE-Selectin.U nbound materials were washed away. HRP-conjugate antibody was added and binds to the captured analyte. Following a wash to remove any unbound substances and/or antibody-enzyme reagent, a substrate solution is added to the wells and blue color develops in proportion to the amount of protein bound. The color development is stopped turning the color in the wells to yellow and the intensity of the color is measured at 450 nm.

Assessment of flow-mediated vasodilation

Evaluations were performed at fasting, between 8.30 am and 10.30 am to exclude circadian variations, abstaining from physical activity and smoking since midnight. Ultrasonic scans were performed in a quiet temperature-controlled (22±2°C) room by using a B-mode ultrasound device (ESAOTE AU4) equipped with a 7.5–10.0 MHz linear array transducer, held throughout the scan at the same point of the

brachial artery (BA) of the non-dominant arm using a stereotactic device. The ultrasonic device was gated to the peak R-wave on ECG and images were collected during the end-diastolic phase of each cardiac cycle and recorded on S-VHS videotapes for off-line measurements.

Images of the BA were continuously recorded: (i) for 1 min at rest, (ii) during 5 min of low-flow obtained by inflating a pneumatic tourniquet placed in the forearm to a pressure 30–50 mmHg above the individual systolic blood pressure and (iii) for 3 min after cuff deflation (i.e. during the reactive hyperemic phase). In each patient, the BA diameter (BAD) was measured using dedicated software, which allows the automatic and continuous detection of the distance between the media–adventitia interfaces of the near and far wall of the vessel. BAD at rest was the average of the sixty BAD values obtained throughout the pre-ischemic phase. BAD max was the highest BAD value in the hyperemic phase. FMD was calculated as the percent change between BAD at rest and BAD max.

HDL purification

HDL was purified by sequential ultracentrifugation from the plasma of 6 homozygotes carrying 4 different LCAT mutations, 10 heterozygotes carrying 6 different LCAT mutations and 10 family controls. Plasma was isolated from 3 ml of blood from each subject. KBr salt was added to plasma to modify density at 1.080 g/ml and 1.080 g/ml plasma was stratified with a KBr solution at the same density and ultracentrifugated overnight. This passage permits first separation of HDL from all other lipoproteins that have density smaller than 1.080 g/ml. Then the 1.080 g/ml plasma was correct with KBr salt to 1.21 g/ml density and stratified with 1.21 g/ml KBr solution and ultracentrifugated. Thus, HDL were separate from other plasmatic protein with greater density and were dialyzed against sterilized saline immediately before use.

HDL protein concentration was determinated by Lowry colorimetric assay and the protein content was expressed as mg of protein/ml.

Shpingosine-1-phosphate evaluation

HDL content of shpingosine-1-phosphate (S1P) was measured by a commercial competitive ELISA assay (Echelon Biosciences) and expressed as pmol/mg of HDL protein. The S1P coated 96-well plate is blocked to reduce non-specific

binding. The S1P standard curve and samples are mixed with the anti-S1P antibody before adding to the plate. The anti-S1P antibody binds to the S1P coated plate or the S1P in the sample. Following an incubation and plate wash, streptavidin- horseradish peroxidase (HRP) is added to the plate and binds to all anti-S1P antibodies (labeled with biotin) bound to the plate. After an additional incubation and plate wash, Tetramethylbenzidine (TMB) substrate is added to the plate and the colorimetric reaction stopped by the addition of 1N sulfuric acid. The absorbance at 450 nm is measured and the concentration of S1P in the samples is determined by comparison to the standard curve.

1.2 STUDIES ON ENDOTHELIAL CELLS

Experiments were performed on primary cultures of human umbilical vein endothelial cells (HUVEC) purchased from Clonetics (Lonza), in M199 with 0.75% BSA, 1% FCS. HDL were used at the protein concentration of 1.0 mg/ml in all experiments and were sterilized with 0.22 μm filters before use.

Cells were growth with complete growth media (M199 with 10% serum, 1% L-Glutamine, 1% antibiotics, EGF 0.1 ng/ml + FGF 1 ng/ml + ECGF 2 ul/ml) in 12-well plates until 90% confluence and starved 18 hours before experiment in M199 with 0.75% BSA, 1% FCS.

<u>VCAM-1 expression</u>

To evaluate VCAM-1 expression, endothelial cells were incubated overnight with HDL, washed with PBS and then stimulated with TNF (10 ng/ml) for 8 hours. After 8 hours media was collected and cell were lysate with Lysis buffer containing 20 mM Tris, pH 6.8

1 mM EDTA, 4% SDS, 20% glycerol,1 mM NaOv, 1 mM NaF, 1 ug/ml leupeptin, 1 mM benzamidin, 10 ug/ml trypsin inhibitor (soybean), 0.5 mM DTT, 1 mM Pefabloc.

VCAM-1 concentration in conditioned medium was evaluated by a commercial matched antibody pairs ELISA kit (BioSource) and normalized by the protein concentration of the total cell lysate. This assay employs the quantitative sandwich enzyme immunoassay technique. Antibody specific for VCAM-1 has been pre-coated onto a microplate. Standards and samples are pipetted into the wells and any VCAM-1 present is bound by the immobilized antibody. After removing any

unbound substances, a biotin-conjugated antibody specific for VCAM-1 is added to the wells. After washing, avidin conjugated Horseradish Peroxidase (HRP) is added to the wells. Following a wash to remove any unbound avidin-enzyme reagent, a substrate solution is added to the wells and color develops in proportion to the amount of VCAM-1 bound in the initial step. The color development is stopped and the intensity of the color is measured.

eNOS expression

To evaluate eNOS expression, endothelial cells were incubated overnight with HDL (1.0 mg/ml), washed with PBS and lysated with Lysis buffer. Expression of eNOS was evaluated by SDS-PAGE and immunoblotting.

Total protein concentration was assayed by micro-BCA method (ThermoScientific) and 25 µg of total protein for each samples were loaded into 8% SDS-polyacrylamide gel. The ratio charge/mass is constant for the presence of the SDS, the separation takes place on the basis of the effects of molecular sieve due to the size of the meshes of the gel. The smaller proteins pass through more easily, while those of larger size are delayed by frictional forces. Electrophoresis is initially performed at 60V so that samples can attributed in stacking gel that, once entered into the Running gel the electrophoresis is raised to 80V. When the electrophoresis finished, the protein were transferred into a nitrocellulose membrane(Schleicher & Schuell) for 1 hour at 180 mA, in buffer containing 25 mM Tris, 192 mM glycin and 15% (v/v) methanol. Membranes were immediately saturated with a TBS-T buffer (0,018 M Tris, 0,25 M NaCl, pH 7.4, and 0,1% (v/v) Tween 20) containing 5% (w/v) nonfat milk, overnight at 4°C. Membranes were developed against total eNOS antibody (BD Biosciences) diluted 1:1000 and incubated overnight at 4°C, washed 50 minutes in T-TBS solution, incubated with a secondary antibody (Dako) conjugated with HRP for 1 hour at 37°C and washed again 50 minutes in T-TBS solution at room temperature. Bands were visualized by enhanced chemiluminescence (GE Healthcare Biosciences) and analyzed with a GS-690 Imaging Densitometer and Multi-Analyst software (Bio-Rad Laboratories).

The membranes were stripped with a buffer solution containing 0.2 M Glycin, pH 2.2, SDS 0.1% (w/v) SDS e 1% (v/v) Tween 20 and reprobed with an antibody against β-actin (Sigma-Aldrich Chemie) diluted 1:2000.

eNOS activation

To evaluate eNOS activation, endothelial cells were incubated 20 minutes with HDL (1.0 mg/ml), washed with PBS and lysated with Lysis buffer.eNOS activation by phosphorylation was evaluated by SDS-PAGE and immunoblotting. Membranes were developed against phosphorylated eNOS (Ser1177, Cell Signalling Technology) diluted 1:1000 overnight 4°C, stripped and reprobed with an antibody against total eNOS with method described previously.

Nitric Oxide production

Nitric oxide (NO) production was evaluated by fluorescence using diacetate 4,5-diaminofluorescein. Endothelial cells were incubated 30 minutes with HDL (1 mg/ml), washed with PBS and incubated 2 hours in dark conditions at room temperature with buffer containing diacetate 4,5-diaminofluorescein (DAF-2 DA, Sigma-Aldrich Chemie). DAF-2DA is a non-fluorescent cell permeable reagent that can measure free Nitric Oxide (NO) and nitric oxide synthase (NOS) activity in living cells under physiological conditions. Once inside the cell the diacetate groups on the DFA-2DA reagent are hydrolyzed by cytosolic esterases thus releasing FAD-2 and sequestering the reagent inside the cell. Production of nitric oxide converts the non-fluorescent dye, DAF-2, to its fluorescent triaole derivative, DAF-2T. Fluorescence intensity was detected (λ excitation= 485 nm, λ emission= 530 nm) with a Synergy Multi-Mode microplate reader equipped with the GEN5 software (BioTek). After detection, cells were lysated with lysis buffer and protein concentration was measured with micro-BCA assay. For each sample, fluorescence was normalized by the protein concentration of the total cell lysate.

1.3 STUDIES ON ANIMAL MODELS

Animal

hLCAT transgenic x hApoA1 transgenic mice, hLCAT transgenic mice, apoE KO mice and wild-type mice (background C57/black6) are involved in this study. Mice were fed to regular chow diet and were sacrificed at the age of 6.0 months-old. The protocol was approved by the National Heart, Lung and Blood Institute Animal Care and Use Committee (NIH, Bethesda, MD, United States).

Plasma Lipid analysis

Plasma levels of total cholesterol, free cholesterol, phospholipid and triglyceride were determined enzymatically by colorimetric assay kits from Sigma Diagnostics and Wako Chemicals.

Plasma lipoproteins were separated by Fast Protein Liquid Chromatography (FPLC) with size exclusion method that separate lipoproteins according to their size. Two Superose 6 columns in series (Akta FPLC; GE Healthcare) were utilized and 2 mM pH 7.4 Phosphate buffer containing 0.15 M NaCl, 0,03% EDTA and 0,02% NaN_3 was used as mobile phase.

The chromatographic bed is composed by the gel beads inside the column and 300 ul of plasma samples were introduced into the injector and carried into the column by the flowing solvent. Columns were equilibrated with buffer before loading sample. Once in the column, the sample mixture separates as a result of different components adhering to or diffusing into the gel. As the solvents is forced into the chromatographic bed by the flow rate, the sample separates into various zones of sample components and were detected by UV absorption at 280 nm.

FPLC is performed at 0.5 mL/min constant flow rate for 84 minutes at room temperature. Forty-two fractions of 0.5 ml each were collected in 96 wells-plate and total cholesterol content was measured in each fraction by Wako enzymatic assay.

Gene expression analysis: RNA isolation and Real Time PCR

Total RNA was extracted from kidneys by Trizol (Invitrogen, Carlsbad, CA) and a PureLink Mini Kit (Invitrogen). Kidneys were homogenized in Trizol by Precellys24 homogenizer and RNA was extracted and purified with a PureLink Mini Kit. RNA was quantified by nanodrop spectrophotometer at 260 nm. Absorbance at 230 and 280 nm was also measured to determine nucleic acid purity. The ratio of absorbance at 260 nm and 280 nm is used to assess the purity of RNA; a ratio greater than 2.0 is generally accepted as “pure” for RNA. A260:A230 ratio is used as a secondary measure of nucleic acid purity and should be greater than 1.7.

0.5 µg of RNA was retrotranscripted in cDNA by a High-capacity cDNA Reverse Transcription Kit (Applied Biosystem).

The gene expression was evaluated through Real Time PCR Arrays (Qiagen), with specific array that analyze the expression of genes involved in cell endothelial

biology. SYBR Green-optimized primers are included in 384-well plate and cDNA with SYBR Green qPCR Mastermix (Qiagen) formulation are addict to the plate. 384 different gene-specific products were amplified simultaneously under uniform cycling conditions. The cDNA templates were mixed with the appropriate ready-to-use PCR mastermix, equal volumes (10 µl) was loaded to each well of the same plate, and then run the real-time PCR cycling program consisted of an initial denaturation of the samples at 95°C for 10 minutes followed by 40 cycles, each cycle consisted of a denaturation step at 95°C for 15 seconds and an annealing step performed at 60°C for 1 minutes. After 40 repeats samples were heated at 95°C for 15 seconds, 60°C for other 15 seconds and the ending step of denaturation of 15 seconds at 95°C. The array monitors the expression of 84 genes related to a disease state or pathway, plus 5 housekeeping genes, also included some elements that permit to evaluate the quality of PCR as genomic DNA contamination detection, RNA sample quality and general PCR performance. Data analysis is based on the ΔΔCT method with normalization of the raw data to either housekeeping genes. Relative quantification is used to compare the gene expression levels between different groups of mice and results are expressed as fold-changes.

1.4 STATISTICAL ANALYSIS

Results are reported as mean ± SD, unless otherwise stated. Group differences were evaluated by one-way ANOVA or unpaired t-test in thehuman studies, and by unpaired t-test in animal studies.

Group differences with a P value <0.05 were considered statistically significant.

2.LCAT AND RENAL DISEASE

2.1 LPX SYNTHESIS AND CHARACTERIZATION

Synthetic LpX was produced by mixing 30% of unesterified cholesterol (Sigma) with 70% of phosphatidylcholine (AvantiLipids) in molar ratio and dried under nitrogen for 1 hour, suspended in sterile saline solution, vortexed and sonicated for 10 minutes.

To evaluate the correct formation of particles, LpX solution was loaded on agarose gel (Sebia gel) and run for 1 hour at 80 V in Barbital Buffer pH 7.4 (Sigma). At the end of electrophoresis gel was fixed in water solution containing acetic acid, methanol and ethanol for 10 minutes, dried and stained with Sudan Black solution (Sigma). Gel was alternatively washed in PBS 1X buffer and stained for one hour with Filipin solution and revealed by UV lamp.

LpX multilamellar structure and size were analyzed by transmission electron microscopy (TEM). 3 µL of the LpX preparation was deposited on carbon film-coated 400 mesh copper grids (Electron Microscopy Sciences) and negatively-stained with 5 droplets of 1% uranyl acetate solution, the excess of solution on the grid was blotted and the grid was dried before TEM observation.

All images were acquired on JEM 1200EX electron microscope (JEOL USA) equipped with an AMT XR-60 digital camera (Advanced Microscopy Techniques Corp). Images were acquired at magnifications from 25,000X to 50,000X.

2.2 STUDIES ON PODOCYTE AND MESANGIAL CELLS

Experiments were performed on mesangial mouse cells and human podocyte cells. Mesangial mouse cells were purchased from ATCC, grown with complete growth media (DMEM:F12 in ratio 3:1, 14 mM Hepes, 5% FBS) on an 8-well chamber slide at a density of 10,000 cells/well.

Human podocytes were kindly donated by Kopp's Laboratory and grown at 33°C in complete growth medium (RPMI 1640, 10% FBS, 1% ITS, 1% Penicillin/Streptomycin/Glutamine solution) and differentiated at 37°C for 15 days on an 8-well chamber slide at a density of 30,000 cells/well.

Cells were starved overnight in media without serum and incubated for 6 hours with 0.5 mg/ml with NBD-LpX. One hour before the end of experiment, red Lysotracker (Life Technologies) was added to the media at a final concentration of

50 nM. Cells were washed with PBS and to each well one drop of DAPI mounting solution (Life Technologies) was added.Images were acquired with a point scanning confocal microscope LSM 510-UV with three detection channels equipped with four lasers: 405 diode, multiline argon, 561 diode, and a 633 diode. Images were acquired and processed using ZEN 2009 (Zeiss) software.

2.3 STUDIES ON TUBULAR CELLS

Experiments were performed on immortalized human tubular cells (HK2 line) grown with complete growth media (DMEM:F12 in ratio 3:1, 10% FBS, 1% L-Glutamine, 1% antibiotics).

Cells were starved and incubated overnight with media containing 2% serum from carriers of LCAT deficiency or from controls and inflammatory parameters and apoptosis were evaluated.

Apoptosis analysis

Apoptosis were evaluated by Annexin V method; Annexin V is an anticoagulant protein that preferentially binds negatively charged phospholipids. In the early phase of apoptotic process, phospholipid asymmetry is disrupted and phosphatidylserine is exposed on the outer leaflet of the cytoplasmic membrane.

After incubation with serum, cells were washed twice with HEPES-buffered saline containing 2 5 mM $CaCl_2$ and 2.5 ug/ml of Annexin V (Biotium) was added for 30 minutes.

Annexin V related fluorescence was measured exciting cells at 495 nm and emission fluorescence was detected at 519 nm. Data were corrected with emission measured in non-treated cells.

Inflammatory parameters

Real Time PCR for inflammatory parameters was performed using SYBER green method (iTaq Universal SYBR Green Supermix -BioRad), primer pairs have been designed on different exons to avoid the amplification of DNA contaminations eventually present in cDNA preparations and the sequences are reported in table 1. Briefly, RNA was extracted from cells after incubation with sera according to Trizol (Invitrogen) method and 0.8 µg of RNA were retrotranscipted using iScript cDNA Synthesis Kit (BioRad). Real-Time PCR consisted of an initial denaturation

of the samples at 95°C for 3 min, followed by 40 cycles. Each cycle consisted of a denaturation step at 95°C for 10s, a 25-s annealing step at the 60°C. At the end, melting curve was evaluted from 60°C to 95°C.

Primers	Sequence
VCAM-1 up	CCACAGTAAGGCAGGCTGTAAAAG
VCAM-1 down	CGCTGGAACAGGTCATGGTCAC
MCP-1 up	CAGCCAGATGCAATCAATGCC
MCP-1 down	GGAATCCTGAACCCACTTCT
GAPDH up	CCCTTCATTGACCTCAACTACATG
GAPDH down	TGGGATTTCCATTGATGACAAGC

Table 1 Sequence of primers utilized in Real Time PCR assay.

Oxidative stress evaluation

For oxidative stress evaluation, HK2 cells were incubated 1 or 2 hours, respectively for ROS and NADPH oxidase evaluation, with medium containing 2% serum from LCAT deficient patients or from controls.`

To evaluate ROS production, cells were incubated 30 minutes with HEPES buffer containing 5 μM of carboxy-H2DCFDA (Molecular Probes, Invitrogen), a carboxyl derivative of fluorescein, before incubation with media containing sera. Reduced and acetylated forms of dichlorofluorescein are non-fluorescent until the acetate groups are removed by intracellular esterases and oxidation occurs within the cells. Oxidation of the probe can be detected by monitoring fluorescence at 517-527 nm.

Cells were lysated and total protein content was measured by microBCA assay (ThermoScientific).

To evaluate NADPH oxidase activity was utilized superoxide-induced lucigenin photoemissions based method.

After 2 hours incubation with 2% serum from carriers of LCAT mutations or controls, cells were lysated with 50mM Phosphate buffer pH 7.0 containing 1 ug/ml of leupeptin and 1 ug/ml of PMSF (phenylmethanesulfonylfluoride or phenylmethylsulfonyl fluoride).

Lysated cells were suspended in a final volume of 1 ml containing 50mM Phosphate buffer, pH 7.0, 1 mM EGTA, 150 mM sucrose, 0.5 mM lucigenin

(Sigma). Enzyme reactions were initiated with the addition of 0.1 mM NADPH (Sigma) and photoemissions, expressed in terms of relative light units (RLU), were measured every min for 5 min using a luminometer.

2.4*IN VIVO* STUDIES

Animal

Wild-type C57BL/6-homozygous LCAT knockout mice backcrossed to strain C57BL/6 for eight generations were involved in both the acute study and the chronic study. Ten-month-old females mice were fed with regular chow diet. Experimental protocol was approved by the National Heart, Lung and Blood Institute Animal Care and Use Committee (NIH, Bethesda, MD, United States).

In the acute study mice received one intravenous injection of dialyzed and sterilized 0.5 mg/ml cholesterol LpX, 0.5 mg/ml cholesterol LDL or an equal volume of sterile saline solution. Blood was collected at 15 minutes, 3, 6 and 24 hours after injection and urine was collected 24 hours after injection.

In the chronic study mice were intravenously injected 3 times per week for one month with LpX or saline solution. Urine was collected at the end of each week and mice were sacrificed 24 hours after the last injection.

Albumin and creatinine measurement in urine

Urine albumin is one of the key markers for chronic kidney disease, however to compensate for variations in urine concentration, the amount of albumin is compared with creatinine concentration. The gold standard to measure the excretion of albumin in urine is a 24-hours urine collection; however microalbumin to creatinine ratio (UACR) measurement in urine is a more convenient method to assess kidney dysfunction and may be less prone to errors due to improper collection methods and variations in 24-hours protein excretion compared with a random urine specimen. It represents a ratio between two measured substances. Both the urine albumin (µg /ml) and the urine creatinine (mg/ml) are measured values. Albumin content in urine was measured with commercial indirect competitive ELISA (Exocell) that recognizes albumin antigen in samples. Samples and rabbit anti-murine albumin antibody were added to plate with mouse albumin-coated wells. The antibody interacts and binds with albumin immobilized to the stationary phase or with that in the fluid phase. A subsequent reaction with anti-

rabbit IgG-HRP conjugate labels the probe with enzyme. After washing, only the antibody-conjugate that bound to the albumin of the stationary phase remains in the well, and it is detected using a chromogenic reaction. Color intensity is inversely proportional to the logarithm of albumin in the fluid phase.Creatinine content was determined by colorimetric assay (Exocell, PA) and is an adaptation of the alkaline picrate method [171]. It entails determination of the differential absorbance in a sample before and after the addition of acid to correct for color generation due to interfering substances [172].

Kidney collection and confocal and histological analysis

24 hours after the last injection mice were sacrificed and kidneys collected. Kidneys were collected in RNAlater (Invitrogen) for gene expression analysis or in 10% formalin buffer solution. For histological analysis kidneys were collected in OCT solution and frozen at -80°C. After sectioning, kidneys in OCT were sectioned with a RM 2050 Microtome (Leica) in 6-10 μm sections, mounted with DAPI solution and analyzed with a point scanning confocal microscope LSM 510-UV with three detection channels equipped with four lasers: 405 diode, multiline argon, 561 diode, and a 633 diode. Images were acquired and processed using ZEN 2009 (Zeiss) software.

Kidneys in 10% formalin buffer were embedded in paraffin, cut in 3-μm sections and stained with Masson-trichrome (WAKO). In Masson's trichrome staining, three dyes are employed to selective stain muscle, collagen fibers, fibrin, and erythrocytes. This stain permits evaluation of glomeruli fibrosis enhancing collagen deposits in glomeruli.

Gene expression analysis

mRNA was isolated from kidney with Trizol and PureLink Mini kit as previously described. Real Time analysis was performed by SYBER green based method with Qiagen Superarray that provides 384-wells plate including primers for 84 genes involved in nephrotoxic pathway. Data were analyzed with ΔΔCT method with normalization of the raw data to either housekeeping genes. Data from mice treated with LpX are expressed as fold-changes to control group.

2.5 STATISTICAL ANALYSIS

Results are reported as mean ± SEM, unless otherwise stated. Group differences in the acute study were evaluated by one-way ANOVA, with post hoc analysis by Tukeys test. Group differences in the chronic study were evaluated by unpaired t-test or by Mann-Whitney test for non-normal data distribution. Data from *in vitro* studies were analyzed by one-way ANOVA. Group differences with a P value <0.05 were considered statistically significant.

Results

1. LCAT AND ATHEROSCLEROSIS

1.1 Human studies

1.1.1 HDL ABILITY TO INHIBIT VCAM-1 EXPRESSION IN ENDOTHELIAL CELLS

The anti-inflammatory capacity of HDL was tested *in vitro* as their ability to inhibit TNFα-induced VCAM-1 expression in endothelial cells. On average, HDL isolated from controls were able to reduce TNFα-induced VCAM-1 expression by 44.4±4.1% (Figure 1). HDL from LCAT deficient subjects proved to be more effective than HDL from controls with a gene-dose dependent effect, since on average HDL from heterozygous carriers reduced VCAM-1 expression by 53.1±7.2% and HDL from homozygous subjects by 65.0±8.6% (Figure 1).

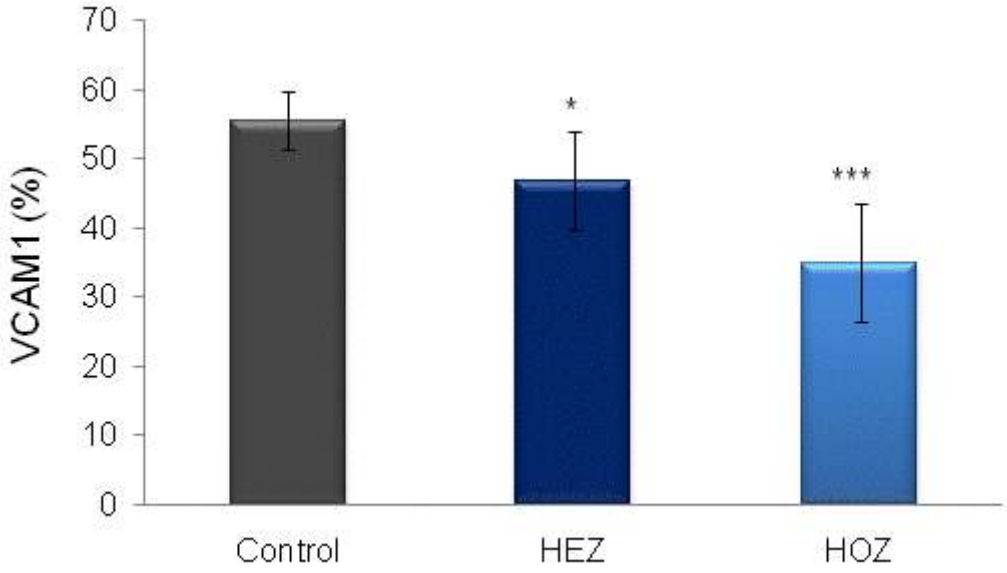

Figure 1.Inhibition of VCAM-1 expression by HDL. HDL from LCAT deficient subjects and controls were tested for their ability to reduce VCAM-1 expression induced by TNFα stimulation in endothelial cells. Data are expressed as percentage of inhibition of VCAM-1 expression in TNFα-stimulated cells, mean±SD. Control n=10 , heterozygous (HEZ) n=10, homozygous (HOZ) n=3. Data are statistically analyzed by ANOVA and P trend is 0.0003

1.1.2 PLASMA LEVELS OF SOLUBLE CAMS

Plasma levels of soluble VCAM-1, ICAM-1 and E-Selectin were assessed as biomarkers of systemic inflammation. No significant changes of soluble VCAM-1, ICAM-1 and E-Selectin plasma levels were detected when values of carriers of two, one or zero mutated alleles were tested for trend (Figure 2). Levels of sVCAM-1 showed a marked degree of variability in carriers of two mutated LCAT alleles and were indeed significantly higher than those of carriers of one mutated allele (*P*=0.017) and controls (*P*=0.046); this is likely due to the presence of renal disease in 9 out of 15 carriers of two mutated alleles (943.5±395.7 ng/ml in carriers with renal disease vs 761.1±394.5 ng/ml in disease-free carriers). On the contrary, independently from the presence/absence of renal disease, carriers of two mutated LCAT alleles did not show a significant increase of sICAM-1 levels, while plasma levels of sE-Selectin were even lower than those of carriers of one mutated allele (*P*=0.026).

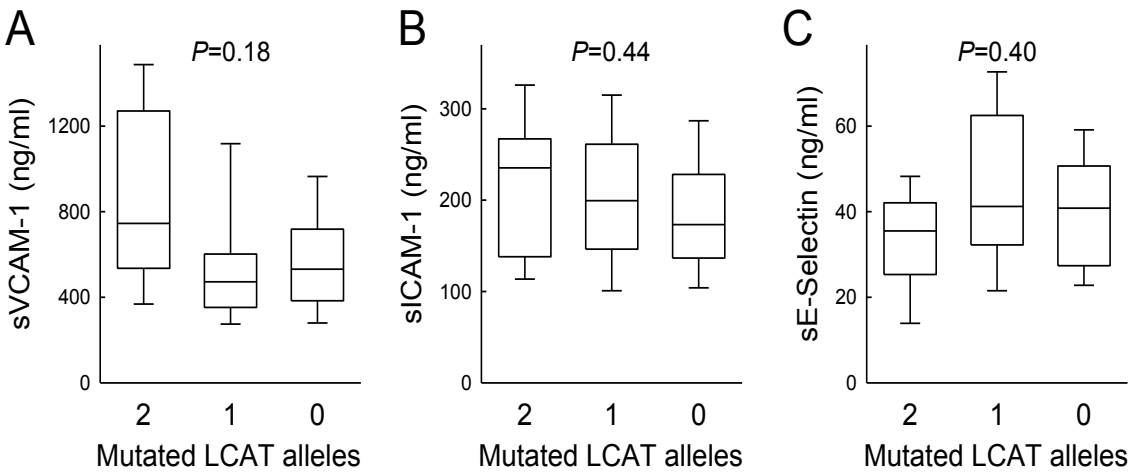

Figure 2. Plasma levels of soluble adhesion molecules

Levels of soluble VCAM-1 (Panel A), ICAM-1 (Panel B) and E-Selectin (Panel C) were measured by ELISA in the plasma of carriers of two or one mutated LCAT alleles and controls. Boxes indicate the median and 25-75th percentiles, capped bars the 10-90th percentiles, n=15 for two mutated alleles, n=62 for one mutated allele and n=32 for controls. P for trend adjusted for age and gender are reported.

1.1.3 HDL ABILITY TO MODULATE eNOS EXPRESSION AND ACTIVITY IN ENDOTHELIAL CELLS

The ability of HDL to modulate endothelial production of nitric oxide was tested *in vitro*. HDL from carriers and controls displayed a comparable capacity to increase eNOS protein abundance (Figure 3), with a slightly reduced effect of HDL from homozygous subjects.

However, HDL from LCAT deficient subjects proved to be more effective than HDL from controls in promoting eNOS activation by phosphorylation with a gene-dose dependent effect; indeed, when compared with HDL from controls, eNOS activation induced by HDL from homozygous subjects was significantly higher. (Figure 4).

As a consequence, NO production induced by carriers' HDL was significantly higher than that of controls' HDL (Figure 5).

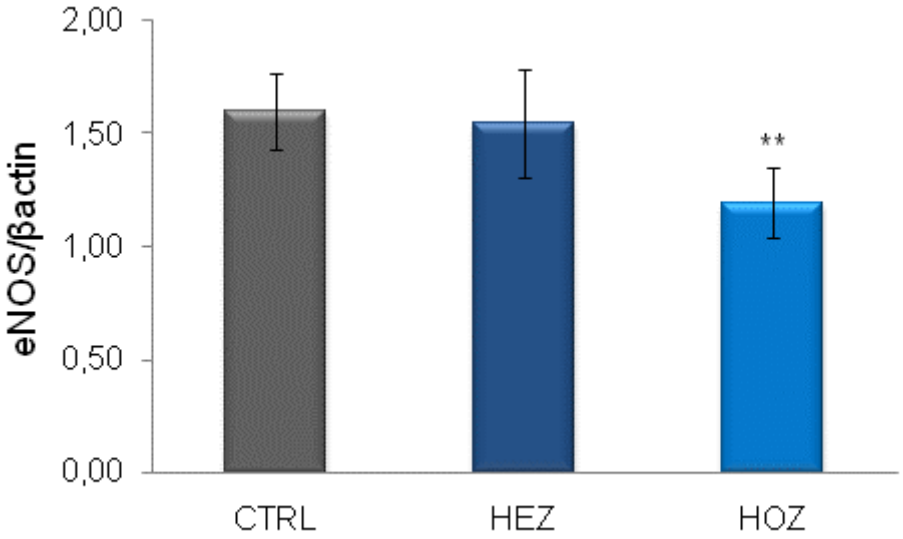

Figure 3.eNOS expression by HDL in endothelial cells. Data are expressed as fold of increase in HDL-treated vs. untreated cells. Data are mean±SD. Control n=10 , heterozygous (HEZ) n=10, homozygous (HOZ) n=3. Data are statistically analyzed by ANOVA and P trend is 0.0016 and compared to control group in post hoc test.

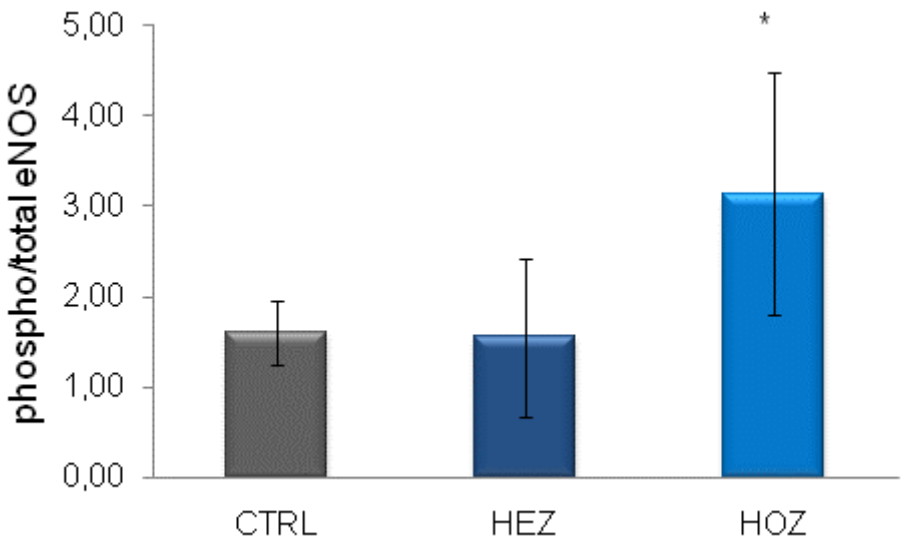

Figure 4.eNOS activation by HDL in endothelial cells. Data are expressed as fold of increase in HDL-treated vs untreated cells. Data are mean±SD. Control n=10 , heterozygous (HEZ) n=10, homozygous (HOZ) n=3.
Data are statistically analyzed by ANOVA and P trend is 0.018 and compared to control group in post hoc test.

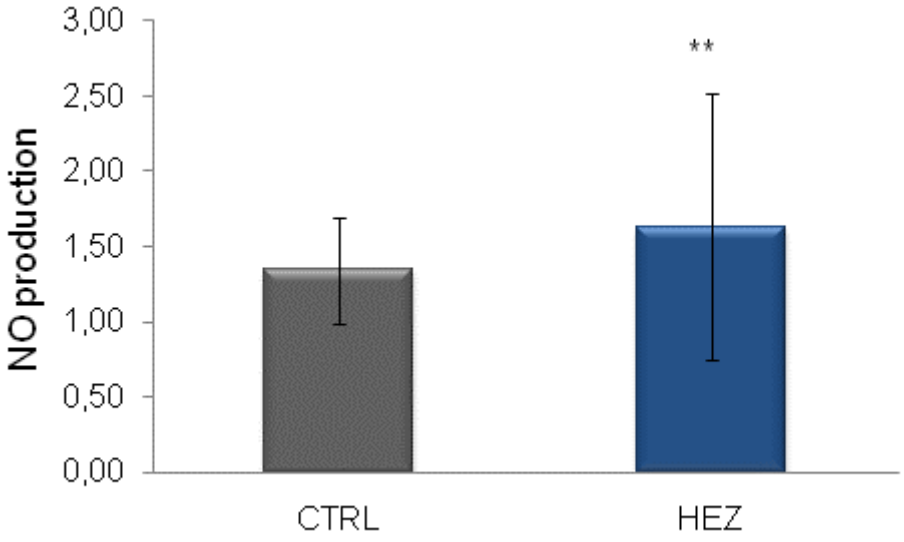

Figure 5.Nitric oxide production mediated by HDL in endothelial cells. Data are expressed as fold of increase in HDL-treated vs untreated cells. Data are mean±SD. Control n=7, heterozygous (HEZ) n=8. Data are statistically analyzed by unpaired t-test and P trend is 0.0091

Sphingosine-1-Phospate (S1P) is a bioactive sphingolipid carried by HDL that can increase the HDL ability to activate eNOS. S1P was measured in HDL isolated from plasma of LCAT deficient carriers and from control in order to assess if the peculiar ability of HDL formed in LCAT deficiency status to activate eNOS is related to S1P content. HDL content of S1P in homozygous LCAT deficiency subjects was comparable to that of controls' HDL (195.0±55.2 pmol/mg protein vs 221.2±28.5 pmol/mg protein, respectively), while HDL from heterozygous carriers showed a slightly higher S1P content (333.8±162.5 pmol/mg protein, P for trend 0.049). (Fig.6)

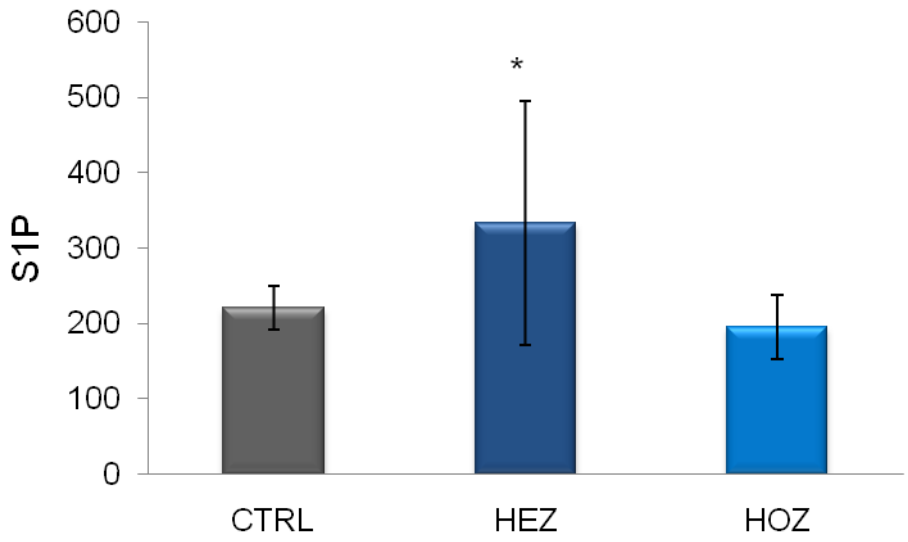

Figure 6.S1P content in HDL. Data are expressed as mean±SD. Control n=9, heterozygous (HEZ) n=9, Homozygous (HOZ) n=3

1.1.4 FLOW-MEDIATED VASODILATION

Arterial function was investigated by measuring flow-mediated vasodilation (FMD). FMD measurement in the brachial artery reflects nitric oxide production and represents a method for assessing endothelial function [173]. Carriers of LCAT mutations displayed FMD values comparable to those of control subjects (7.4±2.5% vs 8.3±2.1%, respectively).

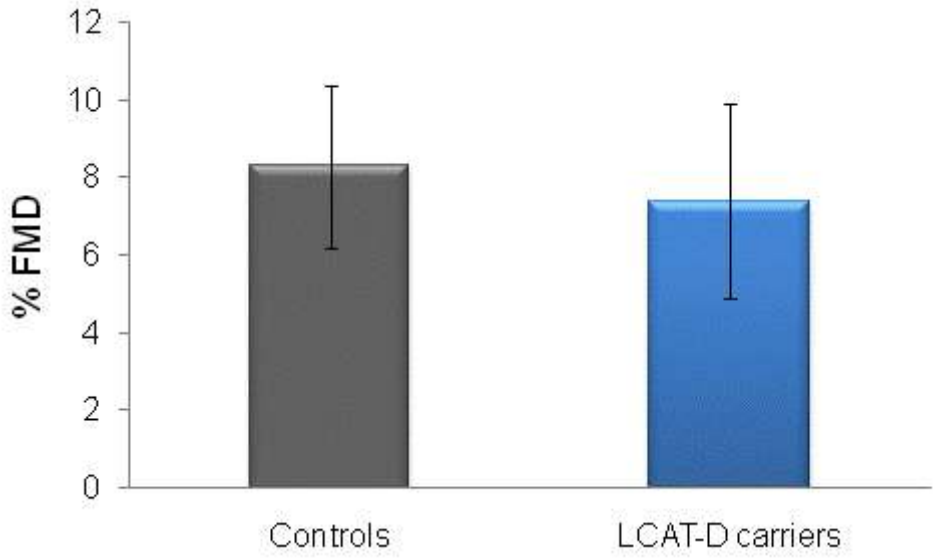

Fig 7.Flow-mediated vasodilation in LCAT deficient and control subjects.
Data are percentage value expressed as mean±SD. LCAT deficient carriers n=7, Controls subjects n=21, every 3 controls are matched for gender and age to each LCAT deficient carrier.

1.2 Animal studies

1.2.1 PLASMA LIPID PROFILE

Plasma lipid levels were measured in mice. hApoA1xhLCAT mice showed dramatic increase in total cholesterol level compared to mice single transgenic for hLCAT or hapoA1, respectively 4.75 and 6 times higher. The observation suggests that the interaction between LCAT and apoA-I is not only addictive, but is synergic. ApoE KO mice, established model for atherosclerosis, present plasma cholesterol levels 8 times higher than control mice but 3 times lower than hApoA1xhLCAT transgenic mice.

	TC (mg/dl)	TG (mg/dl)	PL (mg/dl)	FC (mg/dl)	CE (mg/dl)	CE/TC %
WT	73.9±1.4	81.5±2.5	170.5±4.7	14.7±0.6	58.2±1.3	78.76
hAPOA1	160.0±11.64 ****	110.3±6.6	274.3±14.8 **	42.7±3.2	100.7±6.5	62.94
hApoA1xhLCAT	966.5±16.8 ****	132.5±6.0 **	698.7±12.9 ****	204.6±4.8 ****	805.1±17.6 ****	83.29
hLCAT	216.7±3.3 ****	68.8±2.1	211.1±3.8	46.0±1.0	178.3±3.6 ****	82.14
APOE KO	606.2±11.3 ****	121.4±3.3	310.1±6.5 ****	171.6±6.5 ****	453.5±13.5 ****	74.81

Figure 8.Table of plasma lipid values in female mice. Value are expressed as mean±SEM. WT n=89, hApoA1 n=51, hApoA1xhLCAT n=164, hLCAT n=217, ApoE KO n=178. Lipid values from different mouse model were compared to normal lipid value in WT mice **p<0.01 ****p<0.0001.

1.2.2 FPLC PROFILE

Fast protein liquid chromatography permit to separate lipoprotein in plasma according to size. It is possible to identify three main regions that correspond to VLDL, less retained in column and the first to be eluted, LDL, and HDL, smaller and eluted as the last particles.

It is also possible identify three distinct picks in HDL region, that correspond to large, medium and small HDL.

The analysis of plasma lipoprotein fraction showed that the cholesterol content is concentrated in HDL fraction both in hLCAT and hApoA1xhLCAT transgenic mice. Compared to wild-type (C57Bl/6N green line) and hApoA1 transgenic mice (blue

line) the main HDL pick in hLCAT and hApoA1xhLCATmice is shifted towards particles of larger size that are less retained in column.

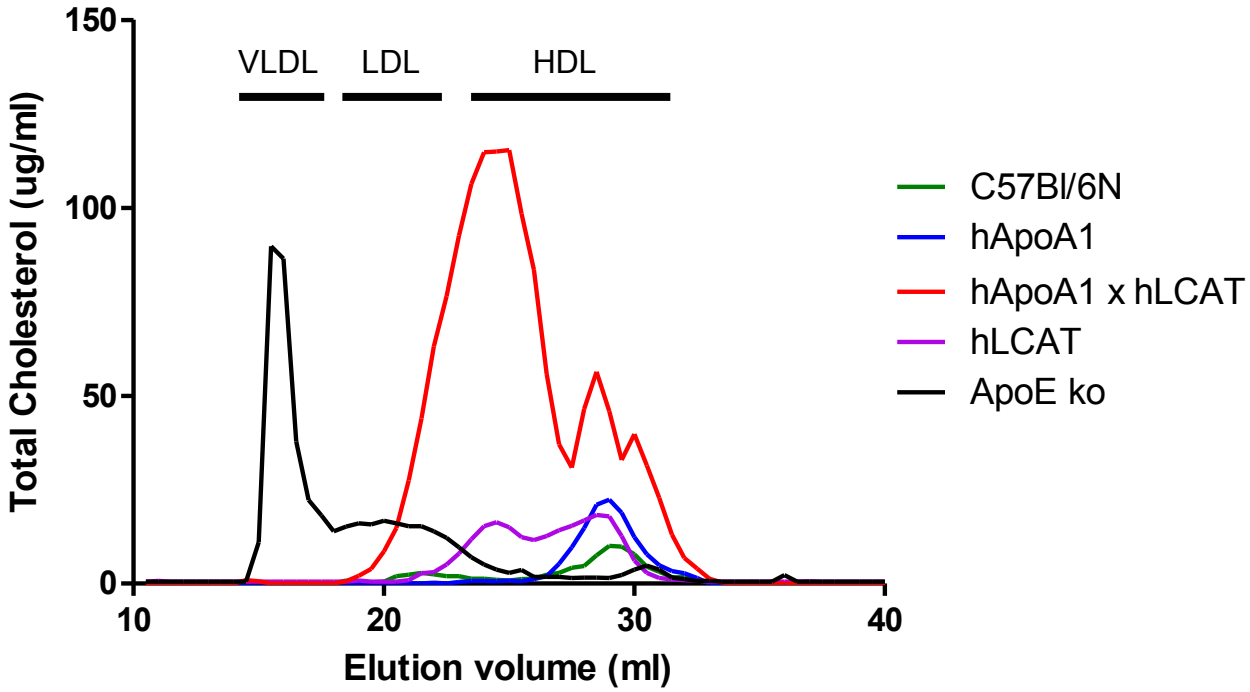

Figure 9. Cholesterol FPLC profile in mice plasma. Plasma lipoproteins were separated by size exclusion chromatography and the cholesterol content was measured in each fraction.

1.2.3 GENE EXPRESSION

Analysis of expression of 84 genes in aorta showed a significant increase in expression of genes involved in inflammation and vasoconstriction in hLCAT transgenic and in hApoA1xhLCAT transgenic mice respect to wild-type mice. Expression of adhesion molecules and integrins is significantly increased as shown in figure 10.

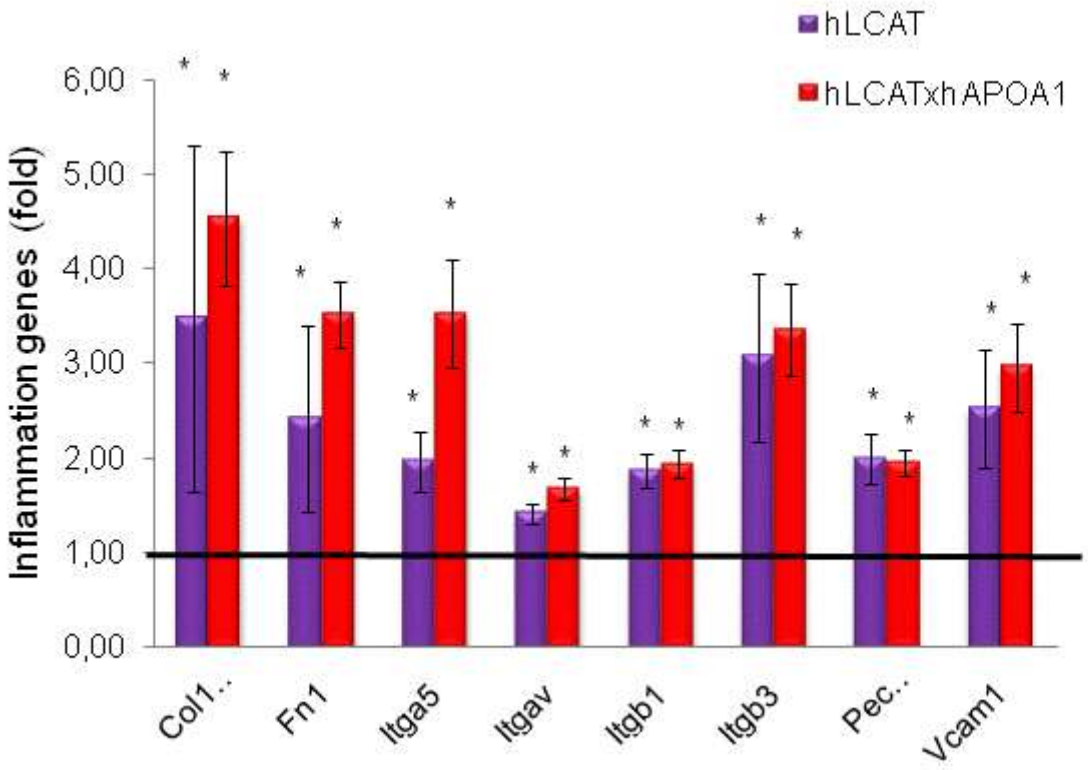

Figure 10. Expression of genes involved in inflammation in hLCAT and hLCATxApoA1 transgenic mice. Results are expressed as fold of increase to value of wild –type mice that are represented by black line. Data are mean±SEM, hLCAT mice n=3, hApoA1xhLCAT n=3. * p value < 0.05

Col18a1= Collagen, type XVIII, alpha 1, hLCAT fold-up 3,48 p value 0,032, hApoA1xhLCAT fold-up 4,54 p value 0,013

Fn1=Fibronectin 1, hLCAT fold-up 2,42 p value 0,016, hApoA1xhLCAT fold-up 3,52 p value 0,006

Itga5=Integrin alpha 5 (fibronectin receptor alpha), hLCAT fold-up 1,97 p value 0,020 hApoA1xhLCAT fold-up 3,52 p value 0,012

Itgav=Integrin alpha V, hLCAT fold-up 1,41 p value 0,016 hApoA1xhLCAT fold-up 1,68 p value 0,007

Itgb1= Integrin beta 1 (fibronectin receptor beta), hLCAT fold-up 1,87 p value 0,027hApoA1xhLCAT fold-up 1,93 p value 0,006

Itgb3=Integrin beta 3 hLCAT fold-up 3,07 p value 0,016 hApoA1xhLCAT fold-up 3,35 p value 0,011

Pecam1=Platelet/endothelial cell adhesion molecule 1 hLCAT fold-up 2,00 p value 0,020 hApoA1xhLCAT fold-up 1,95 p value 0,008

Vcam1=Vascular cell adhesion molecule 1 hLCAT fold-up 2,51 p value 0,024 hApoA1xhLCAT fold-up 2,96 p value 0,038

Expression of genes involved in vasoconstriction was also significantly enhanced in mice with LCAT overexpression (Figure 11).

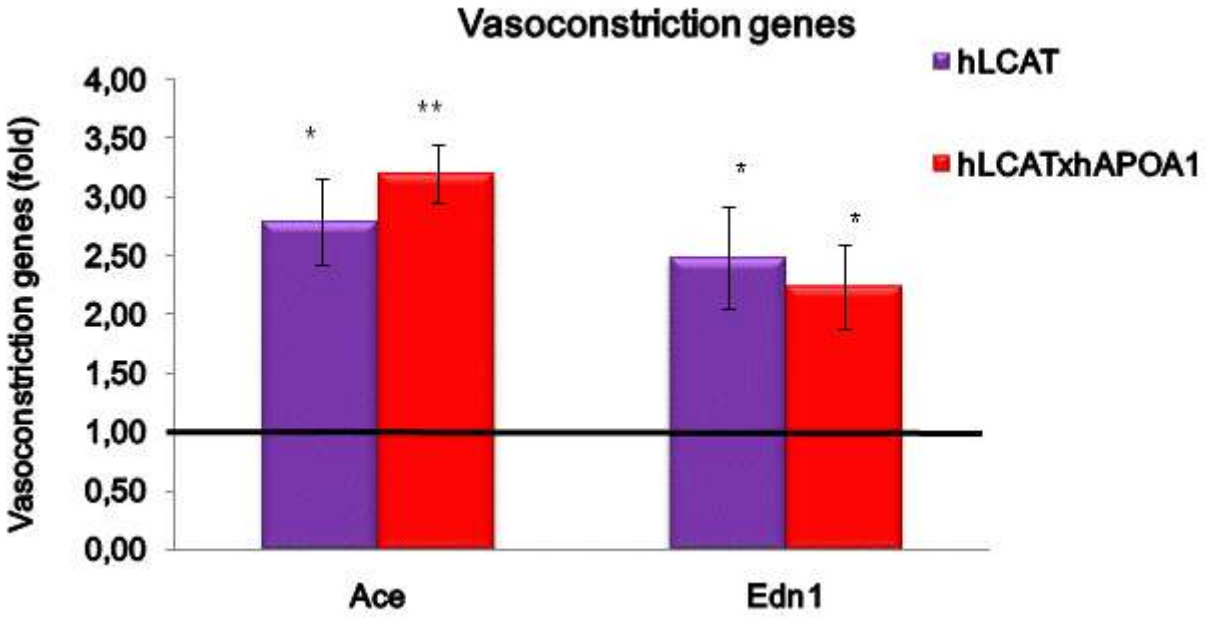

Fig. 11. Expression of genes involved in vasoconstriction in hLCAT and hLCATxapoA1 transgenic mice. Results are expressed as fold of increase to wild-type mice (black line=1). Data are mean±SEM, hLCAT mice n=3, hApoA1xhLCAT n=3. *p value < 0.05, **p value < 0.001
Ace= Angiotensin I converting enzyme (peptidyl-dipeptidase A) hLCAT fold-up 2,79 p
value 0,019 hApoA1xhLCAT fold-up 3,20 p value 0,001
Edn1= Endothelin 1 hLCAT fold-up 2,49 p value 0,018 hApoA1xhLCAT fold-up 2,24 p value 0,036

The results from up regulation of inflammation genes and the increased expression of genes involved in vasoconstriction suggest that there is an alteration in aorta endothelial biology when LCAT is overexpressed.

2.LCAT AND RENAL DISEASE

2.1 In vitro studies

2.1.1 CHARACTERIZATION OF LPX

To evaluate the role of LpX in kidney injury, synthetic LpX were *in vitro* produced and characterized by agarose gel electrophoretic analysis and electron microscopy.

Electrophoretic analysis on agarose gel stained with Sudan Black showed the peculiar property of LpX to migrate towards the anode pole in the opposite direction from other lipoproteins.

However, under specific conditions, such as frozen samples, LpX is difficult to stain with Sudan Black, that preferentially stained neutral lipid, but it is better visualized using Filipin stain as showed in Fig. 12

Electron microscopy analysis confirmed size and shape of synthetic LpX emphasizing the peculiar multilamellar structure (Fig. 13).

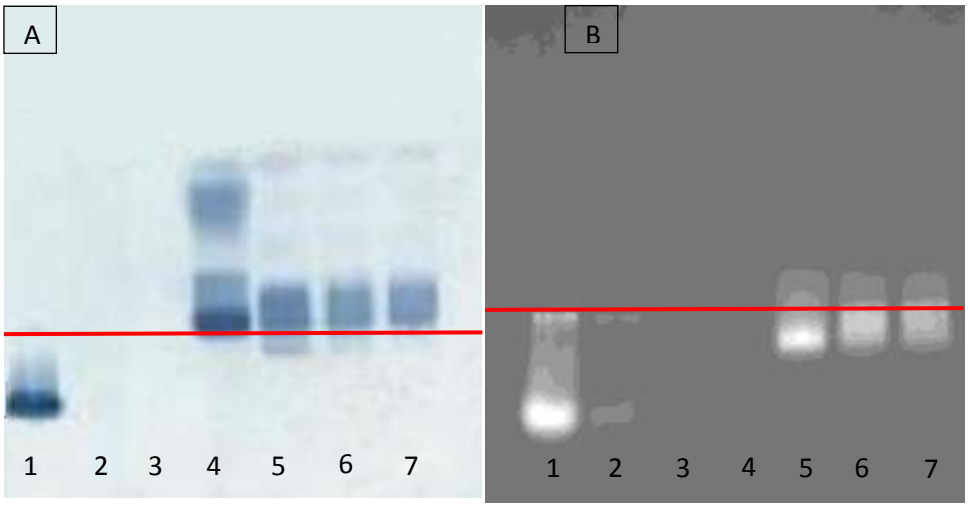

Figure 12. Agarose gel stained with Sudan Black (panel A) and Filipin (panel B). Red line represents loading point, 1= synthetic LpX, 2=synthetic LpX freeze-thawed one time, 3= synthetic LpX freeze-thawed two times, 4=control plasma, 5=FLD plasma, 6= FLD plasma freeze-thawed one time, 7= FLD plasma freeze-thawed two times.

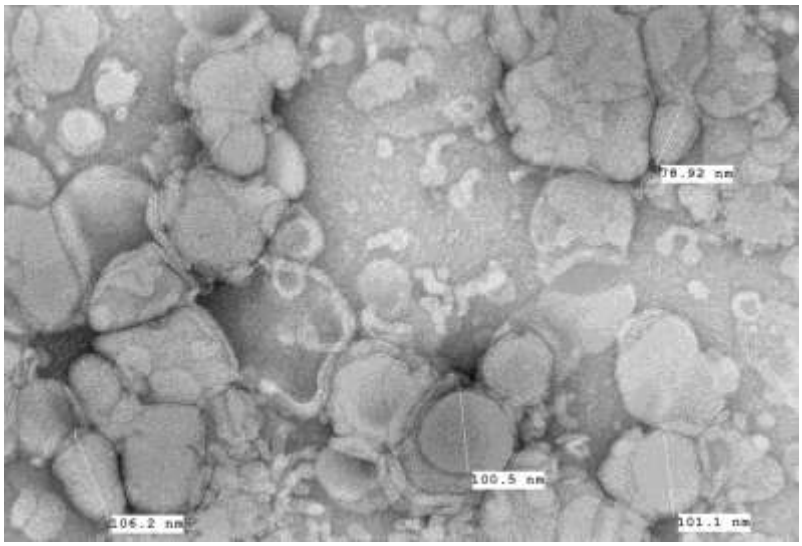

Figure 13. Electron microscopy image of synthetic LpX. Sample is negatively stained with 1% uracil solution and image acquired at 40,000X magnification.

LpX is quickly metabolized in plasma. The detection of fluorescence in plasma obtained from LCAT KO mice injected with NBD-labeled LpX showed a maximum peak of emission 15 minutes after the injection. After 3 hours post injection the emission was reduced to less than the half of the initial peak and after 6 hours the signal was completely absent (Fig. 14).

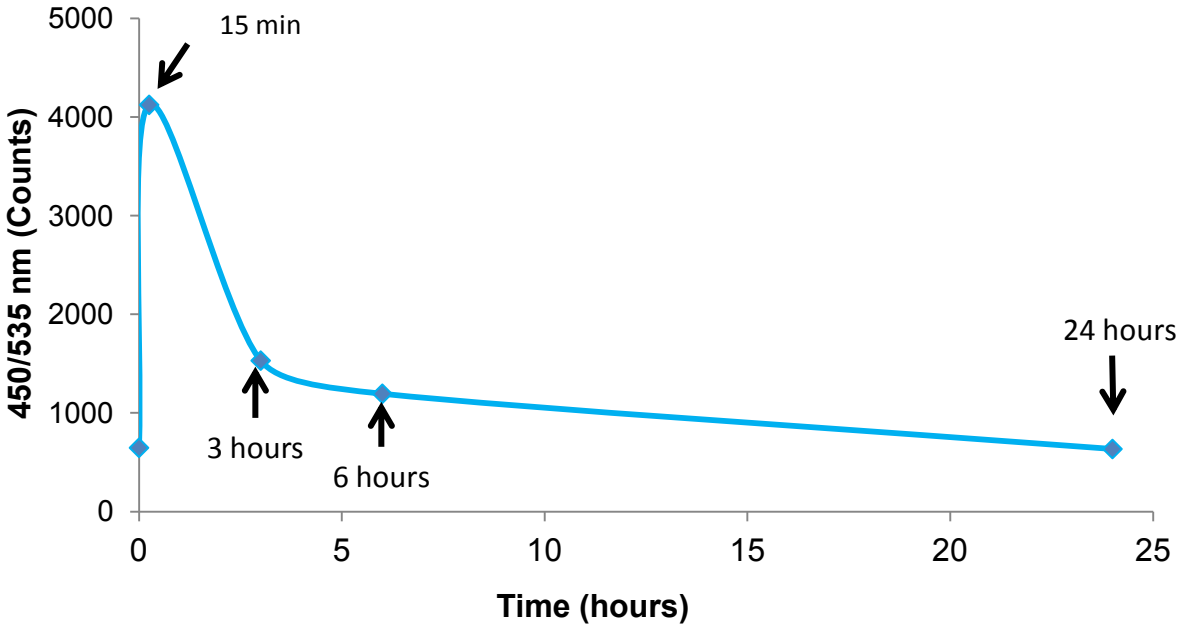

Fig. 14. Time line emission curve of LCAT KO mouse plasma injected with fluorescent LpX. Sample was excited at 450 nm and emission was filtered at 535 nm according to NBD emission spectrum.

2.1.2 LPX INTERNALIZATION BY RENAL CELLS

Glomerular filtration barrier is mainly composed of three layers: endothelial cells with fenestrations (70 to 100 nm in diameter), basal membrane and epithelial regions constituted by podocytes. Intraglomerular mesangial cells are present in the interstitium between endothelial cells of the glomerulus. They also participate indirectly in filtration by contracting and reducing the glomerular surface area.
To assess if LpX affectes the filtration barrier, mesangial and podocyte cells were incubated with LpX and ability of cells to internalize the particle was detected by confocal microscopy. LpX was internalized both in mesangial and podocyte cells 6 hours after incubation. Red Lysotracker was added to visualize lysosome compartments. In the figures is possible to see LpX and lysosomes co-localization.

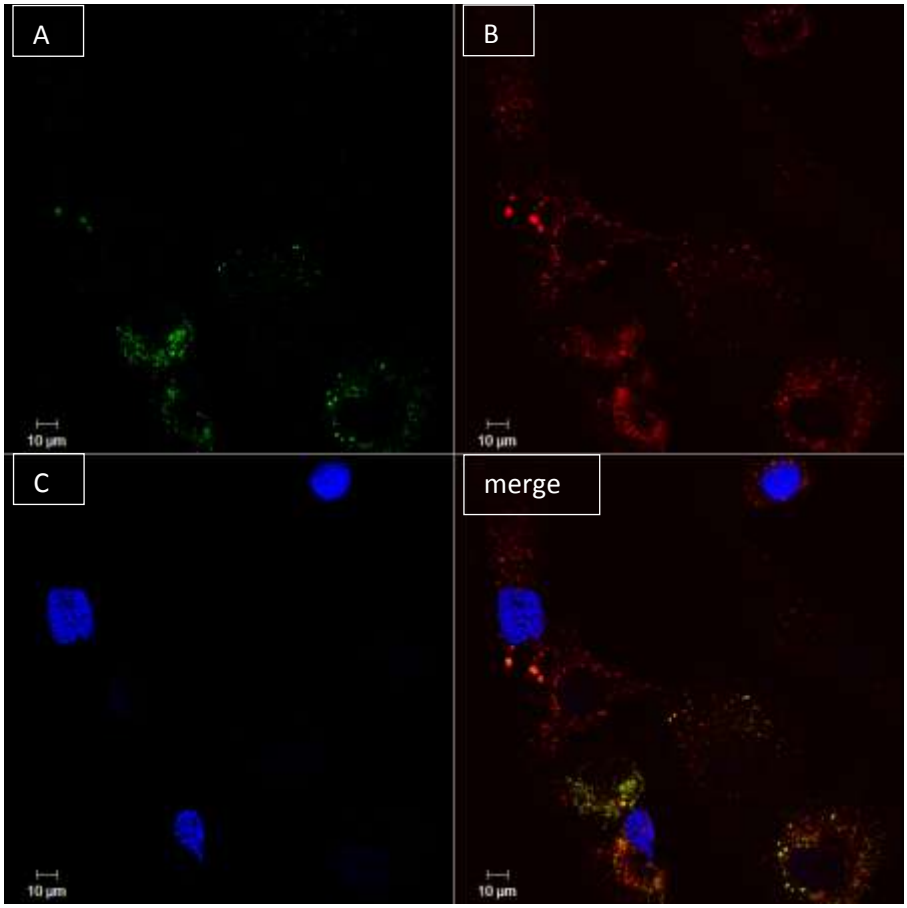

Fig. 15 Podocyte cells under confocal microscopy. Visualization of LpX by green signal (Panel A), lysosomes by red fluorescence (Panel B) and nuclei by blue channel (Panel C) and a merge of the images.

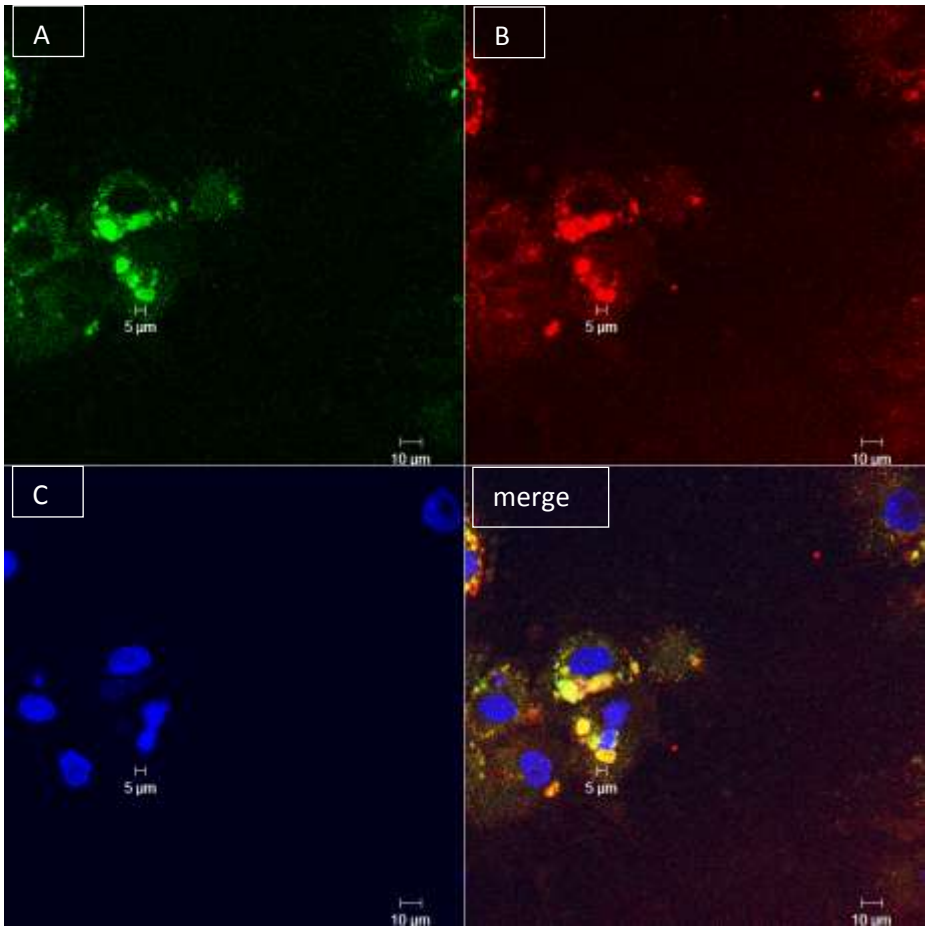

Fig. 16 Mesangial cells under confocal microscopy. Visualization of LpX by green signal (Panel A), lysosomes by red fluorescence (Panel B) and nuclei by blue channel (Panel C) and a merge of the images.

2.1.3 INFLAMMATION, OXIDATIVE STRESS AND APOPTOSIS MEDIATED BY LCAT DEFICIENCY SERUM IN TUBULAR CELLS.

Vasoactive compounds, growth factors and cytokines have a role in the progression of renal disease promoting cell growth and fibrosis. Analysis of VCAM-1 and MCP-1 expression in tubular cells incubated with sera from LCAT deficient patients showed increased inflammatory response in cells incubated with sera from homozygous subjects as shown in Fig. 17.

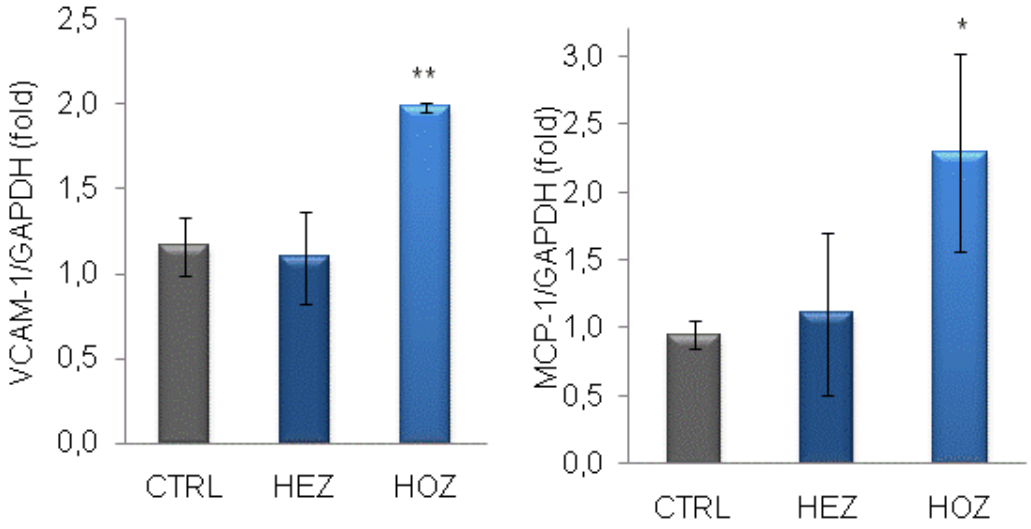

Fig. 17. Gene expression of VCAM-1 and MCP-1 in HK-2 cells incubated with sera. Data are expressed as mean±SD. * $p<0.05$, **$p<0.01$. Control n=3, heterozygous (HEZ) n=3, homozygous (HOZ) n=3.

Oxidative stress is caused by increased production of reactive oxygen species (ROS), nitric oxide, and impaired antioxidant capacity, resulting to necrosis, inflammation, apoptosis, and fibrosis of kidney. The exposure of HK-2 to sera from homozygotes induced an increase of cellular oxidative stress evaluated as NADPH oxidase activity (Fig. 18) and resulting ROS production (Fig. 19).

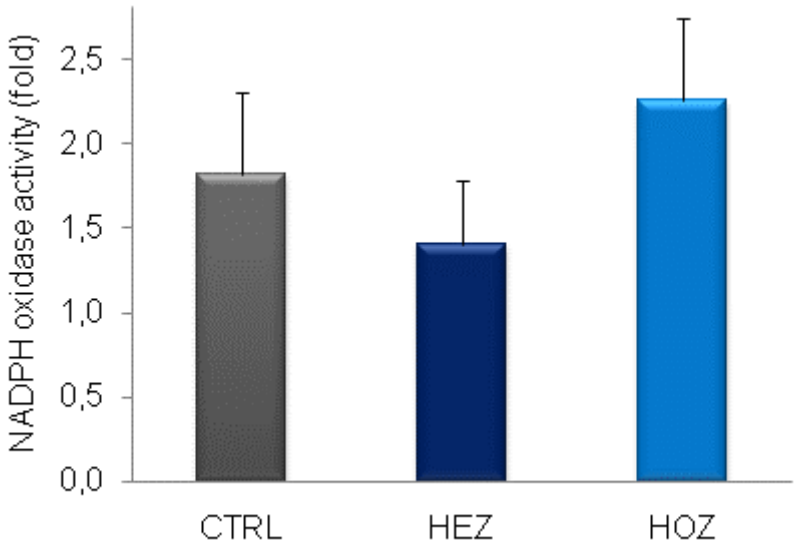

Fig. 18. NADPH oxidase activity in HK-2 cells incubated with sera. Data are expressed as mean±SD. Control n=3, heterozygous (HEZ) n=3, homozygous (HOZ) n=3.

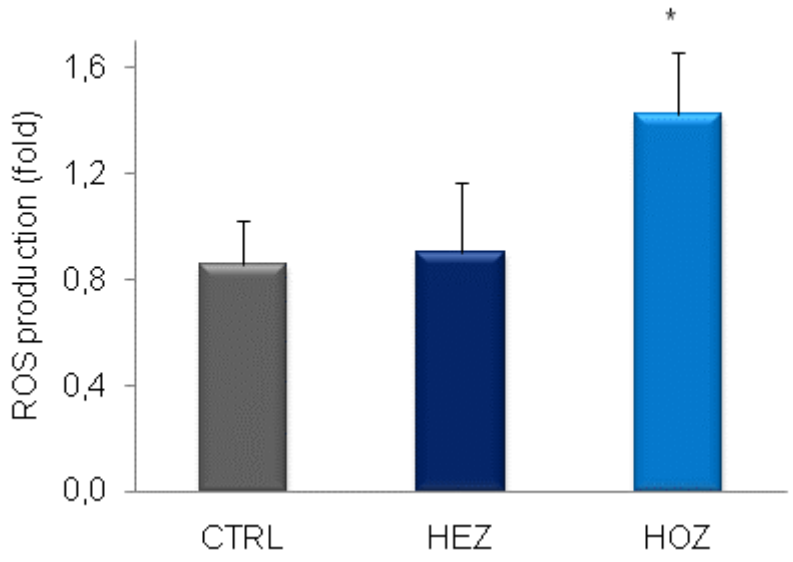

Fig. 19. ROS production in HK-2 cells incubated with sera. Data are expressed as mean±SD. Control n=3, heterozygous (HEZ) n=4, homozygous (HOZ) n=3. Data were analyzed by ANOVA and P trend is 0.0085 and compared to control group in a post hoc test (Dunnett's test).

Apoptosis is involved in the pathophysiologic changes observed in various renal diseases, such as IgA nephropathy, lupus nephritis, and crescentic nephritis [174]. Apoptotic process evaluated by Annexin V staining was measured in HK-2 cells incubated with sera from homozygous and heterozygous LCAT deficient subjects and from controls. The exposure of HK-2 to sera from homozygotes subjects also induced a significant activation of the apoptotic cascade.

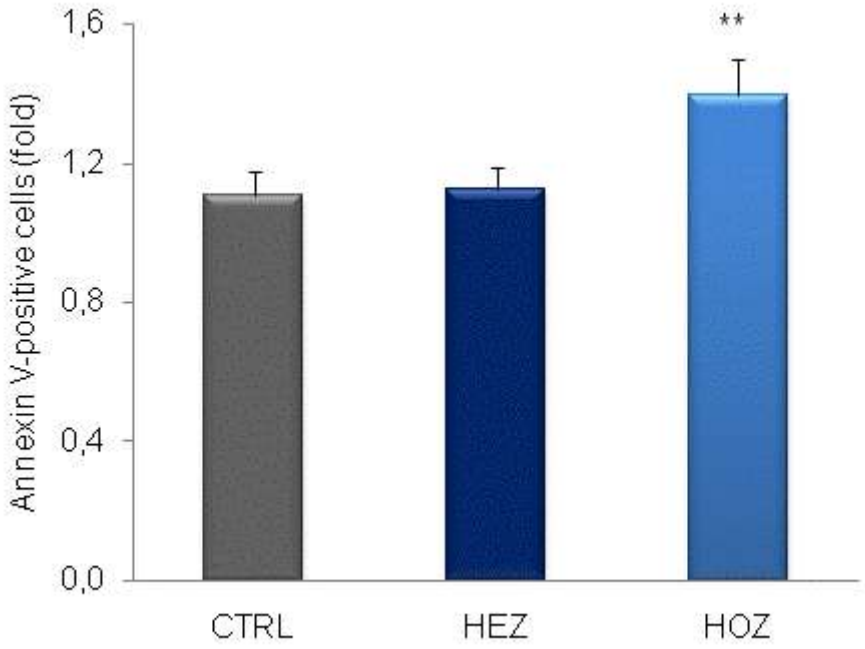

Fig. 20. Apoptosis in HK-2 cells incubated with sera. Data are expressed as mean±SD. Control n=3, heterozygous (HEZ) n=4, homozygous (HOZ) n=3. Data were analyzed by ANOVA and P trend is 0.0016 and compared to control group in a post hoc test (Dunnett's test).

2.2Animal studies

2.2.1 ACUTE KIDNEY INJURY

LCAT KO mice were injected with LpX (0.5 mg/ml cholesterol) or with the same cholesterol amount of LDL or saline solution. Microalbumin-to-creatinine ratio in urine was significantly increased in LCAT KO mice injected with LpX compared to same mutant mice with injected with PBS. However, wild-type mice injected with LpX did not show any differences in basal levels of microalbumin-to-creatinine ratio in urine, suggesting that LCAT activity in normal mice disassembled LpX before arriving in the kidney and causing injury. Although LCAT KO mice injected with LDL showed a mild increase in microalbumin-to-creatinine ratio, but a significantly lower increase was observed in mice injected with LpX.

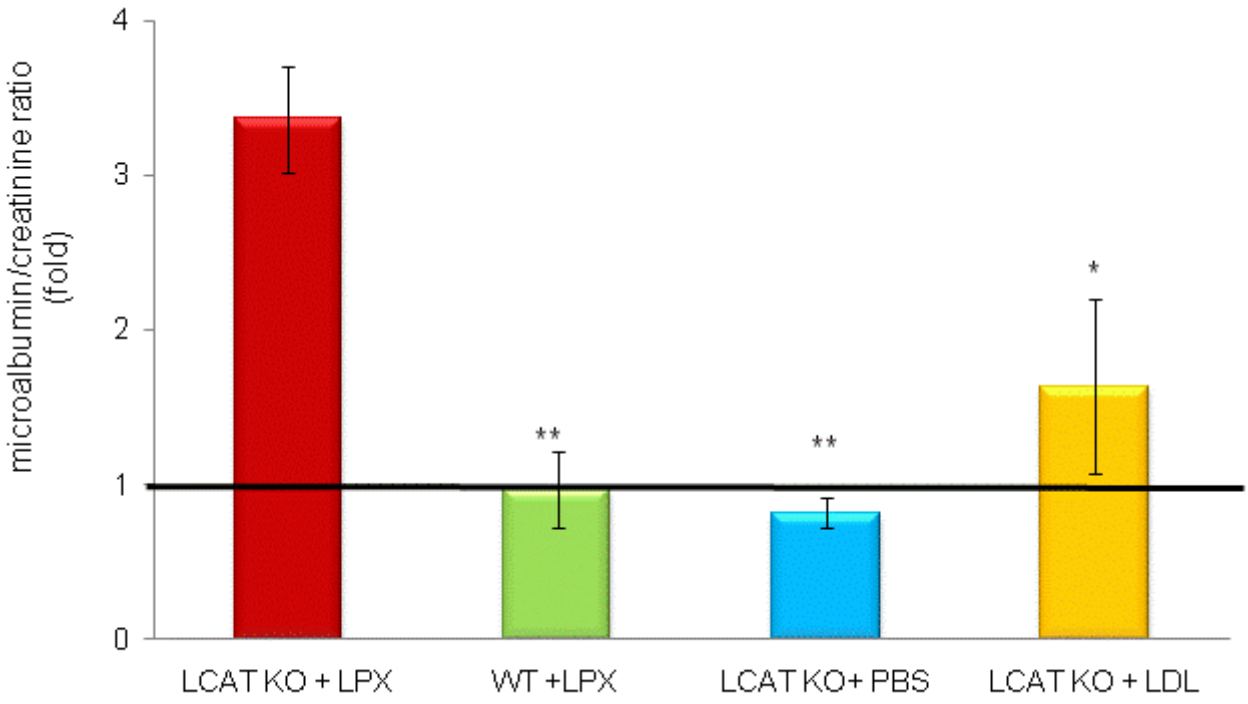

Fig. 21 Microalbumin-to-creatinine ratio in mouse urine.

Microalbumin-to-creatinine ratio fold increase of 3.36± 0.35 in LCAT KO mice (n=6) and 0.97± 0.24 in WT mice (n=3) 24 hours after LpX injection compared to the value measured before injection. Microalbumin-to-creatinine ratio fold increase of 1.63± 0.56 24 hours after LDL injection and 0.81± 0.1 after PBS injection in LCAT KO mice (3 mice for each group).

Values are expressed as fold of change to baseline level (black line), each mouse was normalized on his baseline value measured before the injection. *p<0.05,

**p<0.01. Data were analyzed by ANOVA and groups were compared with Tukey in post hoc analysis.

One week after the injection, microalbumin-to-creatinine ratio decreased but did not returne completely to basal levels, indicating that after only one injection, even if the injury was transitory, the kidney functionality was not completely restored (Fig. 22).

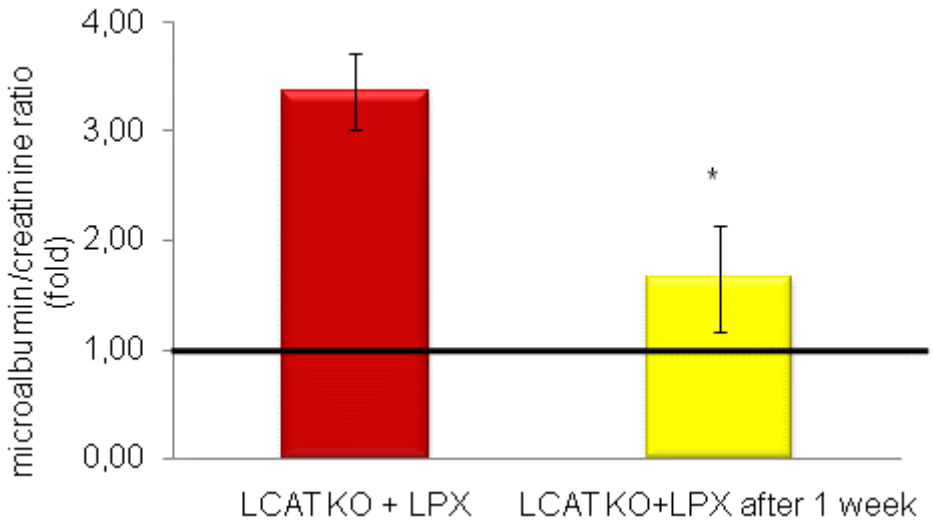

Fig. 22 Microalbumin-to-creatinine ratio in mouse urine.
Microalbumin-to-creatinine ratio in LCAT KO mice injected with LpX measured 1 day (red bar) and after injection and 7 days (yellow bar) after injection. Values are expressed as fold of change to baseline level (black line); each mouse was normalized on his baseline value measured before the injection. Microalbumin-to-creatinine ratio 24 hours after injection fold increase of 3.36± 0.35, 1 week after injection fold increase of 1.65± 0.49. *p<0.05

2.2.2 CHRONIC KIDNEY INJURY: BIOCHEMICAL AND GENE EXPRESSION ANALYSIS

LCAT KO mice were injected with LpX 3 times a week for 4 weeks and microalbumin-to-creatinine ratio was evaluated at the end of each week, 48 hours after the last injection. As shown in Fig. 23, mice injected with LpX showed constant increase in microalbumin-to-creatinine ratio during all the treatment.

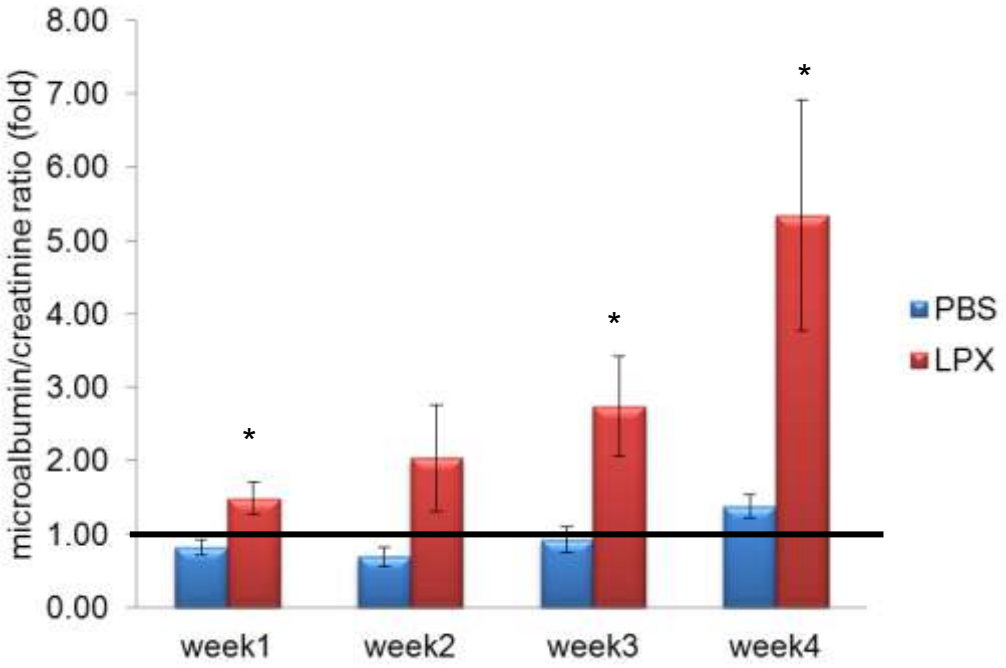

Fig. 23.Microalbumin-to-creatinine ratio in LCAT KO mice after LpX or saline solution injection.

Values are expressed as fold of change to baseline level (black line), each mouse was normalized on his baseline value measured before starting the experiment (6 mice for each group).

Microalbumin-to-creatinine ratio in 1 week injection (48 hours after last injection) fold increase of 1.49±0.22 in LpX group and fold increase of 0.83±0.10 in control group; in 2 weeks fold increase of 2.03±0.72 in LpX group and fold increase of 0.69±0.14 in control group; in 3 weeks fold increase of 2.75±0.68 in LpX group and fold increase of 0.92±0.17 in control group; in 4 weeks fold increase of 5.35±1.57 in LpX group and fold increase of 1.38±0.16 in control group.

After 4 weeks, mice were sacrificed and kidneys collected to evaluate mRNA expression of genes involved in the nephrotoxicity pathway.
Expression of 84 genes was evaluated and the analysis showed that the markers of kidney injury (Fig. 24), genes involved in glomerulus cells apoptosis (Fig. 25), in inflammation (Fig. 26) and oxidative stress (Fig. 27) were significantly up-regulated by chronic presence of LpX in plasma. In the graphs only significant changes in gene expression are reported.

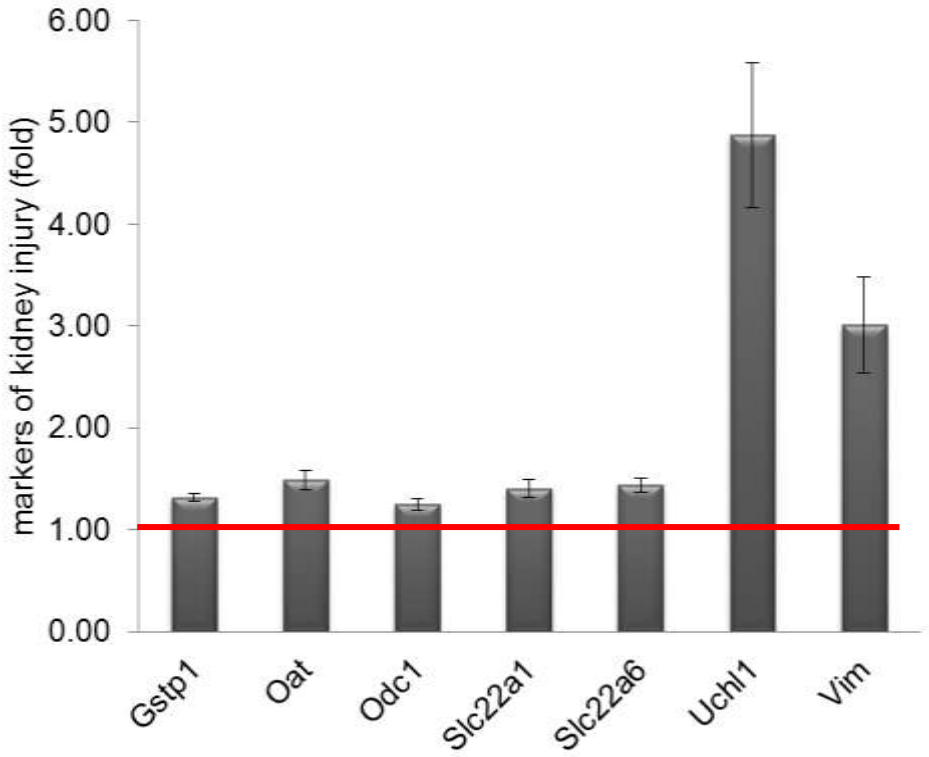

Fig. 24. Gene expression of markers of kidney injury in LCAT KO mice injected with LpX. Results are expressed as fold of increase to LCAT KO mice injected with saline solution (red line = 1). * p value < 0.05.
Gstp1=glutathione S-transferase pi 1 fold increase of 1.32. p value 0.025.
Oat=ornithine aminotransferase fold increase of 1.49. p value 0.018.
Odc1=ornithine decarboxylase 1 fold increase of 1.25.p value 0.021.
Slc22a1=solute carrier family 22 (organic cation transporter), member 1 fold increase of 1.40. p value 0.024.
Slc22a6=solute carrier family 22 (organic anion transporter), member 6 fold increase of 1.44 p value 0.011.
Uchl1=ubiquitin carboxy-terminal hydrolase L1 fold increase of 4.88. p value 0.029

Vim=vimentin fold-up 3.01. p value 0.036.

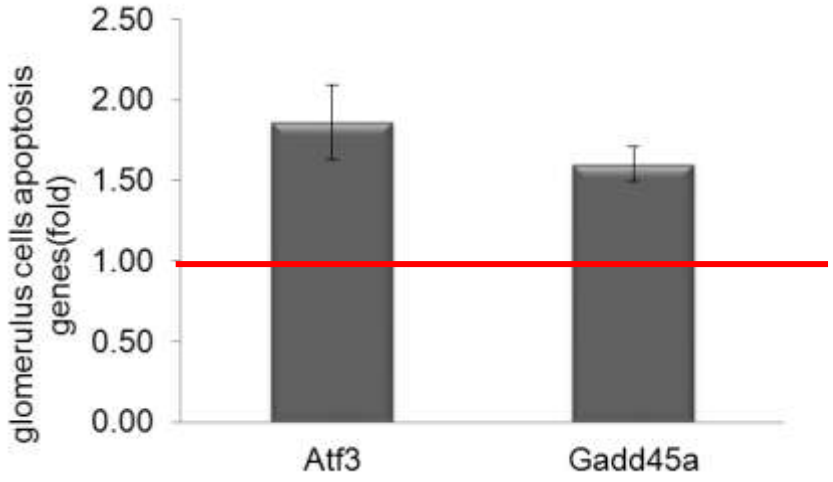

Fig. 25. Expression of genes involved in glomerulus cell apoptosis in LCAT KO mice injected with LpX. Results are expressed as fold of increase compared to LCAT KO mice injected with saline solution (red line = 1). * P value < 0.05. Atf3=activating transcription factor 3, fold increase of 1.86. p value 0.035. Gadd45a=growth arrest and DNA-damage-inducible, alpha fold increase of 1.60. p value 0.015.

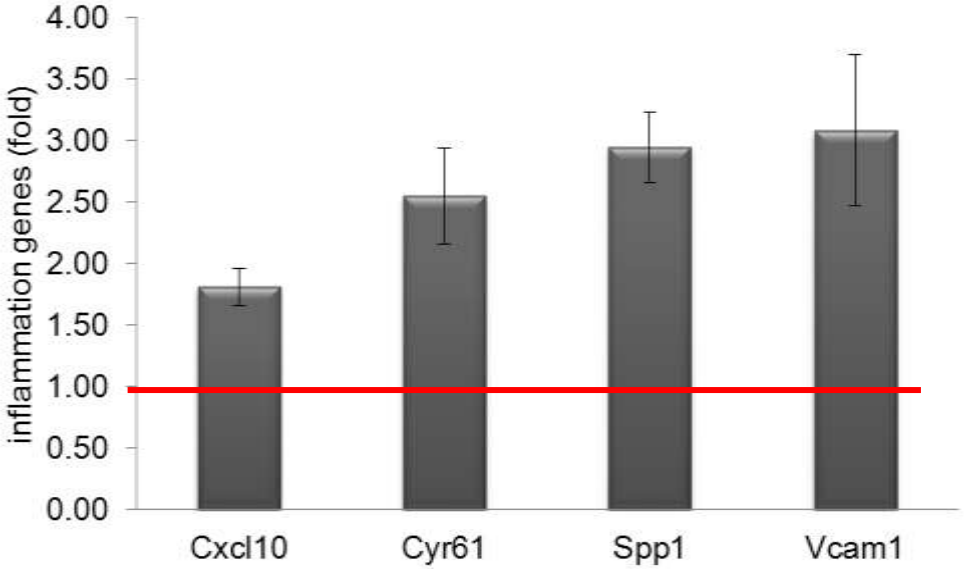

Fig. 26. Expression of genes involved in kidney inflammation in LCAT KO mice injected with LpX. Results are expressed as fold of increase to LCAT KO mice injected with saline solution (red line = 1). * p value < 0.05.

Cxcl10=chemokine (C-X-C motif) ligand 10 fold increase of 1.81. p value 0.017.
Cyr61=cysteine-rich angiogenic inducer 61 fold increase of 2.55. p value 0.028.
Spp1=secreted phosphoprotein 1 fold increase of 2.95. p value 0.017.
Vcam1=vascular cell adhesion molecule 1 fold increase of 3.08. p value 0.059.

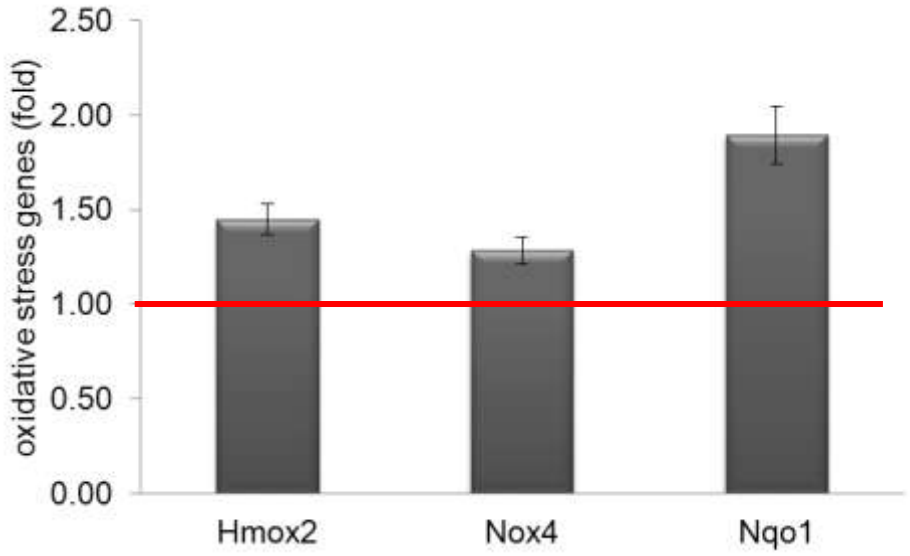

Fig. 27. Expression of genes involved in oxidative stress in LCAT KO mice injected with LpX. Results are expressed as fold of increase to LCAT KO mice injected with saline solution (red line = 1). * p value < 0.05.
Hmox2=heme oxygenase (decycling) 2, fold increase of 1.45. p value 0.031.
Nox4=NADPH oxidase 4, fold increase of 1.28. p value 0.034.
Nqo1=NAD(P)H dehydrogenase, quinone 1, fold increase of 1.89. p value 0.009.

2.2.3 CHRONIC KIDNEY INJURY: CONFOCAL AND HISTOLOGICAL ANALYSIS

Using confocal microscopy it is possible to visualize the emission fluorescence produced by NBD, green fluorescent phospholipid used to tag synthetic LpX. Auto-fluorescence of kidney slice from control mice was subtracted to emission in mice injected with LpX and the net fluorescence was shown in Fig. 28.

By confocal laser scanning microscopy (Z-stack) is possible to obtain high-resolution optical images with depth selectivity. 6 µm-section was optical sectioned by acquiring in-focus images every 1 µm from selected depths. Images were acquired point-by-point and reconstructed with a computer by three-dimensional reconstruction.

The Z-stack overview of sample highlighted the presence of bright green spots mainly in tubular regions with smaller spots in the glomerulus region.

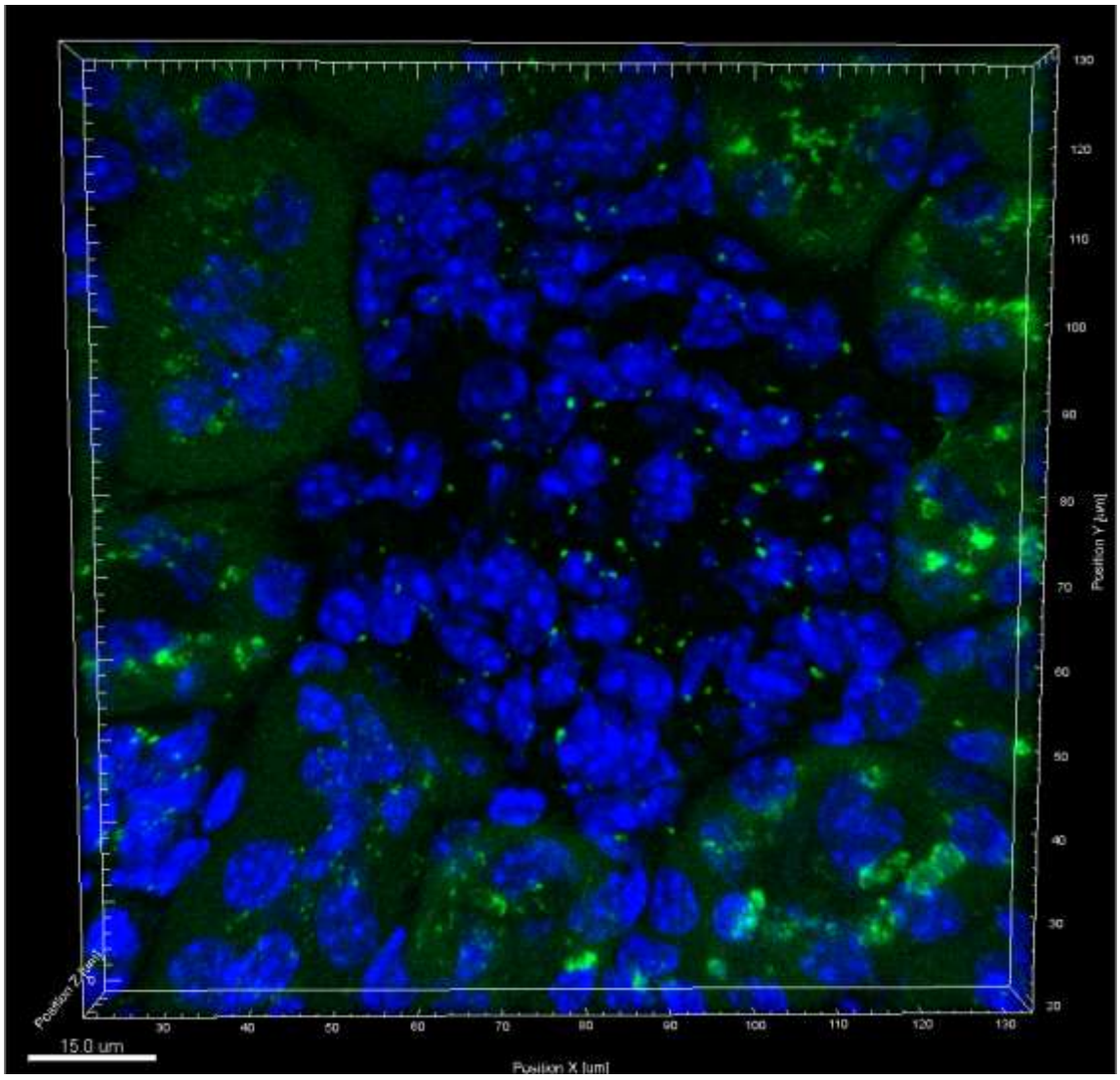

Fig. 28.40x magnification of kidney slice (6 µm). Nuclei are visualized with DAPI and LpX is traced with NBD.

The analysis if distinct glomerulus and tubula area permitted a better visualization of bright green deposition in kidney confirming that 24 hours after injection LpX was mainly accumulated in tubular regions.

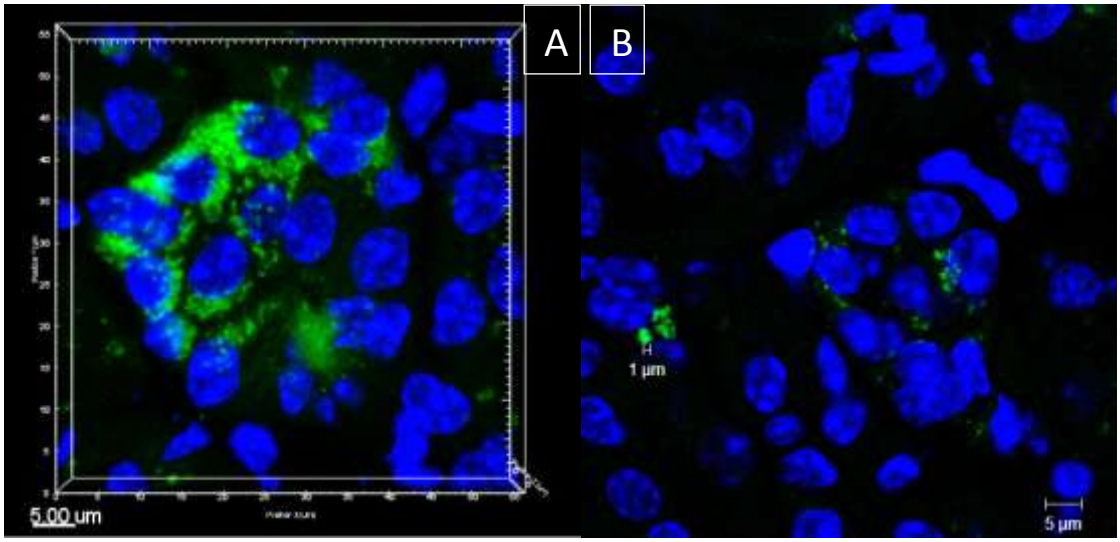

Fig. 29.63x magnification of tubular (Panel A) and glomerulus region (Panel B). Nuclei are visualized with DAPI and LpX is traced with NBD.

Histological analysis emphasizes mainly glomerulosclerosis, with high disorganization in glomerular structures. Moreover, glomeruli presented an expansion of mesangial matrix and the collapse of capillary tubes as showed in Fig 30 (panel A).

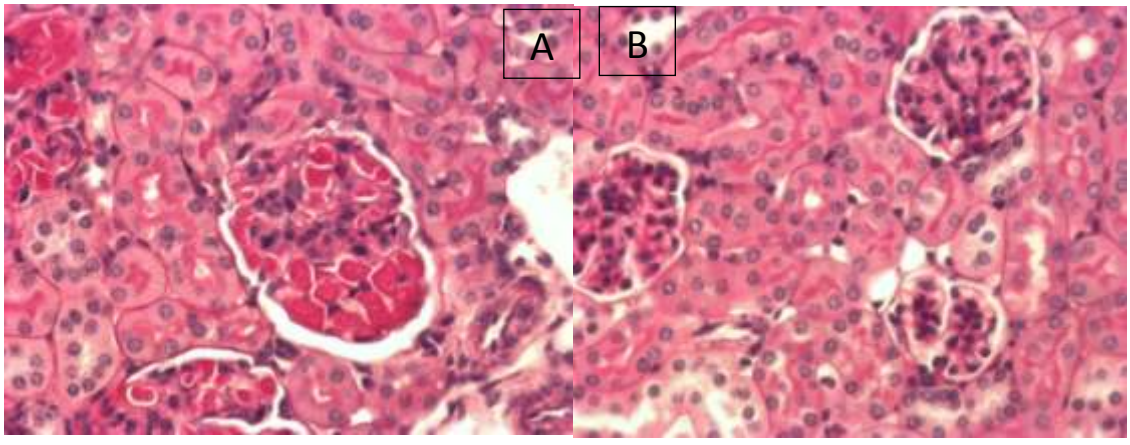

Fig. 30.Histological analysis of glomeruli. Slides were stained with Masson trichrome staining. Panel A, glomeruli from LCAT KO mice treated with LpX; panel B, glomeruli from LCAT KO mice injected with PBS.

Discussion

First objective of the present project was the evaluation of the impact of LCAT deficiency or overexpression on endothelial dysfunction.

Endothelial dysfunction is a peculiar characteristic of atherosclerosis and is characterized by transforming vessels of the endothelial surface from non-adhesive to pro-adhesive surface and is mediated by altered homeostasis balance of particles implicated in regulating vascular tone, inflammation and hemostasis [50]. Among substances that modulate vascular tone, NO plays a major role. HDL are able to stimulate NO production in endothelial cells through eNOS activation. eNOS activation requires binding of apoA-I to SR-BI and the resulting activation of the PI3 K/Akt signaling pathway that phosphorylates eNOS in multiple sites. The enzymatic activity of eNOS is regulated by several post-transcriptional mechanisms such as protein–protein interactions, subcellular localization, and phosphorylation of serine, threonine, and tyrosine residues. Phosphorylation of stimulatory sites and dephosphorylation of inhibitory sites are required for eNOS activation and resulting NO production; among sites involved in eNOS activation, phosphorylation of Ser1177 is mainly implicated in eNOS activation [175].

HDL isolated from LCAT deficient carriers showed an elevated ability to activate eNOS through Ser1177 phosphorylation,resulting in increased NO production with a gene dose-related effect despite the impaired ability to stimulate eNOS expression showed in homozygous carriers of LCAT deficiency. In agreement with the in vitro data, carriers of LCAT mutations have flow-mediated vasodilation values comparable to control subjects despite the low plasma HDL levels. The increased ability of carrier HDL to activate eNOS could be related, at least in part, to the increased content of S1P, a bioactive component of HDL which has been shown to contribute to the HDL-mediated endothelial protection.

In contrast to NO anti-atherogenic activity, Endotelin 1 and ACE (angiotensin converting enzyme) are implicated in vasoconstriction process. Endotelin1 is a potent vasoconstrictor produced by endothelial cells [176] and ACE catalyses the conversion of angiotensin I to angiotensin II, which is a strong vasoconstrictor involved in the renin-angiotensin system [177].The evaluation of the expression of genes involved in endothelial cell homeostasis when LCAT is overexpressed provide additional information to better understand the role of LCAT in atherosclerosis. Increased expression of genes involved in vasoconstriction in mice that overexpress LCAT supports findings from in vitro experiments that LCAT

is not required to maintain vascular tone, but on the contrary mice that overexpressed LCAT showed up-regulation of genes involved in vasoconstriction process such as Ace and Edn1.LCAT is not active in the absence of apoA-I and to exclude any doubt regarding LCAT activation, hApoA1xhLCAT transgenic mice were utilized in this study. Also in the presence of apoA-I, genes involved in vasoconstriction are up-regulated in LCAT transgenic mice.

Another characteristic of endothelial dysfunction is inflammation. Leukocyte recruitment into sites of inflammation is a tightly regulated process in which adhesion molecules and chemokines play crucial roles. Activated endothelium is able to increase the production of adhesion molecules; among these, VCAM-1 is induced by arterial endothelial cells in response to accumulation of cholesterol within the intima and represents a critical feature of atherosclerosis [71]. HDL have been shown to down-regulate the cytokine-induced expression of CAMs [72, 73]. HDL isolated from LCAT deficient subjects shows a higher capacity to inhibit VCAM-1 expression in endothelial cells, with a gene dose-dependent effect; these in vitro data were confirmed by in vivo evaluation of plasma levels of soluble adhesion molecules.

Despite the significant reduction in plasma HDL cholesterol levels, sVCAM-1, sICAM-1 and sE-selectin levels in plasma of LCAT deficiency subjects are not increased, but are comparable to levels measured in control subjects. On the contrary, subjects with low plasma HDL cholesterol levels not associated to genetic disorders show significant increased levels of soluble adhesion molecules [80].

Inflammation parameters were also evaluated in hLCAT and hApoA1xhLCAT transgenic mice, and, once again, LCAT overexpression was related to higher expression in aorta genes coding for integrins and cell adhesion molecules. hApoA1xhLCAT transgenic mice have total cholesterol levels higher than those of apoE knockout mice, a confirmed model of atherosclerosis. However, despite tremendous cholesterol levels, hApoA1xhLCAT transgenic mice are protected against atherosclerosis compared to apoE knockout mice (en face aorta analysis and expression of genes related to endothelial cell homeostasis, data not shown). These data would explain that despite the increased endothelial dysfunction respect wild-type mice, the comparison with mouse model with similar total cholesterol levels did not show increase in atherosclerosis.

This combined analysis suggests that overexpression of LCAT does not improve endothelial protection not does it enhance atherosclerosis.

The in vitro and in vivo data described in the present thesis suggest that the specific HDL subpopulations which accumulate in LCAT deficiency [120], mainly small discoidal pre-β HDL, are more effective in maintaining endothelial homeostasis than control HDL. On the contrary, the large HDL formed when LCAT is overexpressed are less efficient than control HDL in regulating vascular tone and inflammation, probably also due to the lack of CETP in mice.

Data shown in this work together with previous study on efflux cholesterol capacity [146] and carotid intima-media thickness evaluation in LCAT deficient subjects [119] demonstrate that carriers of LCAT mutations are not exposed to higher cardiovascular risk compared to subjects with HDL levels in normal range. Moreover, this finding is also in agreement with recent data on general population in which LCAT mass was positively related to IMT and cardiovascular risk [140, 142].

The second objective of the present study was to evaluate the role of abnormal lipoproteins present in plasma of carriers of LCAT deficiency in renal injury. Renal failure is the first cause of morbility and mortality in LCAT deficient carriers, but the cause of kidney injury is poorly understood. A possible implication of LpX, an abnormal lipoprotein detected in plasma of LCAT deficient homozygous carriers [126], has been suggested in earlier reports [127, 130]. Urine albumin is one of the key markers for chronic kidney disease. The gold standard to measure urine albumin excretion is a 24-h urine collection; however microalbumin to creatinine ratio (UACR) measurement in urine is a more convenient method to assess renal dysfunction and may be less prone to errors due to improper collection methods and variations in 24-h protein excretion compared with a random urine specimen [178]. Microalbumin to creatinine ratio was measured in mice urine before and 24 h after single LpX injection; LCAT KO mice showed significant increase in UACR compared with baseline levels, whereas no change was observed in wild-type mice, suggesting that the LCAT knockout condition is crucial to develop LpX-mediated kidney injury. When LDL with the same amount of cholesterol was injected in mice that lacked LCAT, no significant changes were observed compared with baseline levels. This is probably due to the different forms of cholesterol contained in the two particles; LpX contains only unesterified

cholesterol, whereas in LDL cholesterol is mainly esterified. Previously, it was demonstrated that ratio free cholesterol tocholesterol ester is specifically increased in damaged kidney [179]. Microalbumin to creatinine ratio measured 48 h after multiple LpX injection was consistently increased during the 4 weeks, suggesting that the chronic exposure to LpX increases kidney damage.

The analysis of genes involved in nephrotoxic pathway highlighted the inflammatory status of kidneys of LCAT knockout mice after 4 weeks of chronic LpX exposure. Vasoactive compounds, growth factors and cytokines have a role in the progression of renal disease promoting cell growth and fibrosis; up-regulation of genes associated with adhesion molecule VCAM-1 and cytokines such as CXCL10 and Spp1 was found in LCAT knockout injected with LpX for 1 month. Expression of VCAM-1 and MCP-1, one of the key chemokines that regulate migration and infiltration of monocytes/macrophage [180], was also enhanced in tubular cells exposed to sera from LCAT-deficient patients.These findings underlie inflammatory kidneys status, resulting in associated fibrosis [181].

Oxidative stress in another feature of kidney disease; it mediates a large number of renal impairments, from acute renal failure, rhabdomyolysis, obstructive nephropathy, hyperlipidemia, and glomerular damage to chronic renal failure and hemodialysis [182].

Among genes involved in oxidative stress, Nox4 has been implicated in the basal production of ROS in the kidney. Under pathologic conditions such as diabetic nephropathy and chronic kidney disease, up-regulation of Nox4 was described as crucial in renal oxidative stress and kidney injury [183]. Hmox2 is also implicated in ROS generation and it was up-regulated after LpX injection. Data from in vitro studies on tubular cells showed overexpression of NADPH after incubation with LCAT deficiency serum. The direct measurement of ROS production in tubular cells after exposure to sera from carriers of LCAT mutations confirmed the higher oxidative stress related to abnormal lipoprotein profile in LCAT deficiency compared with normal lipoprotein profile in control subjects.

Pathogenesis of renal disease in LCAT deficient patients is not clear and it is difficult to establish whether it is related to tubular sclerosis or glomerulosclerosis. Evidences of both tubular and glomerular disease are evident in the experiments

performed. Confocal analysis highlighted LpX deposition mainly in tubular cells, but histological Masson trichrome stain showed evidence of severe glomerulosclerosis in mice injected with LpX. Histological analysis showed a disorganization in glomerulus structure with capillary tube collapse and mesangial matrix expansion.In glomerulus, both mesangial and podocyte cells are able to internalize LpX. Once internalized in mesangial cells, LpX could promote apoptosis as demonstrated by overexpression of Atf3 and Gadd45α genes after LpX chronic exposure. Atf3 is an immediate early gene and promotes glomerular mesangial cell apoptosis, which is considered a contributor to the initiation of nephritis. Increase of Atf3 expression has a promoting role in glomerular cells apoptosis with a mechanism that directly involves up-regulation of Gadd45α gene expression [184].

Once internalized in podocytes, LpX promotes up-regulation of UCH-L1 expression. It was previously demonstrated that UCH-L1 expression in podocytes is significantly higher in different kidney diseases such as acute proliferative glomerulonephritis, lupus nephritis,membranous glomerulonephritis and IgA nephropathy than that in focal segmental glomerulosclerosis [185]. On the other hand, LpX has toxic activity also in tubular cells. Significant increase in tubular cells apoptosis was observed after incubation with serum from carriers of two mutant LCAT alleles.

Furthermore, up-regulation of genes related to tubular toxicity, such as Nqo1 and Cyr61, was observed in mice treated for 1 month with LpX. It was previously demonstrated that Cyr61 plays a functional role in the pathogenesis of renal tubulointerstitial fibrosis [186].

In summary, in this work was shown that LpX is involved in renal disease pathogenesis with a non-specific pathway that allows mesangial, podocyte and tubular cell injury. The lack of LCAT enzyme is clearly crucial for kidney injury mediated by LpX; indeed in wild-type mice LpX did not show any signs of kidney injury. Future studies should investigate the reversibility of glomerulosclerosis under LCAT replacement therapy or with other pharmacological treatments.

In conclusion, the experiments described in the present work helped in clarifying the role of the LCAT enzyme, a key player in lipid metabolism, in HDL-mediated

endothelial protection and in the kidney injury observed in LCAT deficiency. The work was made possible by the availability of a large series of American and Italian families carrying LCAT gene mutations collected and characterized in the last decade.

References

1. WHO Atlas of Heart Disease and Stroke, 2008
2. Brown D. Cardiovascular Plaque Rupture.New York; 2002; Marcel Dekker
3. Sirtori C, Colli S. La placca aterosclerotica: basi biologiche, metodi di valutazione e controllo farmacologico. In: Tremoli E, Calabresi L, Franceschini G, Sirtori C. Farmacoterapia cardiovascolare. UTET 2006
4. Kwiterovich PO The John Hopkins Textbook of Dyslipidemia chapter 1. Philadelphia, USA: Lippincott Willams and Wilkins, 2010
5. Medical 2000
6. Franceschini G, Calabresi L, Corsini A. Controllo farmacologico della lesione aterosclerotica: terapia delle displipidemie. In: Tremoli E, Calabresi L, Franceschini G, Sirtori C. Farmacoterapia cardiovascolare. UTET 2006
7. Hegele R. A. Plasma lipoproteins: genetic influences and clinical implications. Nature Reviews Genetics 2009;10, 109-121
8. Calabresi L, Gomaraschi M, Franceschini G. High-Density Lipoprotein Quantity or Quality for Cardiovascular Prevention? Current Pharmaceutical Design, 2010; 16, 1494-1503
9. Gu F, Jones MK, Chen J, Patterson JC, Catte A, Jerome WG, Li L, Segrest JP. Structures of discoidal high density lipoproteins: A combined computational-experimental approach. J Biol Chem 2010; 285: 4652-65.
10. Anantharamaiah GM, Brouillette CG, Engler JA, De Loof H, Venkatachalapathi YV, Boogaerts J, Segrest JP. Role of amphipathic helixes in HDL structure/function. Adv Exp Med Biol 1991; 285:131-40.
11. Tall AR, Jiang X, Luo Y, Silver D. Lipid transfer proteins, HDL metabolism, and atherogenesis. Arterioscler Thromb Vasc Biol 2000; 20: 1185-8.
12. Mishra VK, Palgunachari MN, Segrest JP, Anantharamaiah GM. Interactions of synthetic peptide analogs of the class A amphipathic helix with lipids. Evidence for the snorkel hypothesis. J Biol Chem 1994; 269: 7185-91.
13. Segrest JP, Garber DW, Brouillette CG, Harvey SC, Anantharamaiah GM. The amphipathic alpha helix: a multifunctional structural motif in plasma apolipoproteins. Adv Protein Chem 1994; 45: 303-69.
14. Heinecke JW. The HDL proteome: a marker--and perhaps mediator--of coronary artery disease. J Lipid Res 2009; 50 (Suppl): S167-71.

15. Nichols AV, Krauss RM, Musliner TA. Nondenaturing polyacrylamide gradient gel electrophoresis. Methods Enzymol 1986; 128: 417-31.
16. Ikewaki K, Rader DJ, Schaefer JR, Fairwell T, Zech LA, Brewer HBJr. Evaluation of apoA-I kinetics in humans using simultaneous endogenous stable isotope and exogenous radiotracer methods. J Lipid Res 1993; 34: 2207-15.
17. Huuskonen J, Olkkonen VM, Jauhiainen M, Ehnholm C. The Impact of phospholipid transfer protein (PLTP) on HDL metabolism. Atherosclerosis 2001; 155: 269-81.
18. Chisholm JW, Burleson ER, Shelness GS, Parks JS. ApoA-I secretion from HepG2 cells. Evidence for the secretion of both lipid-poor apoA-I and intracellularly assembled nascent HDL. J Lipid Res 2002; 43: 36-44.
19. Edelstein, C., J. I. Gordon, K. Toscas, H. F. Sims, A. W. Strauss, and A. M. Scanu. In vitro conversion of proapoprotein A-I to apoprotein A-I. Partial characterization of an extracellular enzyme activity. J. Biol. Chem 1983.;258: 11430–11433.
20. Tsujita M, Wu CA, be-Dohmae S, Usui S, Okazaki M, YokoyamaS. On the hepatic mechanism of HDL assembly by the ABCA1/apoA-I pathway. J Lipid Res 2005; 46: 154-62.
21. Jonas A. Lecithin cholesterol acyltransferase. Biochim Biophys Acta 2000; 1529: 245-56.
22. Zechner R, Dieplinger H, Steyer H, Groener JE, Calvert GD, Kostner GM. In vitro formation of HDL-2 from HDL-3 and triacylglycerol-rich lipoproteins by the action of lecithin:cholesterol acyltransferase and cholesterol ester transfer lipoprotein. Biochim Biophys Acta 1987; 918: 27-36.
23. Clay MA, Newnham HH, Forte TM, Barter PJ. Cholesteryl ester transfer protein and hepatic lipase activity promote shedding of apoA-I from HDL and subsequent formation of discoidal HDL.Biochim Biophys Acta 1992; 1124: 52-8.
24. Jahangiri A, Rader DJ, Marchadier D, Curtiss LK, Bonnet DJ, Rye KA. Evidence that endothelial lipase remodels high density lipoproteins without mediating the dissociation of apolipoprotein A-I. J Lipid Res 2005; 46: 896-903.

25. Rye KA, Barter PJ. Formation and metabolism of prebetamigrating, lipid-poor apolipoprotein A-I. Arterioscler Thromb Vasc Biol 2004; 24: 421-8.
26. Rigotti A, Trigatti B, Babitt J, Penman M, Xu S, Krieger M. Scavenger receptor BI--a cell surface receptor for high density lipoprotein. Curr Opin Lipidol 1997; 8: 181-8.
27. Wang N, Arai T, Ji Y, Rinninger F, Tall AR. Liver-specific overexpression of scavenger receptor BI decreases levels of very low density lipoprotein ApoB, low density lipoprotein ApoB, and high density lipoprotein in transgenic mice. J Biol Chem 1998; 273: 32920-6.
28. Webb NR, De Beer MC, Asztalos BF, Whitaker N, Van der Westhuyzen DR, De Beer FC. Remodeling of HDL remnants generated by scavenger receptor class B type I. J Lipid Res 2004; 45: 1666-73.
29. Eckhardt ER, Cai L, Sun B, Webb NR, Van der Westhuyzen DR. High density lipoprotein uptake by scavenger receptor SR-BII. J Biol Chem 2004; 279: 14372-81.
30. Martinez LO, Jacquet S, Esteve JP, Rolland C, Cabezon E, Champagne E, Pineau T, Georgeaud V, Walker JE, Tercé F, Collet X, Perret B, Barbaras R. Ectopic beta-chain of ATP synthase is an apolipoprotein A-I receptor in hepatic HDL endocytosis. Nature 2003; 421: 75-9.
31. Jauhiainen M, Metso J, Pahlman R, Blomqvist S, van Tol A, Ehnholm C. Human plasma phospholipid transfer protein causes high density lipoprotein conversion. J Biol Chem 1993; 268: 4032-6.
32. Glass CK, Pittman RC, Keller GA, Steinberg D. Tissue sites of degradation of apoprotein A-I in the rat. J Biol Chem 1983; 258:7161-7.
33. Moestrup SK, Nielsen LB. The role of the kidney in lipid metabolism. Curr Opin Lipidol 2005; 16: 301-6.
34. Moestrup SK, Kozyraki R. Cubilin, a high-density lipoprotein receptor. Curr Opin Lipidol 2000; 11: 133-40.
35. Kozyraki R, Fyfe J, Kristiansen M, Gerdes C, Jacobsen C, Cui S, Christensen EI, Aminoff M, de la Chapelle A, Krahe R, Verroust PJ, Moestrup SK. The intrinsic factor-vitamin B12 receptor, cubilin, is a highaffinity apolipoprotein A-I receptor facilitating endocytosis of high-density lipoprotein. Nat Med 1999; 5: 656-61.

36. Braschi S, Neville TA, Vohl MC, Sparks DL. Apolipoprotein A-I charge and conformation regulate the clearance of reconstituted high density lipoprotein in vivo. J Lipid Res 1999; 40: 522-32.
37. Schaefer EJ, Zech LA, Jenkins LL, Bronzert TJ, Rubalcaba EA, Lindgren FT, Aamodt RL, Brewer HB Jr. Human apolipoprotein A-I and A-II metabolism. J Lipid Res 1982; 23: 850-62.
38. Brinton EA, Eisenberg S, Breslow JL. Elevated high density lipoprotein cholesterol levels correlate with decreased apolipoprotein A-I and A-II fractional catabolic rate in women. J Clin Invest 1989; 84: 262-9.
39. Rader DJ, Castro G, Zech LA, Fruchart JC, Brewer HB Jr. In vivo metabolism of apolipoprotein A-I on high density lipoprotein particles LpA-I and LpA-I,A-II. J Lipid Res 1991; 32: 1849-59.
40. Lamarche B, Uffelman KD, Carpentier A, Cohn JS, Steiner G, Barrett PH, Lewis GF. Triglyceride enrichment of HDL enhances in vivo metabolic clearance of HDL apo A-I in healthy men. J Clin Invest 1999; 103: 1191-9.
41. Jessup W, Gelissen IC, Gaus K, Kritharides L. Roles of ATP binding cassette transporters A1 and G1, scavenger receptor BI and membrane lipid domains in cholesterol export from macrophages. Curr Opin Lipidol 2006; 17: 247-57.
42. Favari E, Calabresi L, Adorni MP, Jessup W, Simonelli S, Franceschini G, Bernini F. Small discoidal pre-beta1 HDL particles are efficient acceptors of cell cholesterol via ABCA1 and ABCG1. Biochemistry 2009; 48: 11067-74.
43. Favari E, Lee M, Calabresi L, Franceschini G, Zimetti F, Bernini F, Kovanen PT. Depletion of pre-beta-high density lipoprotein by human chymase impairs ATP-binding Cassette Transporter A1- but not Scavenger Receptor Class B Type I-mediated lipid efflux to high density lipoprotein. J Biol Chem 2004; 279: 9930-6
44. Wang X, Collins HL, Ranalletta M, Fuki IV, Billheimer JT, Rothblat GH, Tall AR, Rader DJ. Macrophage ABCA1 and ABCG1, but not SRBI, promote macrophage reverse cholesterol transport in vivo. J Clin Invest 2007; 117: 2216-24.
45. Tanigawa H, Billheimer JT, Tohyama J, Fuki IV, Ng DS, Rothblat GH, Rader DJ. Lecithin: cholesterol acyltransferase expression has minimal effects on macrophage reverse cholesterol transport in vivo. Circulation 2009; 120: 160-9.

46. Calabresi L, Favari E, Moleri E, Adorni MP, Pedrelli M, Costa S, Jessup W, Gelissen IC, Kovanen PT, Bernini F, Franceschini G. Functional LCAT is not required for macrophage cholesterol efflux to human serum. Atherosclerosis 2009; 204: 141-6.
47. Ji Y, Wang N, Ramakrishnan R, Sehayek E, Huszar D, Breslow JL, Tall AR. Hepatic scavenger receptor BI promotes rapid clearance of high density lipoprotein free cholesterol and its transport into bile. J Biol Chem 1999; 274: 33398-402.
48. Tabet F, Rye KA: High-density lipoproteins, inflammation and oxidative stress. Clin.Sci. 2009;116, 87-98.
49. Mineo C, Shaul PW: Novel biological functions of high-density lipoprotein cholesterol. Circ. Res. 2012;111, 1079-1090.
50. Calabresi L, Gomaraschi M, Franceschini G: Endothelial protection by high-density lipoproteins: from bench to bedside. Arterioscler. Thromb. Vasc. Biol. 2003;23, 1724-1731.
51. Kuvin JT, Ramet ME, Patel AR et al: A novel mechanism for the beneficial vascular effects of high-density lipoprotein cholesterol: enhanced vasorelaxation and increased endothelial nitric oxide synthase expression. Am. Heart J. 2002;144, 165-172.
52. Ramet ME, Ramet M, Lu Q et al: High-density lipoprotein increases the abundance of eNOS protein in human vascular endothelial cells by increasing its half-life. J. Am. Coll. Cardiol. 2003;41, 2288-2297.
53. Gomaraschi M, Baldassarre D, Amato M et al: Normal vascular function despite low levels of high-density lipoprotein cholesterol in carriers of the apolipoprotein AI(Milano) mutant. Circulation 2007;116, 2165-2172.
54. Yuhanna IS, Zhu Y, Cox BE et al: High-density lipoprotein binding to scavenger receptor-BI activates endothelial nitric oxide synthase. Nat. Med. 2001;7, 853-857.
55. Fulton D, Gratton JP, Sessa WC: Post-translational control of endothelial nitric oxide synthase: why isn't calcium/calmodulin enough? J. Pharmacol. Exp. Ther. 2001;299, 818-824.
56. Mineo C, Yuhanna IS, Quon MJ, Shaul PW: High density lipoprotein-induced endothelial nitric-oxide synthase activation is mediated by Akt and MAP kinases. J. Biol. Chem. 2003;278, 9142-9149.

57. Nofer JR, van der Giet M, Tolle M et al: HDL induces NO-dependent vasorelaxation via the lysophospholipid receptor S1P3. J. Clin. Invest. 2004;113, 569-581.
58. Christoffersen C, Obinata H, Kumaraswamy SB et al: Endothelium-protective sphingosine-1-phosphate provided by HDL-associated apolipoprotein M. Proc. Natl.Acad. Sci. U. S. A. 2001;108, 9613-9618.
59. Pomerantz KB, Fleisher LN, Tall AR, Cannon PJ: Enrichment of endothelial cell arachidonate by lipid transfer from high density lipoproteins: relationship to prostaglandin I2 synthesis. J. Lipid Res. 1985;26, 1269-1276.
60. Tamagaki T, Sawada S, Imamura H et al: Effects of high-density lipoproteins on intracellular pH and proliferation of human vascular endothelial cells. Atherosclerosis 1996;123, 73-82 .
61. Van Sickle WA, Wilcox HG, Malik KU, Nasjletti A: High density lipoprotein-induced cardiac prostacyclin synthesis in vitro: relationship to cardiac arachidonate mobilization. J. Lipid Res. 1986;27, 517-522.
62. Kaul S, Coin B, Hedayiti A et al: Rapid reversal of endothelial dysfunction in hypercholesterolemic apolipoprotein E-null mice by recombinant apolipoprotein AI(Milano)-phospholipid complex. J. Am. Coll. Cardiol. 2004;44, 1311-1319.
63. Kuvin JT, Patel AR, Sidhu M et al: Relation between high-density lipoprotein cholesterol and peripheral vasomotor function. Am. J. Cardiol. 2003;92, 275-279.
64. Lupattelli G, Marchesi S, Roscini A et al: Direct association between high-density lipoprotein cholesterol and endothelial function in hyperlipemia. Am. J. Cardiol. 2002;90, 648-650.
65. O'Brien SF, Watts GF, Playford DA et al: Low-density lipoprotein size, high-density lipoprotein concentration, and endothelial dysfunction in non-insulin-dependent diabetes. Diabet. Med. 1997;14, 974-978.
66. Zhang X, Zhao SP, Li XP, Gao M, Zhou QC: Endothelium-dependent and -independent functions are impaired in patients with coronary heart disease. Atherosclerosis 2000;149, 19-24.
67. Spieker LE, Sudano I, Hurlimann D et al: High-density lipoprotein restores endothelial function in hypercholesterolemic men. Circulation 2002;105, 1399-1402.

68. Bisoendial RJ, Hovingh GK, Levels JH et al: Restoration of endothelial function by increasing high-density lipoprotein in subjects with isolated low high-density lipoprotein. Circulation 2003;107, 2944-2948.
69. Davies MJ, Gordon JL, Gearing AJ et al: The expression of the adhesion molecules ICAM-1, VCAM-1, PECAM, and E-selectin in human atherosclerosis. J. Pathol. 1993;171, 223-229.
70. Gearing AJ, Newman W: Circulating adhesion molecules in disease. Immunol. Today 1993;14, 506-512.
71. Galkina E, Ley K.Vascular adhesion molecules in atherosclerosis. Arterioscler Thromb Vasc Biol. 2007;27(11):2292-301
72. Barter PJ, Baker PW, Rye KA: Effect of high-density lipoproteins on the expression of adhesion molecules in endothelial cells. Curr. Opin. Lipidol. 2002;13, 285-288.
73. Calabresi L, Franceschini G, Sirtori CR et al: Inhibition of VCAM-1 expression in endothelial cells by reconstituted high density lipoproteins. Biochem. Biophys. Res. Commun. 1997;238, 61-65.
74. Xia P, Vadas MA, Rye KA, Barter PJ, Gamble JR: High density lipoproteins (HDL) interrupt the sphingosine kinase signaling pathway. A possible mechanism for protection against atherosclerosis by HDL. J. Biol. Chem. 1999;274, 33143-33147.
75. Kimura T, Tomura H, Mogi C et al: Role of scavenger receptor class B type I and sphingosine 1-phosphate receptors in high-density lipoprotein-induced inhibition of adhesion molecule expression in endothelial cells. J. Biol. Chem. 2006;281, 37457-37467.
76. McGrath KC, Li XH, Puranik R et al: Role of 3beta-hydroxysteroid-Delta 24 reductase in mediating antiinflammatory effects of high-density lipoproteins in endothelial cells. Arterioscler. Thromb. Vasc. Biol. 2009;29, 877-882.
77. Ashby DT, Rye KA, Clay MA et al: Factors influencing the ability of HDL to inhibit expression of vascular cell adhesion molecule-1 in endothelial cells. Arterioscler. Thromb. Vasc. Biol. 1998;18, 1450-1455.
78. Gomaraschi M, Calabresi L, Rossoni G et al: Anti-inflammatory and cardioprotective activities of synthetic high-density lipoprotein containing apolipoprotein A-I mimetic peptides. J. Pharmacol. Exp. Ther. 2008;324, 776-783.

79. Baker PW, Rye KA, Gamble JR, Vadas MA, Barter PJ: Phospholipid composition of reconstituted high density lipoproteins influences their ability to inhibit endothelial cell adhesion molecule expression. J. Lipid Res. 2000;41, 1261-1267.
80. Calabresi L, Gomaraschi M, Villa B et al: Elevated soluble cellular adhesion molecules in subjects with low HDL-cholesterol. Arterioscler. Thromb. Vasc. Biol. 2002;22, 656-661.
81. Birjmohun RS, van Leuven SI, Levels JH et al: High-density lipoprotein attenuates inflammation and coagulation response on endotoxin challenge in humans. Arterioscler. Thromb. Vasc. Biol. 2007;27, 1153-1158.
82. Nicholls SJ, Lundman P, Harmer JA et al: Consumption of saturated fat impairs the anti-inflammatory properties of high-density lipoproteins and endothelial function. J. Am. Coll. Cardiol. 2006;48, 715-720.
83. Deanfield JE, Halcox JP, Rabelink TJ: Endothelial function and dysfunction: testing and clinical relevance. Circulation 2007;115, 1285-1295.
84. Nofer JR, Levkau B, Wolinska I et al: Suppression of endothelial cell apoptosis by high density lipoproteins (HDL) and HDL-associated lysosphingolipids. J. Biol. Chem. 2001;276, 34480-34485.
85. Sugano M, Tsuchida K, Makino N: High-density lipoproteins protect endothelial cells from tumor necrosis factor-alpha-induced apoptosis. Biochem. Biophys. Res. Commun. 2000;272, 872-876.
86. Tso C, Martinic G, Fan WH et al: High-density lipoproteins enhance progenitormediated endothelium repair in mice. Arterioscler. Thromb. Vasc. Biol. 2006;26, 1144-1149.
87. Noor R, Shuaib U, Wang CX et al: High-density lipoprotein cholesterol regulates endothelial progenitor cells by increasing eNOS and preventing apoptosis. Atherosclerosis 2007;192, 92-99.
88. Huang CY, Lin FY, Shih CM et al: Moderate to high concentrations of high-density lipoprotein from healthy subjects paradoxically impair human endothelial progenitor cells and related angiogenesis by activating rho-associated kinase pathways. Arterioscler. Thromb. Vasc. Biol. 2012;32, 2405-2417.

89. Gomaraschi M, Ossoli A, Vitali C, Calabresi L. HDL and endothelial protection: examining evidence from inherited HDL disorders. Clinical Lipidology 2013;8(3):361-370
90. Calabresi L, Pisciotta L, Costantin A et al: The molecular basis of lecithin:cholesterol acyltransferase deficiency syndromes: a comprehensive study ofmolecular and biochemical findings in 13 unrelated Italian families. Arterioscler Thromb Vasc Biol 2010;25, 1972-1978.
91. Asztalos BF, Schaefer EJ, Horvath KV et al: Role of LCAT in HDL remodeling: investigation of LCAT deficiency states. J. Lipid Res. 2007;48, 592-599.
92. Calabresi L, Simonelli S, Gomaraschi M, Franceschini G.: Genetic lecithin:cholesterol acyltransferase deficiency and cardiovascular disease. Atherosclerosis. 2012;222(2):299-30
93. Rousset X, Vaisman B, Amar M, Sethi AA, Remaley AT. Lecithin: cholesterol acyltransferase--from biochemistry to role in cardiovascular disease. Curr Opin Endocrinol Diabetes Obes. 2009;16(2):163-71.
94. Kosek AB, Durbin D, Jonas A. Binding affinity and reactivity of lecithin cholesterol acyltransferase with native lipoproteins.Biochem Biophys Res Commun. 1999;258(3):548-51.
95. Chang TY, Li BL, Chang CC, Urano Y. Acyl-coenzyme A:cholesterol acyltransferases. Am J Physiol Endocrinol Metab 2009;297(1):E1–9.
96. Liu M, Subbaiah PV . Activation of plasma lysolecithin acyltransferase reaction by apolipoproteins A-I, C-I and E. Biochim Biophys Acta. 1993;1168(2):144-52.
97. Cho KH, Durbin DM, Jonas A. Role of individual amino acids of apolipoprotein A-I in the activation of lecithin:cholesterol acyltransferase and in HDL rearrangements. J Lipid Res 2001;42(3):379–89.
98. Segrest JP, Jones MK, Catte A, Thirumuruganandham SP. Validation of previous computer models and MD simulations of discoidal HDL by a recent crystal structure of apoA-I. J Lipid Res 2012;53(9):1851–63.
99. Hirsch-Reinshagen V, Donkin J, Stukas S, Chan J, Wilkinson A, Fan J, Parks JS, Kuivenhoven JA, Lütjohann D, Pritchard H, Wellington CL. LCAT synthesized by primary astrocytes esterifies cholesterol on glia-derived lipoproteins. J Lipid Res. 2009;50(5):885-93

100. Subbaiah PV, Liu M. Role of sphingomyelin in the regulation of cholesterol esterificationin the plasma lipoproteins. Inhibition of lecithin-cholesterol acyltransferase reaction. J Biol Chem 1993;268(27):20156–63.
101. Subbaiah PV, Jiang XC, Belikova NA, Aizezi B, Huang ZH, Reardon CA. Regulation of plasma cholesterol esterification by sphingomyelin: effect of physiological variations of plasma sphingomyelin on lecithin-cholesterol acyltransferase activity. Biochim Biophys Acta 2012;1821(6):908–13.
102. Subbaiah PV, Liu M. Disparate effects of oxidation on plasma acyltransferase activities:inhibition of cholesterol esterification but stimulation of transesterification of oxidized phospholipids. Biochim Biophys Acta 1996;1301(1-2):115–26.
103. Subbaiah PV, Subramanian VS, Liu M. Trans unsaturated fatty acids inhibit lecithin:cholesterol acyltransferase and alter its positional specificity. J Lipid Res 1998;39(7):1438–47.
104. Soutar AK, Garner CW, Baker HN, Sparrow JT, Jackson RL, Gotto AM, Smith LC. Effect of the human plasma apolipoproteins and phosphatidylcholine acyl donor on the activity of lecithin: cholesterol acyltransferase. Biochemistry. 1975;14(14):3057-64.
105. Escolà-Gil JC, Marzal-Casacuberta A, Julve-Gil J, Ishida BY, Ordóñez-Llanos J, Chan L, González-Sastre F, Blanco-Vaca F.Human apolipoprotein A-II is a pro-atherogenic molecule when it is expressed in transgenic mice at a level similar to that in humans: evidence of a potentially relevant species-specific interaction with diet. J Lipid Res. 1998;39(2):457-62
106. Clay MA, Pyle DH, Rye KA, Barter PJ. Formation of spherical, reconstituted high density lipoproteins containing both apolipoproteins A-I and A-II is mediated by lecithin:cholesterol acyltransferase. J Biol Chem. 2000;275(12):9019-25.
107. Nakamura Y, Kotite L, Gan Y, Spencer TA, Fielding CJ, Fielding PE. Molecular mechanism of reverse cholesterol transport: reaction of pre-beta-migrating high-density lipoprotein with plasma lecithin/cholesterol acyltransferase. Biochemistry 2004;43:14811–20.
108. Rye KA, Barter PJ. Formation and metabolism of prebeta-migrating, lipid-poor apolipoprotein A-I. Arterioscler Thromb Vasc Biol 2004;24:421–8.

109. Glomset JA. The plasma lecithin:cholesterol acyltransferase reaction. J Lipid Res 1968;9:155–62.
110. Matsuura F, Wang N, Chen W, Jiang XC, Tall AR. HDL from CETP-deficient subjects shows enhanced ability to promote cholesterol efflux from macrophages in an apoE- and ABCG1-dependent pathway. J Clin Invest 2006;116:1435–42.
111. Favari E, Lee M, Calabresi L, Franceschini G, Zimetti F, Bernini F, Kovanen PT. Depletion of pre-beta-high density lipoprotein by human chymase impairs ATP-binding Cassette Transporter A1- but not Scavenger Receptor Class B Type I-mediated lipid efflux to high density lipoprotein.J Biol Chem 2004;279:9930–6.
112. Cuchel M, Rader DJ. Macrophage reverse cholesterol transport: key to the regression of atherosclerosis? Circulation 2006;113:2548–55
113. Norum KR, Gjone E. Familial serum-cholesterol esterification failure. A new inborn error of metabolism. Biochim Biophys Acta 1967;144:698–700.
114. Torsvik H, Gjone E, Norum KR. Familial plasma cholesterol ester deficiency.Clinical studies of a family. Acta Med Scand 1968;183:387–91.
115. http://www.lcat.it/database.html. Interrogated July10, 2011.
116. Santamarina-Fojo S, Hoeg JM, Assmann G, Brewer Jr HB. Lecithin cholesterol acyltransferase deficiency and fish eye disease. In: Scriver CR, Beaudet AL, Sly WS, Valle D, editors. The metabolic and molecular bases of inherited diseases. New York: McGraw-Hill; 2001. p. 2817–33
117. Holleboom AG, Kuivenhoven JA, van Olden CC, Peter J, Schimmel AW, Levels JH, Valentijn RM, Vos P, Defesche JC, Kastelein JJ, Hovingh GK, Stroes ES, Hollak CE. Proteinuria in early childhood due to familial LCAT deficiency caused by loss of a disulfide bond in lecithin:cholesterol acyl transferase. Atherosclerosis 2011;216:161–5.
118. Calabresi L, Pisciotta L, Costantin A, Frigerio I, Eberini I, Alessandrini P, Arca M, Bon GB, Boscutti G, Busnach G, Frascà G, Gesualdo L, Gigante M, Lupattelli G, Montali A, Pizzolitto S, Rabbone I, Rolleri M, Ruotolo G, Sampietro T, Sessa A, Vaudo G, Cantafora A, Veglia F, Calandra S, Bertolini S, Franceschini G. The molecular basis of lecithin:cholesterol acyltransferase deficiency syndromes: a comprehensive study of molecular and biochemical

findings in 13 unrelated Italian families. Arterioscler Thromb Vasc Biol 2005;25:1972–8.

119. Calabresi L, Baldassarre D, Castelnuovo S, Conca P, Bocchi L, Candini C, Frigerio B, Amato M, Sirtori CR, Alessandrini P, Arca M, Boscutti G, Cattin L, Gesualdo L, Sampietro T, Vaudo G, Veglia F, Calandra S, Franceschini G.. Functional lecithin:cholesterol acyltransferase is not required for efficient atheroprotection in humans. Circulation 2009;120:628–35.
120. Asztalos BF, Schaefer EJ, Horvath KV, Yamashita S, Miller M, Franceschini G, Calabresi L. Role of LCAT in HDL remodeling: investigation of LCAT deficiency states. J Lipid Res. 2007;48(3):592-9
121. Cogan DG, Kruth HS, Datilis MB, Martin N. Corneal opacity in LCAT disease. Cornea 1992;11(6):595–9.
122. Suda T, Akamatsu A, Nakaya Y, Masuda Y, Desaki J. Alterations in erythrocyte membrane lipid and its fragility in a patient with familial Lecithin:cholesterol acyltrasferase (LCAT) deficiency. J Med Invest. 2002;49(3-4):147-55.
123. Miarka P, Idzior-Waluś B, Kuźniewski M, Waluś-Miarka M, Klupa T, Sułowicz W. Corticosteroid treatment of kidney disease in a patient with familial lecithin-cholesterol acyltransferase deficiency. Clin Exp Nephrol. 2011;15(3):424-9
124. Boscutti G, Calabresi L, Pizzolitto S, Boer E, Bosco M, Mattei PL, Martone M, Milutinovic N, Berbecar D, Beltram E, Franceschini G. LCAT deficiency: a nephrological diagnosis. G Ital Nefrol. 2011;28(4):369-82
125. Borysiewicz LK, Soutar AK, Evans DJ, Thompson GR, Rees AJ. Renal failure in familial lecithin: cholesterol acyltransferase deficiency. Q J Med 1982;51(204):411–26.
126. Imbasciati E, Paties C, Scarpioni L, Mihatsch MJ. Renal lesions in familial lecithincholesterol acyltransferase deficiency. Ultrastructural heterogeneity of glomerular changes. Am J Nephrol 1986;6(1):66–70.
127. Lager DJ, Rosenberg BF, Shapiro H, Bernstein J. Lecithin cholesterol acyltransferase deficiency: ultrastructural examination of sequential renal biopsies. Mod Pathol1991;4(3):331–5.
128. Sessa A, Battini G, Meroni M, Daidone G, Carnera I, Brambilla PL, Viganò G, Giordano F, Pallotti F, Torri Tarelli L, Calabresi L, Rolleri M, Bertolini S.

Hypocomplementemic type II membranoproliferative glomerulonephritis in a male patient with familial lecithin-cholesterol acyltransferase deficiency due to two different allelic mutations. Nephron. 2001;88:268–72

129. Stoekenbroek RM, van den Bergh Weerman MA, Hovingh GK, Potter van Loon BJ, Siegert CE, Holleboom AG. Familial LCAT deficiency: from renal replacement to enzyme replacement. Neth J Med. 2013;71(1):29-31
130. Narayanan, S. Biochemistry and clinical relevance of lipoproteinX. Ann. Clin. Lab. Sci. 1984;14371-374.
131. Norum, K. R., and E. Gjone. X The effect of plasma transfusion on the plasma cholesterol esters in patients with familial plasma lecithin:cholesterol acyltransferase deficiency.Scand.J Clin. Lab. Invest. 1984;22:339-342.
132. O K, Frohlich J. Role of lecithin:cholesterol acyltransferase and apolipoprotein A-I in cholesterol esterification in lipoprotein-X in vitro. J Lipid Res. 1995;36(11):2344-54.
133. Solajic Bozicevic N, Stavljenic A, Sesto M. Lecithin:cholesterol acyltransferase activity in patients with acute myocardial infarction and coronary heart disease. Artery 1991;18:326–40.
134. Solajic-Bozicevic N, Stavljenic-Rukavina A, Sesto M. Lecithin-cholesterol acryltransferase activity in patients with coronary artery disease examined bycoronary angiography. Clin Investig 1994;72:951–6.
135. Brown BG, Zhao XQ, Chait A, Fisher LD, Cheung MC, Morse JS, Dowdy AA, Marino EK, Bolson EL, Alaupovic P, Frohlich J, Albers JJ. Simvastatin and niacin, antioxidant vitamins,or the combination for the prevention of coronary disease. N Engl J Med2001;345:1583–92.
136. Frohlich J, Dobiasova M. Fractional esterification rate of cholesterol and ratio of triglycerides to HDL-cholesterol are powerful predictors of positive findings on coronary angiography. Clin Chem 2003;49:1873–80
137. Dobiasova M, Frohlich J, Sedova M, Cheung MC, Brown BG. Cholesterol esterification and atherogenic index of plasma correlate with lipoprotein size and findings on coronary angiography. J Lipid Res 2011;52:566–71.
138. Stein JH, Korcarz CE, Hurst RT, Lonn E, Kendall CB, Mohler ER, Najjar SS, Rembold CM, Post WS. Use of carotid ultrasound to identify subclinical vascular disease and evaluate cardiovascular disease risk: a consensus statement from the American Society of Echocardiography Carotid Intima-

Media Thickness Task Force. Endorsed by the Society for Vascular Medicine.J Am Soc Echocardiogr 2008;21:93–111.

139. Dullaart RP, Perton F, Sluiter WJ, De VR, Van TA. Plasma lecithin:cholesterol acyltransferase activity is elevated in metabolic syndrome and is an independent marker of increased carotid artery intima media thickness. J Clin Endocrinol Metab 2008;93:4860–6.
140. Calabresi L, Baldassarre D, Simonelli S, Gomaraschi M, Amato M, Castelnuovo S, Frigerio B, Ravani A, Sansaro D, Kauhanen J, Rauramaa R, de Faire U, Hamsten A, Smit AJ, Mannarino E, Humphries SE, Giral P, Veglia F, Sirtori CR, Franceschini G, Tremoli E. Plasma lecithin:cholesterol acyltransferase and carotid intima-media thickness in European individuals at high cardiovascular risk. J Lipid Res 2011;52:1569–74.
141. Dullaart RP, Perton F, van der Klauw MM, Hillege HL, Sluiter WJ. High plasma lecithin:cholesterol acyltransferase activity does not predict low incidence of cardiovascular events: possible attenuation of cardioprotection associated with high HDL cholesterol. Atherosclerosis 2010;208:537–42.
142. Holleboom AG, Kuivenhoven JA, Vergeer M, Hovingh GK, van Miert JN, Wareham NJ, Kastelein JJ, Khaw KT, Boekholdt SM. Plasma levels of lecithin:cholesterol acyltransferase and risk of future coronary artery disease in apparently healthy men and women: a prospective case-control analysis nested in the EPIC-Norfolk population study. J Lipid Res 2010;51:416–21.
143. Kuivenhoven JA, Pritchard H, Hill J, Frohlich J, Assmann G, Kastelein J. The molecular pathology of lecithin:cholesterol acyltransferase (LCAT) deficiency syndromes. J Lipid Res 1997;38:191–205.
144. Ayyobi AF, McGladdery SH, Chan S, John Mancini GB, Hill JS, Frohlich JJ. Lecithin:cholesterol acyltransferase (LCAT) deficiency and risk of vascular disease: 25 year follow-up. Atherosclerosis 2004;177:361–6.
145. Hovingh GK, Hutten BA, Holleboom AG, Petersen W, Rol P, Stalenhoef A, Zwinderman AH, de Groot E, Kastelein JJ, Kuivenhoven JA. Compromised LCAT function is associated with increased atherosclerosis. Circulation 2005;112:879–84.
146. Calabresi L, Favari E, Moleri E, Adorni MP, Pedrelli M, Costa S, Jessup W, Gelissen IC, Kovanen PT, Bernini F, Franceschini G. Functional LCAT is not

required for macrophage cholesterol efflux to human serum. Atherosclerosis. 2009;204(1):141-6

147. Gelissen IC, Harris M, Rye KA, Quinn C, Brown AJ, Kockx M, Cartland S, Packianathan M, Kritharides L, Jessup W. ABCA1 and ABCG1 synergize to mediate cholesterol export to apoA-I. Arterioscler Thromb Vasc Biol 2006;26:534–40.
148. Yancey PG, Bortnick AE, Kellner-Weibel G, Llera-Moya M, Phillips MC, Rothblat GH. Importance of different pathways of cellular cholesterol efflux. Arterioscler Thromb Vasc Biol 2003;23:712–9.
149. Vaisman , B. L. , H. G. Klein , M. Rouis , A. M. Bérard, M. R. Kindt, G. D. Talley, S. M. Meyn, R. F. Hoyt, Jr., S. M. Marcovina, J. J. Albers, et al. Overexpression of human lecithin cholesterol acyltransferase leads to hyperalphalipoproteinemia in transgenic mice. J. Biol. Chem. 1995;270 : 12269 – 12275
150. Francone , O. L. , E. L. Gong , D. S. Ng , C. J. Fielding , and E. M. Rubin . Expression of human lecithin-cholesterol acyltransferase in transgenic mice. J. Clin. Invest. 1995;96 : 1440 – 1448 .
151. Mehlum , A. , B. Staels , N. Duverger , A. Tailleux , G. Castro , C. Fievet , G. Luc, J. C. Fruchart , G. Olivecrona , G. Skretting , et al .Tissue-specifi c expression of the human gene for lecithin: cholesterol acyltransferase in transgenic mice alters blood lipids, lipoproteins and lipases towards a less atherogenic profile. Eur. J. Biochem. 1995;230 : 567 – 575
152. Kunnen S, Van Eck M. Lecithin:cholesterol acyltransferase: old friend or foe in atherosclerosis? J Lipid Res. 2012 Sep;53(9):1783-99.
153. Bérard , A. M. , B. Föger , A. Remaley , R. Shamburek , B. L. Vaisman , G. Talley , B. Paigen , R. F. Hoyt , Jr ., S. Marcovina , H. B. Brewer , Jr ., et al . High plasma HDL concentrations associated with enhanced atherosclerosis in transgenic mice overexpressing lecithin-cholesteryl acyltransferase. Nat. Med. 1997;3 : 744 – 749 .
154. Berti , J. A. , E. C. de Faria , and H. C. Oliveira . Atherosclerosis in aged mice over-expressing the reverse cholesterol transport genes. Braz. J. Med. Biol. Res. 2005;38 : 391 – 398 .
155. Föger , B. , M. Chase , M. J. Amar , Vaisman BL, Shamburek RD, Paigen B, Fruchart-Najib J, Paiz JA, Koch CA, Hoyt RF, Brewer HB Jr, Santamarina-

Fojo S. Cholesteryl ester transfer protein corrects dysfunctional high density lipoproteins and reduces aortic atherosclerosis in lecithin cholesterol acyltransferase transgenic mice. J. Biol. Chem. 1999;274 : 36912 – 36920 .

156. Sakai , N. , B. L. Vaisman , C. A. Koch , R. F. Hoyt , Jr ., S. M. Meyn ,G. D. Talley , J. A. Paiz , H. B. Brewer , Jr ., and S. Santamarina-Fojo . Targeted disruption of the mouse lecithin:cholesterol acyltransferase (LCAT) gene. Generation of a new animal model for human LCAT defi ciency. J. Biol. Chem. 1997;272 : 7506 – 7510.
157. Ng , D. S. , O. L. Francone , T. M. Forte , J. Zhang , M. Haghpassand , and E. M. Rubin . Disruption of the murine lecithin:cholesterol acyltransferase gene causes impairment of adrenal lipid delivery and up-regulation of scavenger receptor class B type I. J. Biol.Chem. 1997;272 : 15777 – 15781
158. Lambert G, Sakai N, Vaisman BL, Neufeld EB, Marteyn B, Chan CC, Paigen B, Lupia E, Thomas A, Striker LJ, Blanchette-Mackie J, Csako G, Brady JN, Costello R, Striker GE, Remaley AT, Brewer HB Jr, Santamarina-Fojo S. Glomerulosclerosis and atherosclerosis in lecithin cholesterolacyltransferase-deficient mice. J. Biol. Chem. 2001;276 : 15090 – 15098
159. Furbee Jr JW, Sawyer JK, Parks JS. Lecithin:cholesterol acyltransferase deficiency increases atherosclerosis in the low density lipoprotein receptor and apolipoprotein E knockout mice. J Biol Chem 2002;277(5):3511–9.
160. Hoeg JM, Santamarina-Fojo S, Bérard AM, Cornhill JF, Herderick EE, Feldman SH, Haudenschild CC, Vaisman BL, Hoyt RF Jr, Demosky SJ Jr, Kauffman RD, Hazel CM, Marcovina SM, Brewer HB Jr.. Overexpression of lecithin: cholesterol acyltransferase in transgenic rabbits prevents diet-induced atherosclerosis. Proc. Natl. Acad. Sci. USA . 1996;93 :11448 – 11453 .
161. Brousseau , M. E. , S. Santamarina-Fojo , L. A. Zech , A. M. Bérard , B. L. Vaisman , S. M. Meyn , D. Powell , H. B. Brewer , Jr ., and J. M. Hoeg . Hyperalphalipo-proteinemia in human lecithin cholesterol acyltransferase transgenic rabbits. J. Clin. Invest. 1996;97 : 1844 – 1851
162. Zhu X, Herzenberg AM, Eskandarian M, Maguire GF, Scholey JW, Connelly PW, Ng DS. A novel in vivo lecithin-cholesterol acyltransferase (LCAT)-deficient mouse expressing predominantly LpX is associated with spontaneous glomerulopathy. Am J Pathol. 2004;165(4):1269-78

163. Yee MS, Pavitt DV, Richmond W, Cook HT, McLean AG, Valabhji J, Elkeles RS.Changes in lipoprotein profile and urinary albumin excretion in familial LCAT deficiency with lipid lowering therapy.Atherosclerosis. 2009;205(2):528-32.
164. Aranda P, Valdivielso P, Pisciotta L, Garcia I, Garcã A-Arias C, Bertolini S, Martã N-Reyes G, Gonzã Lez-Santos, Calandra S. Therapeutic management of a new case of LCAT deficiency with a multifactorial long-term approach based on high doses of angiotensin II receptor blockers (ARBs).Clin Nephrol. 2008;69(3):213-8.
165. Panescu V., Grignon Y., Hestin D., Rostoker G., Frimat L., Renoult E., Gamberoni J., Grignon G. and Kessler M. Recurrence of lecithin cholesterol acyltransferase deficiency after kidney transplantation. Nephrol Dial Transplant 1997;12: 2430–2432.
166. Murayama N, Asano Y, Kato K, Sakamoto Y, Hosoda S, Yamada N, Kodama T, Murase T, Akanuma Y. Effects of plasma infusion on plasma lipids, apoproteins and plasma enzyme activities in familial lecithin: cholesterol acyltransferase deficiency. European Journal of Clinical Investigation 1984;14:122-9.
167. Wood S. Recombinant human LCAT raises HDL in rare lipoprotein disorder. http://www theheart org/article/1547141 do 2013.
168. Frank Kayser ML, Bei Shan, Jian Zhang, Mingyue Zhou, inventor Amgen Inc.,assignee. Methods for Treating Atherosclerosis. United States patent US 2008/0096900 A1. 04/24/2008.
169. Zhou MFP, Zhang J. Novel small molecule LCAT activators raise HDL levels inrodent models. Arterioscler Thromb Vasc Biol 2008;28:E65–6.
170. Chen Z, Wang SP, Krsmanovic ML, Castro-Perez J, Gagen K, Mendoza V, et al. Small molecule activation of lecithin cholesterol acyltransferase modulates lipoprotein metabolism in mice and hamsters. Metabolism 2012;61(4):470–81.
171. Murray RL: in Methods in Clinical Chemistry, AJ Pesce and LA Kaplan, ed, CV Mosby Co, St. Louis, pp 10-17, 1987
172. Heinegard D and Tiderstrom G. Determination of serum creatinine by a direct colorimetric method Clin Chim Acta 1973;43:305.

173. Yeboah J, Folsom AR, Burke GL, Johnson C, Polak JF, Post W, Lima JA, Crouse JR, Herrington DM. Predictive value of brachial flow-mediated dilation for incident cardiovascular events in a population-based study: the multi-ethnic study of atherosclerosis. Circulation 2009;120:502–9
174. Savill JS, Mooney AF, Hughes J: Apoptosis in acute renal inflammation. In: Immunologic Renal Disease, edited by Neilson G, Couser WG, Philadelphia, Lippincott-Raven, 1997;309 -329
175. Activation of nitric oxide synthase in endothelial cells by Akt-dependent phosphorylation. Nature. 1999; 399, 601-605.
176. Yanagisawa M, Kurihara H, Kimura S, Tomobe Y, Kobayashi M, Mitsui Y, Yazaki Y, Goto K, Masaki T. A novel potent vasoconstrictor peptide produced by vascular endothelial cells. Nature. 1988; 332(6163):411-5.
177. Schweisfurth H, Kment A, Dahlheim H, Strauer BE. Klin Wochenschr. Elevated angiotensin-I-converting enzyme (ACE) in patients with essential hypertension. 1982 Jan 4;60(1):49-50.
178. Keane WF, Eknoyan G: Proteinuria, albuminuria, risk, assessment, detection, elimination (PARADE): A position paper of the National Kidney Foundation. Am J Kidney Dis 1999; 33: 1004–1010.
179. Zager RA, Andoh T, Bennett WM. Renal cholesterol accumulation: a durable response after acute and subacute renal insults. Am J Pathol. 2001;159(2):743-52
180. Deshmane SL, Kremlev S, Amini S, Sawaya BE. Monocyte chemoattractant protein-1 (MCP-1): an overview. J Interferon Cytokine Res. 2009 Jun;29(6):313-26.
181. Klahr S, Morrissey JJ. The role of vasoactive compounds, growth factors and cytokines in the progression of renal disease. Kidney Int Suppl. 2000 Apr;75:S7-14
182. Popolo A, Autore G, Pinto A, Marzocco. Oxidative stress in patients with cardiovascular disease and chronic renal failure. S.Free Radic Res. 2013;47(5):346-56.
183. Sedeek M, Nasrallah R, Touyz RM, Hébert RL. NADPH Oxidases, Reactive Oxygen Species, and the Kidney: Friend and Foe. J Am Soc Nephrol. 2013;24(10):1512-1518

184. Xu K, Zhou Y, Qiu W, Liu X, Xia M, Liu L, Liu X, Zhao D, Wang Y. Activating transcription factor 3 (ATF3) promotes sublytic C5b-9-induced glomerular mesangial cells apoptosis through up-regulation of Gadd45α and KLF6 gene expression. Immunobiology. 2011;216(8):871-81.

185. Liu Y, Wu J, Wu H, Wang T, Gan H, Zhang X, Liu Y, Li R, Zhao Z, Chen Q, Guo M, Zhang Z.UCH-L1 expression of podocytes in diseased glomeruli and in vitro.J Pathol. 2009;217(5):642-53

186. Lai CF, Chen YM, Chiang WC, Lin SL, Kuo ML, Tsai TJ.Cysteine-rich protein 61 plays a proinflammatory role in obstructive kidney fibrosis. PLoS One. 2013;8(2):e56481.